

**ADVANCED APPLICATIONS  
OF MINIEMULSION TECHNOLOGY**  
*DEVELOPMENT OF A VIABLE EMULSIFICATION PROCESS*

By

ULA EL-JABY

A thesis submitted to the Department of Chemical Engineering  
in conformity with the requirements for  
the degree of Doctor of Philosophy

Queen's University

Kingston, Ontario, Canada

**April 2010**

**Copyright © Ula El-Jaby, 2010**

## ABSTRACT

---

Miniemulsion technology is attracting increasing interest for the preparation of nano-size particles. However, the barrier to industrialising miniemulsion-based products is the lack of an energy efficient and scalable homogenisation device. Current laboratory techniques consist of batch units, however trends are leaning towards developing continuous processes. The objective of the work presented here is to investigate the use of the rotor-stator (RS) and static mixers (SM) as homogenisation devices and ultimately develop a continuous emulsification/polymerisation process for the preparation of miniemulsions.

Initially we investigated the RS as a homogenisation device and found that we were able to generate droplets ranging from 300 nm to 2  $\mu$ m, at industrially pertinent solids content. Subsequently, we investigated the use of SM and compared their performance in terms of mean droplet size evolutions with the rotor-stator. We were able to generate droplets < 200 nm in size and polymerise them in a stable fashion.

All the available emulsification devices were then compared in terms of power/energy consumption, droplet size distributions and shear rates. It was observed that with energy costs being of similar orders of magnitude, SM imposed less shear, produced relatively narrow distributions and were better adapted to scale-up, making them the optimal choice for miniemulsification.

Energy savings were increased by reducing coalescence during the emulsification step by using *in situ* generated surfactants, ultimately reducing emulsification time. Neutralising a water-soluble base with an oil-soluble acid almost instantaneously generates *in situ* surfactants at the oil-water interface. The reduction in emulsification time was partially attributed to the elimination of the relatively slow adsorption step

typical of preformed surfactants.

These results were used to show that emulsifying *in situ* formulations at moderate flow rates in line with SMX mixers can substantially reduce emulsification time from 30 minutes, with preformed surfactants, to ~30 seconds. With such a rapid emulsification step, it was possible to test the feasibility of the continuous emulsification process followed by polymerisation in a tubular reactor. Comparing this process with a batch operation, similar results for the ratio of  $N_p/N_D$  and conversion were obtained, but the continuous process was accomplished in a single step.

## ACKNOWLEDGMENTS

---

I am very thankful to my supervisors, Dr. Timothy McKenna and Dr. Michael Cunningham, whose encouragement, supervision and support from the beginning to the end, helped me grow as a professional, a researcher and as a writer.

Over the last four years, I have had the wonderful opportunity to spend half my time studying in France and the other half in Canada. I have had the pleasure to work with a number of colleagues from around the world, all of whom taught me a little something about their own countries. I would like to thank you for being there to talk and help me brainstorm ideas, to ask me good questions and to help me think through my problems.

To my friends in Ottawa, Kingston, Lyon and all over the world. I would like to extend a sincere thank you for your patience, understanding, encouragement and for teaching me how to work hard, yet play hard! I will always hold dear the discussions over coffee breaks, the long late night phone calls, the frustrations, the tears, the smiles and most importantly the laughs. Without your support I would not be able to solve the unsolvable!

Finally, to my family and to my loved ones. I will forever be indebted to you for educating me, for your unconditional support, your unconditional love, your endless patience, your kindness, your words of wisdom and of course your delicious meals! I will forever be grateful for encouraging me to pursue my interests, even when that meant the interests were across the ocean. For that I will always thank you.

I am fortunate to have you all in my life and I want to thank you for having faith in me.

# TABLE OF CONTENTS

---

<b>ABSTRACT</b>	i
<b>ACKNOWLEDGMENTS</b>	iii
<b>LIST OF FIGURES</b>	viii
<b>LIST OF TABLES</b>	xi
<b>NOMENCLATURE</b>	xii
<b>LIST OF PUBLICATIONS</b>	xv
<b>CHAPTER 1: INTRODUCTION</b>	1
1.1 LITERATURE CITED	6
<b>CHAPTER 2: BACKGROUND AND LITERATURE REVIEW</b>	7
2.1 EMULSION POLYMERISATION	8
2.2 MINIEMULSION POLYMERISATION	10
2.2.1 <i>COSTABILISERS IN MINIEMULSION SYSTEMS</i>	12
2.2.2 <i>SURFACTANTS IN MINIEMULSION SYSTEMS</i>	15
2.3 EMULSIFICATION DEVICES	19
2.3.1 <i>ULTRASONICATION</i>	20
2.3.2 <i>HIGH PRESSURE HOMOGENISERS</i>	21
2.3.3 <i>ROTOR-STATORS</i>	23
2.3.4 <i>STATIC MIXERS</i>	28
2.4 CONTINUOUS POLYMERISATION	35
2.5 LITERATURE CITED	38
 <b>CHAPTER 3: POLYMERISABLE MINIEMULSIONS USING ROTOR-STATOR HOMOGENISERS</b>	 44
3.1 EXPERIMENTAL	45
3.1.1 <i>MATERIALS</i>	45
3.1.2 <i>HOMOGENISATION</i>	46
3.1.3 <i>POLYMERISATION</i>	47
3.1.4 <i>CHARACTERISATION</i>	48
3.1.5 <i>CONDUCTIVITY MEASUREMENTS</i>	48

3.2	RESULTS AND DISCUSSION	49
3.2.1	<i>HOMOGENISATION AND POLYMERISATION</i>	49
3.2.1.1	POLYMERISATION OF 300 NM MINIEMULSIONS (R1)	52
3.2.1.2	POLYMERISATION OF 400 NM MINIEMULSIONS (R2)	54
3.2.1.3	POLYMERISATION OF 600 NM MINIEMULSIONS (R4)	57
3.2.2	<i>POLYMERISATION OF 400 NM DROPLETS</i>	59
3.2.2.1	PREPARATION OF MINIEMULSION WITH DIFFERENT COSTABILISERS	59
3.2.2.2	POLYMERISATION OF MINIEMULSIONS WITH DECREASING AGITATION SPEED IN THE REACTOR	61
3.2.2.3	POLYMERISATION OF MINIEMULSIONS WITH A LOWER SOLID CONTENT	63
3.2.2.4	POLYMERISATION OF MINIEMULSIONS WITH THE ADDITION OF PROTECTIVE COLLOID DISPERSANTS	65
3.2.2.5	PREPARATION OF MINIEMULSION WITH INCREASED SURFACE COVERAGE	66
3.3	CONCLUSIONS	70
3.4	LITERATURE CITED	71
	 <b>CHAPTER 4: EMULSIFICATION FOR LATEX PRODUCTION: COMPARING IN LINE MIXERS TO ROTOR-STATORS</b>	 72
4.1	EXPERIMENTAL	73
4.1.1	<i>MATERIALS</i>	73
4.1.2	<i>HOMOGENISATION</i>	73
4.1.3	<i>POLYMERISATION</i>	74
4.1.4	<i>CHARACTERISATION</i>	75
4.2	RESULTS AND DISCUSSION	75
4.2.1	<i>HOMOGENISATION</i>	75
4.3	CONCLUSIONS	83
4.4	LITERATURE CITED	84

<b>CHAPTER 5: COMPARISON OF EMULSIFICATION DEVICES FOR THE PRODUCTION OF MINIEMULSIONS</b>	<b>85</b>
5.1 EXPERIMENTAL	86
5.1.1 MATERIALS	86
5.1.2 HOMOGENISATION	86
5.1.2.1 ULTRASONICATION	86
5.1.2.2 ROTOR-STATOR	87
5.1.2.3 STATIC MIXERS	88
5.1.3 POLYMERISATION	89
5.1.4 CHARACTERISATION	89
5.2 RESULTS AND DISCUSSION	90
5.3 CONCLUSIONS	98
 <b>CHAPTER 6: MINIEMULSIONS VIA <i>IN SITU</i> SURFACTANT GENERATION</b>	 <b>99</b>
6.1 EXPERIMENTAL	100
6.1.1 MATERIALS	100
6.1.2 HOMOGENISATION	102
6.1.3 POLYMERISATION	102
6.1.4 CHARACTERISATION	103
6.2 RESULTS AND DISCUSSION	103
6.2.1 INCREASING SURFACTANT CONCENTRATION	106
6.2.2 INCREASING SOLIDS CONTENT	110
6.2.3 ROLE OF SA AS SURFACTANT AND COSTABILISER	112
6.2.4 REDUCING ODA CONCENTRATION	114
6.2.5 VARYING CARBOXYLIC ACID CHAIN LENGTH	116
6.2.6 VARYING SURFACTANT COUNTERION	118
6.3 CONCLUSIONS	120
6.4 LITERATURE CITED	122

<b>CHAPTER 7: CONTINUOUS PRODUCTION OF MINIEMULSIONS USING IN LINE SMX ELEMENTS</b>	123
7.1 EXPERIMENTAL	124
7.1.1 MATERIALS	124
7.1.2 HOMOGENISATION	124
7.1.3 POLYMERISATION	126
7.1.4 CHARACTERISATION	128
7.2 RESULTS AND DISCUSSION	128
7.2.1 EFFECT OF VARYING FLOW RATE	128
7.2.2 INCREASING THE NUMBER OF ELEMENTS IN SERIES	134
7.2.3 VARYING BOTH FLOW RATE AND THE NUMBER OF ELEMENTS IN SERIES	137
7.2.4 CONTINUOUS EMULSIFICATION/POLYMERISATION OF MINIEMULSIONS	142
7.3 CONCLUSIONS	144
7.4 LITERATURE CITED	146
 <b>CHAPTER 8: SIGNIFICANT CONTRIBUTIONS</b>	 147
<b>CHAPTER 9: FUTURE WORK</b>	151
<b>APPENDIX A</b>	156



## LIST OF FIGURES

<b>Figure 2.1</b>	Emulsion Polymerisation process explained in three intervals:	9
<b>Figure 2.2</b>	Miniemulsion Polymerisation.	11
<b>Figure 2.3</b>	Ostwald Ripening.	13
<b>Figure 2.4</b>	A - Droplets coalescing in the absence of surfactants due to attractive van der Waals forces. B – Droplets stabilised with surfactants repel each other due to the repulsive forces induced by surfactants.	16
<b>Figure 2.5</b>	A – Generating a surfactant <i>in situ</i> at the oil-water interface by neutralizing an oil-soluble carboxylic acid with a water-soluble base, reducing the amount of coalescence and enhancing droplet stability and emulsification time. B – When using preformed surfactants, which are predissolved in the aqueous medium, droplet stability is dependent on the rate of transport to, collision with and adsorption onto the oil-water interface; adsorption being the rate limiting step.	18
<b>Figure 2.6</b>	Branson VC 750 Vibra-Cell Ultrasonic Processor.	21
<b>Figure 2.7</b>	A - Cross section of a HPH outlining the flow path. B - Droplet elongation, fragmentation and recalescence process.	22
<b>Figure 2.8</b>	Flow paths through a rotor-stator mixing head.	24
<b>Figure 2.9</b>	Flow patterns of the jets emerging from different stators.	25
<b>Figure 2.10</b>	Commercially available static mixers, differing in design and material.	29
<b>Figure 2.11</b>	Breaking positions in and SMX mixing element.	31
<b>Figure 2.12</b>	Droplet deformation in an SMX mixing element as described by Streiff <i>et al.</i> <sup>[67]</sup>	32
<b>Figure 2.13</b>	Droplet deformation in turbulent flow.	34
<b>Figure 3.1</b>	Top view of vessels used during emulsification with the rotor stator.	47
<b>Figure 3.2</b>	Droplet diameter distribution of ~ 300 nm (R1) and ~ 400 nm (R2) droplets generated using the rotor-stator.	51
<b>Figure 3.3</b>	Conversion profile for ~ 300 nm droplets (R1) polymerised initiated at 70°C using AIBN and BPO.	52
<b>Figure 3.4</b>	Conversion profile of ~ 400 nm droplets (R2) initiated with AIBN, LPO and BPO) at 70°C.	56
<b>Figure 3.5</b>	Evolution of the particle diameter ( $D_v$ ) over time as a function of the costabilisers ODA and HD for ~ 400 nm miniemulsions polymerised at 70°C using BPO.	60
<b>Figure 3.6</b>	Evolution of the particle diameter ( $D_v$ ) and relative conductivity with time as a function of the reactor impeller speeds: 300, 150 and 50 RPM for ~ 400 nm droplets polymerised at 70°C using BPO.	62
<b>Figure 3.7</b>	Evolution of the particle diameter ( $D_v$ ) over time as a function of the solid contents 47 and 34 wt% for ~ 400 nm miniemulsions polymerised at 70°C using BPO.	64

<b>Figure 3.8</b>	Evolution of the particle diameter ( $D_v$ ) over time as a function of the protective colloids PVOH, Acacia Powder and the non-ionic surfactant Disponil for ~ 400 nm miniemulsions polymerised at 70°C using BPO.	66
<b>Figure 3.9</b>	Evolution of the particle diameter ( $D_v$ ) over time as a function of the 30, 60, and 90% surface coverage for ~ 400 nm miniemulsions polymerised at 70°C using BPO.	67
<b>Figure 4.1</b>	Evolution of droplet diameter ( $D_v$ ) over time for formulation S2 made using the static mixer and the rotor-stator.	76
<b>Figure 4.2</b>	Evolution of the PDI for S2 droplets generated using the static mixer and the rotor-stator.	77
<b>Figure 4.3</b>	Evolution of droplet sizes ( $D_v$ ) for a 38 % solids content MMA miniemulsion system homogenised with SMX and PAC separately at 114 g/s.	78
<b>Figure 4.4</b>	A: Evolution of droplet diameter ( $D_v$ ) over time as a function of the surfactant quantity. B: Evolution of conversion and PDI as a function of time for formulations SM 1 and SM 2.	80
<b>Figure 4.5</b>	Particle size distributions at 0, 90, and 180 minutes for the polymerised S1 and S2 formulations.	82
<b>Figure 5.1</b>	Homogenisation set up for the static mixers.	89
<b>Figure 5.2</b>	Droplet diameter evolutions for miniemulsions generated using the rotor-stator (5.5 and 7.5 cm stator head), static mixer and sonicator	91
<b>Figure 5.3</b>	Final volume average droplet size distribution for miniemulsions generated using the rotor-stator, static mixer and sonicator.	92
<b>Figure 5.4</b>	Particle diameter evolutions for miniemulsion prepared using the rotor-stator, static mixer and sonicator.	97
<b>Figure 6.1</b>	Droplet size evolution for droplets prepared with a rotor-stator (3000 RPM) using equal amounts (9.0 mmol) of preformed KSA, <i>in situ</i> KSA or SDBS. (○ = minimum droplet size)	104
<b>Figure 6.2</b>	Droplet size evolutions for miniemulsions at 40 % solids content prepared with varying amounts of <i>in situ</i> and preformed potassium stearate (assuming 100% neutralisation) and emulsified using an ultrasonic dismembrator for four minutes.	107
<b>Figure 6.3</b>	The ratios of the number of particles to the number of droplets throughout the polymerisations for systems prepared with <i>in situ</i> KSA ranging in amounts from 2.5 to 25.8 mmol.	109
<b>Figure 6.4</b>	Droplet size evolutions for systems prepared with increasing solids content (40-60%); keeping the weight percent of costabiliser (7.0 wt%) and <i>in situ</i> KSA (2.0 wt%) constant. All systems were emulsified using ultrasonication.	111
<b>Figure 6.5</b>	Droplet diameters for miniemulsions prepared with <i>in situ</i> KSA and SDBS separately with varying amounts of ODA.	114
<b>Figure 6.6</b>	The ratios of the number of particles to the number of droplets throughout the polymerisations for systems prepared with 9.0 mmol <i>in situ</i> KSA and 4-7 wt% ODA.	116

<b>Figure 6.7</b>	Droplet diameter by volume ( $D_v$ ) measurements for miniemulsions prepared with equimolar amounts (9.0 mmol) of potassium laurate (KLA), potassium stearate (KSA) and potassium behenoate (KDA).	117
<b>Figure 6.8</b>	Droplet diameter by volume ( $D_v$ ) measurements for miniemulsions prepared with equimolar amounts (9.0 mmol) of lithium stearate (LiSA), sodium stearate (NaSA) and potassium stearate (KSA).	119
<b>Figure 7.1</b>	Homogenisation apparatus using static mixers, consisting of a closed loop system with a pump, tubing, product reservoir and temperature bath.	125
<b>Figure 7.2</b>	Continuous emulsification/polymerisation process set up for the production of miniemulsions.	128
<b>Figure 7.3</b>	A - Mean droplet size evolution for miniemulsions emulsified using 1 bank of SMX elements (7 mixers) and pumped through at flow rates ranging from 50 to 75 g/s (350 to 600 RPM). B - Mean droplet size evolution for miniemulsions prepared with increasing RPM and ~ 30 passes through 1 bank of SMX mixing elements.	129
<b>Figure 7.4</b>	Pressure drop evolution for miniemulsion formulation FM 1 emulsified at varying RPM.	132
<b>Figure 7.5</b>	The ratios of the number of particles to the number of droplets throughout the polymerisations for miniemulsions prepared with 2.0 wt% <i>in situ</i> KSA and homogenised at various RPM ranging from 350 to 600 (50 to 75 g/s).	133
<b>Figure 7.6</b>	Mean droplet size evolution for droplets emulsified at 350 RPM using 1, 2 and 3 banks of mixers.	135
<b>Figure 7.7</b>	Mean droplet size evolution as a function of the number of passes for droplets emulsified at 350 RPM using 1, 2 and 3 banks of mixers.	136
<b>Figure 7.8</b>	Time (A) and energy (B) evolution for 170 to 180 nm droplets generated at various flow rates (350 to 600 RPM) with varying number of elements in series.	138
<b>Figure 7.9</b>	Conversion and $N_p/N_D$ profiles for miniemulsions emulsified in the static mixers at 600 RPM with 3 banks of elements in series and polymerised in a batch (■) or one step emulsification/polymerisation process with a tubular reactor (○).	143

## LIST OF TABLES

<b>Table 3.1</b>	Dissociation rate constants at 70 °C and solubility in water constants of AIBN, BPO and LPO.	45
<b>Table 3.2</b>	Effect of surfactant concentration (SDBS) and rotational speed on mean droplet diameter by volume (D <sub>v</sub> ) and polydispersity (PDI).	50
<b>Table 3.3</b>	Evolution of the conversion, droplet diameters (D <sub>v</sub> & D <sub>N</sub> ) and PDI during polymerisation as a function of the initiator (AIBN or LPO) used for ~ 300 nm miniemulsions (R1). T=70°C.	54
<b>Table 3.4</b>	Evolution of the conversion and droplet diameters (D <sub>v</sub> & D <sub>N</sub> ) during polymerisation as a function of the initiator (AIBN, BPO and LPO) used for ~ 400 nm miniemulsions (R2). T=70°C.	55
<b>Table 3.5</b>	Evolution of the conversion and droplet diameters (D <sub>v</sub> & D <sub>N</sub> ) during polymerisation as a function of the initiator (AIBN and BPO) used for ~ 600 nm miniemulsions (R4). T=70°C.	58
<b>Table 3.6</b>	Evolution of the N <sub>p</sub> and droplet diameters (D <sub>v</sub> & D <sub>N</sub> ) during polymerisation as a function of the surfactant coverage (30, 60, and 90%) used for ~ 400 nm miniemulsions (R2). T=70°C.	69
<b>Table 4.1</b>	Formulations prepared to be used in the static mixer and the rotor-stator.	74
<b>Table 5.1</b>	Formulation used for emulsifications using the RS, SM and US.	86
<b>Table 5.2</b>	Estimation of the amount of power and energy required by the rotor-stator, static mixer and sonicator to generate droplets ranging between 160-200 nm.	95
<b>Table 6.1</b>	Formula and molecular weight of behenic, stearic and lauric acid.	100
<b>Table 6.2</b>	Solubility and molecular weight data for potassium, sodium and lithium hydroxide.	101
<b>Table 6.3</b>	Miniemulsion formulations containing MMA and BA in a 50:50 w/w ratio, ODA and either <i>in situ</i> generated (FM 1) or preformed surfactant (FM 2).	101
<b>Table 6.4</b>	Formulations prepared with varying amounts of <i>in situ</i> KSA to assess the roles of <i>in situ</i> KSA as costabiliser and surfactant.	113
<b>Table 7.1</b>	Flow rates at varying RPM and the time required for a single pass through 1 bank of elements.	126
<b>Table 7.2</b>	Miniemulsion formulations containing MMA and BA monomer in a 50:50 w/w ratio, ODA and <i>in situ</i> generated KSA (FM 1)	126
<b>Table 7.3</b>	Estimation of the energy consumption required by ultrasonication, the rotor-stator and static mixers in the preparation of miniemulsion systems.	141

## NOMENCLATURE

---

### *Acronyms*

AIBN	2,2'-azobis(2-methylpropionitrile)
BA	Butyl Acrylate
BPO	Dibenzoyl Peroxide
CFD	Computational Fluid Dynamics
CMC	Critical Micelle Concentration
D	Diameter of the Stator Head
DA	Behenic Acid (Docosanoic Acid)
DIW	Deionised Water
DP	Disponil
DSD	Droplet Size Distribution
FM	Formulation
HD	Hexadecane
HPH	High Pressure Homogenisers
ID	Inside Diameter
KDA	Potassium behenoate
KLA	Potassium Laureate
KOH	Potassium Hydroxide
KPS	Potassium Persulphate
KSA	Potassium Stearate
LA	Lauric Acid
LiOH	Lithium Hydroxide
LPO	Dilauryl Peroxide
LiSA	Lithium Stearate
MMA	Methyl Methacrylate
MW	Molecular Weight
N	Revolutions Per Minute
NaOH	Sodium Hydroxide
NaSA	Sodium Stearate
ODA	Octadecyl Acrylate
PAC	Polyacetal Mixers
PDI	Polydispersity Index
<i>p</i> KSA	Preformed Potassium Stearate
PSD	Particle Size Distribution
PVOH	Polyvinyl Alcohol
RPM	Rotations Per Minute
RS	Rotor-Stators
SA	Stearic Acid
SDBS	Sodium dodecylbenzene sulphonate
SM	Static Mixers
SMX	Static Mixers provided by Sulzer Chemtech
US	Ultrasonication
VOC	Volatile Organic Compounds

## Greek

$\gamma$	Oil-water interfacial tension (mN/m)
$\dot{\gamma}$	Shear rate (1/s)
$\Delta$	Change
$\delta$	Gap width between rotor and stator (m)
$\eta$	Viscosity (cP)
$\pi$	Pi
$\rho$	Density (kg/m <sup>3</sup> )
$\tau$	Torque (N cm)
$\phi_c$	Volume fraction of costabiliser
$\phi_m$	Volume fraction of monomer
$\chi_{mc}$	Monomer polymer interaction parameter

## Variables

A	Surface Area
A <sub>s</sub>	Specific Surface Area
D	Diameter of the stator head (m)
D <sub>D</sub>	Diameter of droplet (nm)
D <sub>Max</sub>	Maximum stable droplet size
D <sub>N</sub>	Number average droplet diameter
D <sub>P</sub>	Diameter of the particle
d <sub>pol</sub>	Density of polymer (kg/m <sup>3</sup> )
D <sub>S</sub>	Tube Diameter (m)
D <sub>V</sub>	Volume average droplet diameter (nm)
j <sub>crit</sub>	Critical hydrophobic chain length
K	Constant
k <sub>d</sub>	Dissociation rate constant (1/s)
K <sub>S</sub>	Metzner-Otto Constant
m	Exponent
m <sub>mc</sub>	Ratio of equivalent number of molecular segments between the monomer and costabiliser
M <sub>pol</sub>	Mass of polymer (kg)
m <sub>SDBS</sub>	Amount of SDBS (kg)
M <sub>SDBS</sub>	Molecular Weight of SDBS (g/mol)
M <sub>TOT</sub>	Total mass of monomer (kg)
MW	Molecular Weight (g/mol)
n	Exponent
N	Revolutions per minute (RPM)
N <sub>A</sub>	Avagadro's number (1/mol)

$N_P$	Number of Particles
$N_D$	Number of Droplets
$P$	Pressure (bar)
$P_W$	Power (W)
$Q$	The flow rate (kg/s)
$R$	Gas constant
$Re$	Reynolds Number
$r_1$	Radius of droplet distribution 1
$r_{1e}$	Radius of particle 1 in equilibrium
$r_2$	Radius of droplet distribution 2
$r_{2e}$	Radius of particle 2 in equilibrium
$T$	Temperature
$u_m$	Chemical potential
$V$	Fluid Velocity (m/s)
$V_m$	Molar volume of monomer
$V_{tip}$	Tip Speed (m/s)
$We$	Weber Number
$W_{Breakage}$	Energy required to break/form an interface

## LIST OF PUBLICATIONS

---

1. U. El-Jaby, M. Cunningham, T.F.L. McKenna. Continuous Production of Miniemulsions Using SMX Static Mixers. *AIChE Journal* –Submitted **2010**
2. U. El-Jaby, M. Cunningham, T.F.L. McKenna. Miniemulsions via *In Situ* Surfactant Generation. *Macromolecular Chemistry and Physics* – Submitted **2010**.
3. U. El-Jaby, M. Cunningham, T.F.L. McKenna. *In situ* Surfactant Generation for Miniemulsions. *Macromolecular Rapid Communication*. **2010**, 31, 558.
4. U. El-Jaby, M. Cunningham, T.F.L. McKenna. Investigation of the Production of Miniemulsions using an SMX Static Mixer. *Industrial & Engineering Chemistry Research*. **2009**, 48, 10147.
5. U. El-Jaby, G. Farzi, E. Bourgeat-Lami, M. Cunningham, T.F.L. McKenna. Emulsification for Latex Production using Static Mixers. *Macromolecular Symposia*. **2009**, 281, 77.
6. U. El-Jaby, M. Cunningham, T. Enright, T.F.L. McKenna. Polymerisable Miniemulsions Using Rotor-Stator Homogenisers. *Macromolecular Reaction Engineering*. **2008**, 4, 350.
7. U. El-Jaby, M. Cunningham, T.F.L. McKenna. Miniemulsification: An Analysis of the Use of Rotor Stators as Emulsification Devices. *Macromolecular Symposia*. **2007**, 259, 1.



# 1

## ***INTRODUCTION***

---

The production of polymers via free radical polymerisation in colloidal dispersions continues to be of economic significance for a number of reasons including: a desire to substitute current solvent-based systems with an aqueous medium for environmental reasons, a reduction in the bulk viscosity of the reactor contents (better heat transfer, easier handling) and the ease of manipulating sticky or film forming materials. Traditionally a large majority of products (i.e. paints, adhesives, textiles, etc.), has been made by suspension and conventional emulsion polymerisation; however we are reaching the limits in terms of the range of materials that can be produced.

More recently, the ease with which one can incorporate a wide range of organic

and inorganic materials into the final product, as well as the ability to directly produce and emulsify dispersions with solids contents  $\geq 45$  % by volume have made miniemulsions more and more attractive as an alternative means for production of heterogeneous aqueous dispersions of polymer particles. Miniemulsions have been extensively researched within the academic community (<http://www.ehu.es/napoleon/>) and have recently sparked an increasing amount of industrial attention due to their versatile nature, thereby offering a technology capable of producing a range of new value-added specialty latexes. It is therefore clear that a significant amount of effort is being invested in moving miniemulsion technology from the laboratory to the market place. However, one of the major barriers preventing the market expansion of this technology is the lack of a commercially viable emulsification technique; indicating that the development of a scalable and energy efficient homogenisation device for commercial scale operations is extremely important and timely.

Miniemulsions are chemically similar to conventional emulsions in the sense that they can employ the same monomers and surfactants; however they differ in their method of preparation and polymerisation. Roughly speaking, latex particles made with miniemulsions are created by provoking polymerisation directly in mechanically generated droplets rather than by causing the reaction to occur in monomer swollen micelles as is typically the case in a conventional emulsion. However, these droplets need to be small enough (on the order of 50 to 500 nm) that they can be polymerised at a commercially-viable rate. Therefore, generation of miniemulsions requires the input of mechanical energy through high shearing devices to yield nano-scale droplets, and the use of a two component stabilisation system consisting of surfactant(s) and a costabiliser

to prevent the degradation of the resulting droplets via coalescence and Ostwald ripening. Ideally, polymerisation of a miniemulsion proceeds in such a manner that each droplet acts as a mini batch reactor, yielding a polymer particle. Therefore, if we manage to incorporate organic or inorganic materials in the droplets and polymerise in an ‘ideal’ fashion, we can begin to create a new range of materials that cannot be produced using established techniques.

The most common homogenisation device at the laboratory scale is ultrasonication (US) due to its simplicity of use and rapidity. Nonetheless, it is an energy-intensive device and its use in the preparation of composite or hybrid miniemulsions is questionable, as the high shear inherent to the technique may rupture the droplets and release their contents. The use of high pressure homogenisers (HPH) on the bench scale is also well documented (POLYMAT<sup>\*</sup>). HPH require more energy than devices like the static mixers (SM) as they generate 5 to 50 MPa of pressure compared to 0.5 to 1.5 MPa for pumps used in static mixer set ups. This raises the question, are there any more efficient homogenisation methods for making miniemulsions on an industrial scale?

Ouzineb *et al.* previously investigated the use of the rotor-stator and static mixers as emulsification devices and successfully showed that it was possible to produce stable miniemulsion droplets with both devices.<sup>[1]</sup> Both of these types of equipment are commonly used in different industrial sectors for applications such as food homogenisation and petroleum processing. While Ouzineb *et al.*’s work has yielded promising results the application of these homogenisation techniques for the preparation of miniemulsions has not been studied in-depth. The overall objective of the thesis work presented herein is to more deeply investigate the potential of the rotor-stator and static

---

<sup>\*</sup> Institute of Polymer Technology, University of the Basque Country

mixers for the preparation of miniemulsions and to develop a single step commercially viable emulsification/polymerisation process for the generation of miniemulsions.

In the initial part of the investigation, we studied the preparation of miniemulsions with the rotor-stator and focused on the preparation and polymerisation of stable systems. Droplets ranging from 300 nm to 2  $\mu$ m in size were prepared and polymerised. It was found that stable droplets do not necessarily produce stable particles (Chapter 3) and in some cases the final polymer particles nearly doubled in diameter with respect to the initial miniemulsion drops. This problem was not encountered at later stages using the static mixers (Chapter 4). A preliminary study demonstrated that static mixers produced smaller and narrower average size distributions that polymerised in a nearly 1 to 1 mapping of droplets to particles (Chapter 5). Therefore, the investigation focused on the development of static mixers as homogenisation devices and we compared their efficiency to that of the rotor-stator and ultrasonication in terms of the magnitude of shear imposed, emulsification time scale and energy consumption (Chapter 5).

The next phase of the study centred on improving the emulsification, stabilisation and polymerisation of miniemulsion systems by modifying the stabilisation system used (Chapter 6). We found that the time to reach the minimum droplet equilibrium size can be significantly shortened ( $\sim 50\%$ ) by using an *in situ* generated surfactant. *In situ* surfactants almost instantaneously stabilise the newly generated interfaces, thus reducing the amount of droplet coalescence and the amount of secondary nucleation due to its hydrophobic nature.

The combination of static mixers with *in situ* generated surfactants was studied with regard to possible development of a continuous polymerisation process (Chapter 7).

The effect of increasing the flow rate at a fixed number of SMX elements and increasing the number of SMX elements at fixed flow rate was studied separately. Increasing both flow rate and the number of elements simultaneously was investigated and it was found to have a nonlinear impact on reducing both the time required to reach minimum droplet size at the same number of passes as well as reducing the total energy required. By combining a continuous emulsification unit in series with a tubular reactor we were able to develop a single step continuous emulsification/polymerisation process for the production of miniemulsions.

## 1.1 LITERATURE CITED

1. Ouzineb, K.; Lord, C.; Lesauze, N.; Graillat, C.; Tanguy, P. A.; McKenna, T. Homogenisation Devices for the Production of Miniemulsions. *Chem. Eng. Sci.* **2006**, *61*, 2994-3000.

## ***BACKGROUND AND LITERATURE REVIEW***

---

This chapter begins by providing a brief overview of both the emulsion and miniemulsion polymerisation processes. The general mechanism of each method is described in order for the reader to grasp the advantages of miniemulsions and the usefulness of this technology in generating a new range of value-added products. For a more in-depth review of emulsion polymerisation, the reader is referred to reviews written by Thickett *et al.*<sup>[1]</sup>, Chern *et al.*<sup>[2]</sup> and references therein. We then delve into miniemulsion technology, highlighting the area most relevant to the objectives of this study. An introduction is given on the role of costabilisers, surfactants and a number of different

emulsification devices; with an emphasis on the latter given its importance in the thesis. When necessary, a more detailed examination will be addressed in the following chapters as we investigate their impact on the preparation and preservation of miniemulsion systems.

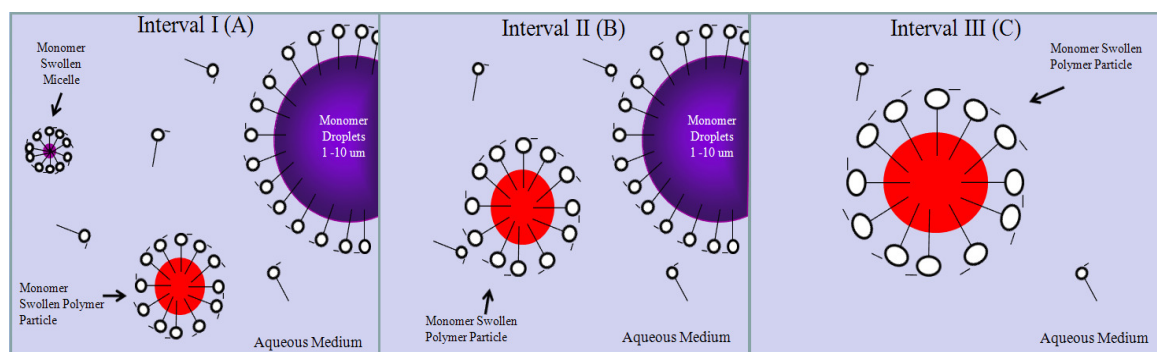
## 2.1 EMULSION POLYMERISATION

Emulsion polymerisation processes are traditionally used in the commercial production of a multitude of products such as paints, coatings, adhesives and rubbers just to name a few.<sup>[3]</sup> The formulation of a conventional oil in water emulsion polymerisation process contains one or more monomers and an excess of surfactant (in quantities above the critical micelle concentration (CMC)) dispersed in a continuous phase.<sup>[4]</sup>

Harkins was the first to demonstrate emulsion polymerisation in a batch process.<sup>[5]</sup> The Harkins framework is still the most widely used in academia and industry, although it has evolved considerably under the guidance of notable researchers such as Priest<sup>[6]</sup>, Smith and Ewert<sup>[7]</sup>, Fitch<sup>[8]</sup> and Ugelstad<sup>[9]</sup>. The process is typically broken down into three separate and distinct intervals (Figure 2.1). Mixing the emulsion components under moderate agitation ( $\geq 300$  RPM) leads to the creation of a system containing large monomer droplets (1-10  $\mu\text{m}$ ), micelles (10-20 nm) and free dissolved surfactant. Water is an appropriate (but not the only) choice for the continuous phase as it is non-toxic, has a high heat capacity and low viscosity, all of which are good characteristics for heat transfer (in the rest of this thesis we will study oil-in-water emulsions). During interval I (Figure 2.1A), waterborne radicals arising from initiator decomposition propagate in the medium adding dissolved monomer units and forming



oligomers. At a certain chain length, the oligomers become surface active and enter a micelle or continue to grow until they reach a critical hydrophobic chain length ( $j_{crit}$ ).<sup>[6]</sup> In the latter case, the chains precipitate forming primary particles in the aqueous phase and are stabilised by free surfactant molecules (homogeneous nucleation).<sup>[8]</sup> With respect to micellar nucleation, 1 out of every ~ 100 to 1000 micelles is directly converted to particles; the remaining micelles disband and help stabilise growing polymer particles, marking the end of interval I.<sup>[2]</sup> Interval II (Figure 2.1B) is characterised by a constant rate of polymerisation as monomer diffuses from the droplet reservoirs to the growing particles, through the aqueous medium. Once the monomer reservoirs have been depleted, interval III (Figure 2.1C) commences and the concentration of monomer within the particles decreases as the polymerisation progresses.



**Figure 2.1 Emulsion Polymerisation process explained in three intervals: Interval 1 (A) - particle nucleation stage; Interval II (B) - monomer diffusion/consumption stage; Interval III (C) - monomer depletion stage.**

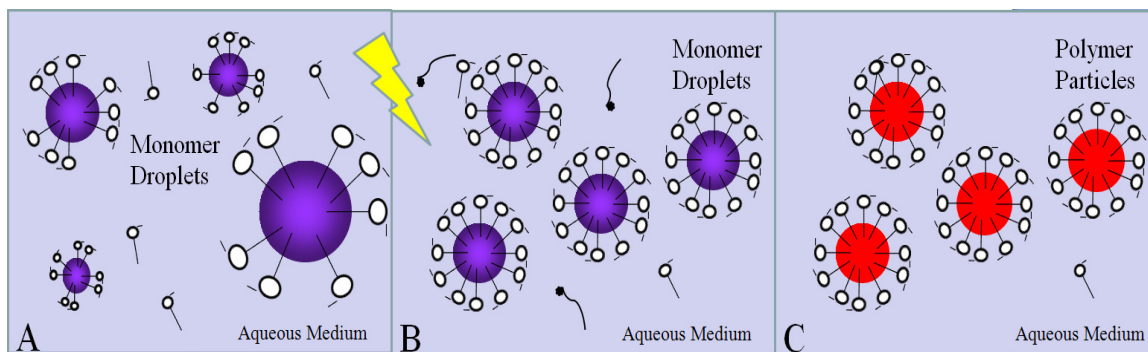
Statistically, the predominant form of nucleation is micellar when surfactant is present in quantities above the CMC, due to the abundant number of available micelles ( $\sim 10^{18-22}$  per litre), followed by homogeneous (described earlier) and droplet nucleation.<sup>[4]</sup> Droplet nucleation can also occur if an oligoradical enters the monomer reservoirs. However, in conventional emulsion polymerisation droplet nucleation is generally considered negligible since the specific surface area of the droplets is several orders of

magnitude lower than that of the micelles and growing polymer particles.<sup>[4]</sup> It will become important if the droplets are as small and as numerous as the polymer particles. The significance of this will become apparent in the next section.

## 2.2 MINIEMULSION POLYMERISATION

Miniemulsion technology has been extensively researched within the academic community for the past 2 decades or so, and has recently attracted an increasing amount of industrial attention. The growing interest in this technique is in large part due to the fact that it provides a means of incorporating hydrophobic materials directly into the polymer phase and can be directly produced at industrially relevant solids content (i.e.  $\geq 45\%$ ); thereby offering the possibility of producing a range of new value-added specialty latexes.

Miniemulsions are prepared by emulsifying two immiscible phases using a mechanical agitator (Figure 2.2A), generating colloidally dispersed oil droplets in an aqueous medium. Droplet systems range anywhere from 50 to 500 nm in size depending on the intensity of shear and the stabilisation system (Figure 2.2B) used. The distinct feature of miniemulsion systems is that in an ideal situation, each droplet behaves as a miniature batch reactor. Upon radical nucleation from the aqueous (or oil<sup>[10, 11, 12, 13]</sup>) phase, each droplet yields a polymer particle and the number of particles ( $N_P$ ) at the end of the polymerisation equals the number of droplets ( $N_D$ ) initially present ( $N_P/N_D=1$ ) (Figure 2.2C).



**Figure 2.2 Miniemulsion Polymerisation. A- Initial coarse emulsion system containing monomer droplets ranging in size and free dissolved surfactant. B – Application of high shear generates a more uniform distribution of monomer droplets. C- Aqueous phase radicals entering each droplet yielding a polymer particle.**

However, the keys to a successful polymerisation are: to get the droplets small enough that they can capture aqueous phase radicals (otherwise need to use oil-soluble systems) and to generate as uniform a distribution as possible, significantly reducing the effect of monomer transfer from smaller to larger droplets. Agitation/shearing is important when generating a desired average droplet size and distribution. The use of surfactant(s) and costabiliser are required to stabilise the droplet systems against Ostwald ripening (sec. 2.2.1) and coalescence (sec. 2.2.2), respectively. The costabiliser is typically a low molecular weight compound dissolved within the oil droplets, creating an osmotic pressure gradient and significantly reducing the amount of monomer transfer from smaller to larger droplets.<sup>[14, 15, 16]</sup> Surfactants (electrostatic and/or steric) play two very important roles. During emulsification they lower the interfacial tension and facilitate droplet breakage. Surfactants also prevent, to varying degrees, recoalescence of droplets.

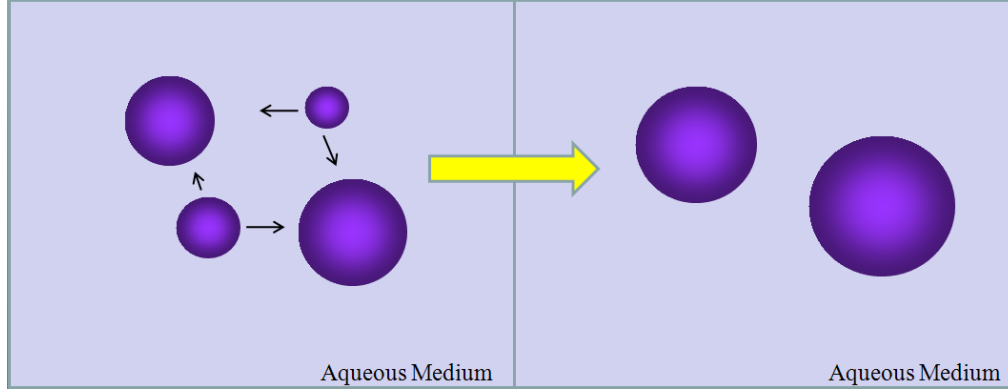
Mechanical homogenisation devices (sec. 2.3) are a vital component for breaking droplets down to desired size range.<sup>[17]</sup> Ultrasonication (US) (sec. 2.3.1) is the preferred homogenisation method for laboratory scale experiments because of its rapidity and simplicity, however, the large energy consumption is not practical at commercial scales.

High pressure homogenisers (HPH) (sec. 2.3.2) have also been found to be effective for laboratory and commercial scale experiments, but similar to US, HPH devices are energy intensive and sometimes require a prehomogenisation step. More recently it has been shown that devices such as the rotor-stator (RS) (sec. 2.3.3) and static mixers (SM) (sec. 2.3.4) impose less shear and are capable of generating larger volumes of polymerisable miniemulsions comparable in size to those prepared with the sonicator (Chapter 5).

Given that a considerable amount of work has been done in the field of miniemulsion technology, we will concentrate the discussion to touch upon the major aspects of miniemulsions; explaining the importance and use of costabilisers, surfactants and the need for efficient emulsification devices.

### *2.2.1 COSTABILISERS IN MINIEMULSION SYSTEMS*

Higushi and Misra were the first to propose that Ostwald ripening, the diffusion of monomer from smaller to larger droplets can be significantly delayed when a second water insoluble component is added to the dispersed phase.<sup>[14]</sup> The diffusion is driven by chemical potential differences of the dispersed phase within a distribution of droplets sizes, whereby smaller droplets are lost at the expense of larger ones (Figure 2.3) as described using the Morton equation (Equation 1).



**Figure 2.3 Ostwald Ripening.** The loss of the smaller droplets at the expense of larger ones due to differences in chemical potentials.

To simplify our explanation of the ripening process, Morton's equation has been expanded assuming that only two sizes exist, where  $r_1 < r_2$  <sup>[18]</sup>:

$$\ln\left(\frac{\varphi_{m_1}}{\varphi_{m_2}}\right) + (1 - m_{mc})(\varphi_{c_1} - \varphi_{c_2}) + \chi_{mc}(\varphi_{c_1}^2 - \varphi_{c_2}^2) + \frac{2\gamma V_m}{RT}\left(\frac{1}{r_{1e}} - \frac{1}{r_{2e}}\right) = \frac{\Delta u_m}{RT} \approx 0 \quad (1)$$

Where,  $\varphi_m$  and  $\varphi_c$  are the volume fraction of monomer and costabiliser in droplets 1 and 2 respectively,  $m_{mc}$  is the ratio of equivalent number of molecular segments between the monomer and costabiliser,  $\chi_{mc}$  is the monomer polymer interaction parameter,  $\gamma$  is the oil-water interfacial tension,  $V_m$  is the molar volume of monomer,  $r_{1e}$  and  $r_{2e}$  are the radii of particles 1 and 2 at equilibrium,  $R$  is the gas constant,  $T$  is the temperature and  $\Delta u_m$  is the difference in chemical potential. The first two terms on the left-hand side of the equation describe the fractional composition of the droplets. The third term, containing the interaction parameter ( $\chi_{mc}$ ), accounts for the enthalpy of mixing between the monomer and costabiliser and the fourth term represents the interfacial energy at the oil-water interface for droplets of different sizes.

After homogenisation, a distribution of droplet sizes exists with relatively similar fractional compositions. However, if only two droplet distributions 1 and 2 existed,

where  $r_1 < r_2$ , the chemical potential in the smaller droplet,  $r_1$ , would be greater than that of the larger droplet,  $r_2$ . As all systems naturally tend to minimize their free energy, monomer will diffuse out of the smaller droplet,  $r_1$  towards droplet  $r_2$  in order to counteract the high potential. As monomer diffuses out of the smaller droplet, the monomer concentration begins to decrease ( $\downarrow \varphi_{m_1}$ ) and the concentration of the costabiliser begins to increase ( $\uparrow \varphi_{c_1}$ ). Similarly, the concentration of monomer in the larger droplet increases ( $\uparrow \varphi_{m_2}$ ) and the concentration of costabiliser decreases ( $\downarrow \varphi_{c_2}$ ). The increase in the fractional amount of costabiliser in the smaller droplet offsets the chemical potential of said droplet and helps eliminate the driving force needed for ripening. The dynamic process continues until pseudo-equilibrium is reached, hence  $\Delta u_m \rightarrow 0$ .<sup>[18]</sup> Other changes such as costabiliser type and molecular weight, which also affect the interaction parameter, can be quantified using Equation 1. However, since we are only interested in the phenomenology, the reader is referred to references written by Taylor *et al.*<sup>[16]</sup>, Schork *et al.*<sup>[17]</sup> and Asua *et al.*<sup>[18]</sup> for a further examination.

The use of costabilisers is well documented in early miniemulsion research, in particular by Ugelstad *et al.* who pioneered the work using cetyl alcohol, what was then termed a cosurfactant.<sup>[15]</sup> In addition to reducing the rate of ripening, a cosurfactant possesses surface activity and helps lower the interfacial energy, facilitating the formation of smaller droplets. The use of a long chain hydrocarbon, hexadecane, was explored shortly thereafter.<sup>[19]</sup> Hexadecane was found to be more efficient than cetyl alcohol at stabilising droplets of comparable size due to its increased hydrophobicity. Either compound is satisfactory for the theoretical development of miniemulsion

technology; however replacements for these volatile organic compounds (VOC's) are needed if eco-friendly products are to be made with miniemulsion based systems. The use of low molecular weight polymers (i.e. polystyrene<sup>[20]</sup>, polymethyl methacrylate<sup>[21]</sup>, polyvinyl acetate<sup>[22]</sup>) has been investigated as an alternative; they are hydrophobic and can be tailored to not influence the physical properties of the latex.

Acrylate monomers were also found to be effective, if not better than polymeric costabilisers, as they are low molecular weight compounds which are chemically incorporated into the polymer backbone, reducing VOC concerns.<sup>[23, 24, 25]</sup>

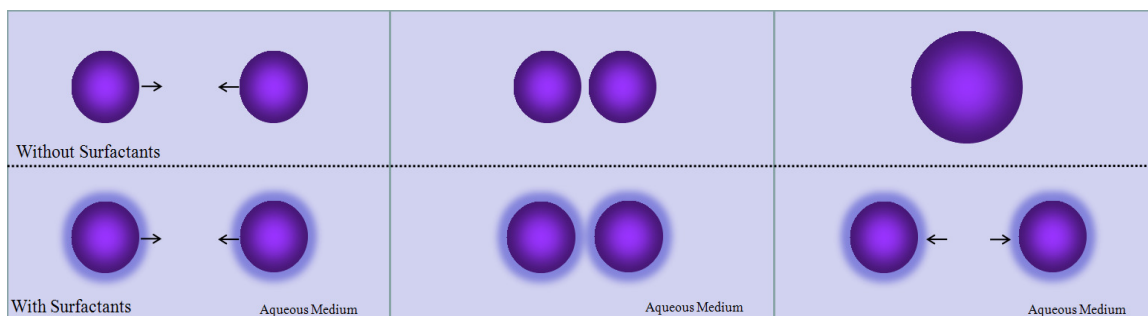
### 2.2.2 SURFACTANTS IN MINIEMULSION SYSTEMS

Surfactants play two very important roles in the preparation of miniemulsions. During emulsification, surfactant molecules lower the interfacial tension, facilitating droplet breakage.<sup>[26]</sup> They also prevent, to varying degrees, recoalescence of droplets (Figure 2.4). It has been shown that as the surfactant concentration increases ( $\downarrow\gamma$ ), for a given amount of shear ( $W_{\text{Breakage}}$ ), the overall surface area increases ( $\Delta A$ ):

$$W_{\text{Breakage}} = \gamma \times \Delta A \quad (2)$$

However, in the early stages of droplet formation, surfactant partitioning favors the oil-water interface, although not exclusively. As the interface approaches saturation, the surfactant partitioning into the water phase becomes more and more significant. Once the surface is completely saturated, for a given quantity of monomer and water, any additional surfactant molecules remain in the aqueous phase. It is essential, once droplets are formed, that the concentration of surfactant in the aqueous phase remains below the CMC to avoid competitive micellar nucleation, which would have a negative impact on

the polymerisation process.<sup>[27]</sup>



**Figure 2.4 A - Droplets coalescing in the absence of surfactants due to attractive van der Waals forces. B – Droplets stabilised with surfactants repel each other due to the repulsive forces induced by surfactants.**

During emulsification, the adsorption of surfactants onto newly formed surfaces is a very complex process. Stabilisation of new surfaces is dependent on the rate of droplet-droplet collisions and the rate of surfactant adsorption which is a function of diffusion. The rate at which surfactants diffuse to the interface is determined by the flow regime, the size and type (ionic or non-ionic) of surfactant.<sup>[28]</sup>

Urbina-Villalbla *et al.* numerically predicted a rough estimation of adsorption times for an emulsion system at varying volume fractions (0.1 to 0.4).<sup>[28]</sup> They found that, for a given diffusion coefficient, as the surfactant concentration decreased from  $5 \times 10^{-4}$  to  $1 \times 10^{-4}$  M, the rate of surfactant adsorption decreased by  $\sim 24$  fold. Similarly, as the diffusion coefficient decreased from  $10^{-9}$  to  $10^{-12}$  m<sup>2</sup>/s for a constant surfactant concentration, the rate of surfactant adsorption varied from fractions to hundreds of seconds compared to a time frame of just under a minute for droplet collision, suggesting that the rate of surfactant adsorption is much slower than the rate of droplet coalescence.<sup>[28]</sup>

It should be strongly noted that determining the rate of surfactant adsorption comes with a number of stipulations that depend on the method of emulsification and the

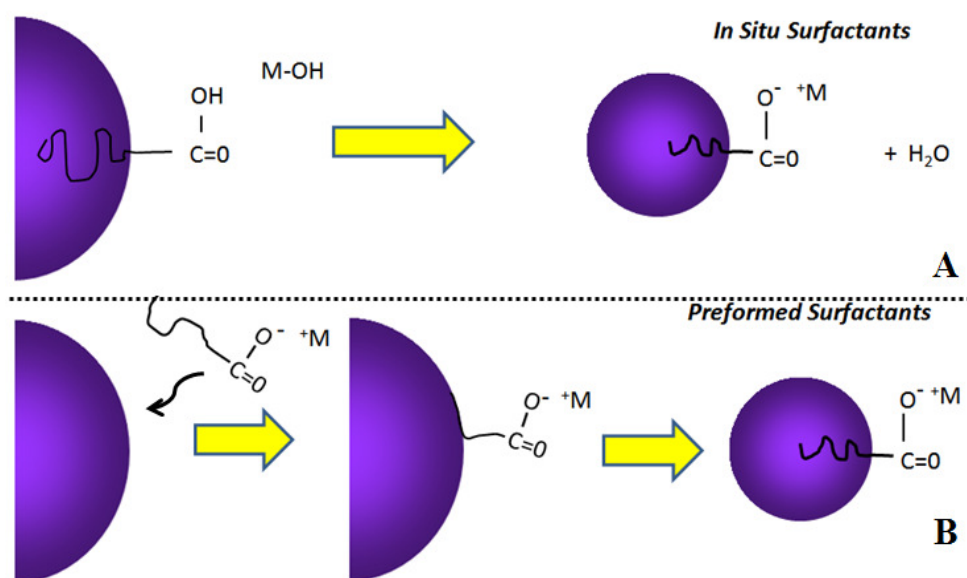


formulation used. Adsorption of ionic surfactants is kinetically limited; approaching surfactants experience repulsion from previously adsorbed molecules, progressively reducing the rate of diffusion. On the other hand, adsorption of non-ionic surfactants is solely diffusion limited.<sup>[28]</sup> The balance between collision and adsorption is also susceptible to changes in the surfactant concentration gradient between the bulk and the interface (if homogeneously dispersed), the flow regime, volume fraction of the dispersed phase, the number (and total surface area) of droplets, the dynamic droplet size distribution and the attractive forces between the droplets.<sup>[28]</sup>

As the total surface area increases, the rate of adsorption changes to accommodate adjustments at the interface.<sup>[28]</sup> Since the rate of adsorption is a local phenomenon (varying from fractions to hundreds of seconds), a certain amount of droplet coalescence is inevitable, especially during the early stages of emulsification when droplet rupture occurs and size distribution is broad (Figure 2.5B). After repetitive cycles of rupture followed by some stabilisation and coalescence, equilibrium between droplet breakage and coalescence is eventually established and the system reaches a minimum droplet size

It has been observed that the homogenisation process could be significantly improved by generating a surfactant *in situ* at the oil-water interface by neutralising an oil-soluble carboxylic acid with a water-soluble base (Chapter 6). *In situ* surfactant generation is a phenomenon first described in the second half of the nineteenth century by Johannes Gad; who observed the formation of a milky white emulsion when an oil (containing fatty acids) was brought together with an aqueous alkaline solution.<sup>[29]</sup> It was initially stated that spontaneous emulsification, via *in situ* surfactant generation, occurs in the absence of shear.<sup>[29]</sup> However, the emulsification process could be enhanced when

under the influence of high shear mixing devices as the *in situ* surfactants almost instantaneously stabilise newly formed surfaces, reducing the amount of coalescence and most importantly the time to reach a stable droplet size (Figure 2.5A); allowing for a more rapid reproducible homogenisation/polymerisation process compared to when using preformed conventional surfactants. The advantage, when using *in situ* generated surfactants, implies that the characteristic reaction time is less than the characteristic time for adsorption of surfactant on a surface.



**Figure 2.5 A** – Generating a surfactant *in situ* at the oil-water interface by neutralizing an oil-soluble carboxylic acid with a water-soluble base, reducing the amount of coalescence and enhancing droplet stability and emulsification time. **B** – When using preformed surfactants, which are predissolved in the aqueous medium, droplet stability is dependent on the rate of transport to, collision with and adsorption onto the oil-water interface; adsorption being the rate limiting step.

The physico - chemical aspects of carboxylate salts as emulsifiers have been extensively studied. Lawrence and separately McBain and Field, collectively examined the fundamentals of soap systems and their colloidal behavior.<sup>[30, 31, 32, 33, 34]</sup> It was reported that the dissolution of *in situ* generated salts in aqueous media requires elevated temperatures ( $\geq 40^\circ\text{C}$ ), which vary depending on the counterion used and the hydrocarbon chain length.<sup>[30, 35]</sup>

*In situ* surfactant generation has been successfully used in a number of other applications, for example crude oil recovery processes where water is displaced and the oil is separated.<sup>[36, 37]</sup> These processes rely on the inherent impurities in the oil to react with alkaline solutions causing them to spontaneously emulsify. Carboxylate salts have been employed as simple emulsifiers in emulsion coagulation studies, where the change in distribution and diameter of micron sized droplets was observed over time.<sup>[38]</sup> Niraula *et al.* found that, in addition to micelles, multilamellar vesicles existed in solution and helped stabilise emulsion droplets.<sup>[39]</sup>

Prokopov and Gritskova synthesised surfactant at the interface of a microsuspension process. The neutralisation reaction at the oil-water interface led to instantaneous phase separation and formation of micron-sized droplets in the aqueous phase.<sup>[40]</sup> They suggested that if the concentration of surfactant in the system was sufficient to only stabilise the droplets, then each droplet could ideally be polymerised as a self-contained batch reactor. Saygi-Arslan *et al.* prepared miniemulsion systems using preformed and *in situ* generated potassium laurate, as well as examined the effectiveness of the carboxylic acid as both a surfactant and costabiliser. However, they found that all of the systems phase separated (with or without costabiliser) within a short period of time.<sup>[41]</sup> A recent investigation from our group suggests that increasing the base to acid ratio by 50% (to a ratio of 3:2) allows us to successfully produce and polymerise miniemulsions (Chapter 6).

## 2.3 EMULSIFICATION DEVICES

Homogenisation devices are rarely investigated in theoretical miniemulsion studies but

play a fundamental role in droplet breakage/formation. At the laboratory scale, high shear is typically applied to a coarse emulsion to generate miniemulsion droplets comparable in size to emulsion polymerisation particles. Miniemulsions have proven to be an effective technique for developing innovative materials at the research stage, but have yet to be exploited at the industrial level due to scale up issues associated with homogenisation devices. In order to accelerate the commercialisation of miniemulsion technology, it is essential to develop a simple inexpensive means of generating droplets by implementing a device/process which is scalable, reproducible and, most importantly, economically and energy efficient.

### 2.3.1 *ULTRASONICATION*

Ultrasonication (Figure 2.6) is well-suited for laboratory scale experiments due to its simplicity and ease of operation.<sup>[42, 43]</sup> Ultrasonication is a fairly quick and simple technique but has significant drawbacks preventing commercialisation, such as large energy requirements per unit volume and tremendous heat loss.<sup>[44]</sup>

The mechanism of droplet breakage during emulsification using ultrasonication is attributed to intensified mechanical vibrations in the probe which create pressure waves in the emulsion that leads to the formation of bubbles.<sup>[45]</sup> Once the bubble reaches a critical size it will implode violently; a phenomenon commonly referred to as cavitation. At this point, a substantial amount of energy is released consequently generating high shear rates, temperatures, pressures and shockwaves.<sup>[45]</sup> For instance, it has been shown that the magnitude of shear rates needed to break liposomes segments down to 150-300 nm were on the order of  $10^6$  to  $10^7$  s<sup>-1</sup>.<sup>[45]</sup>

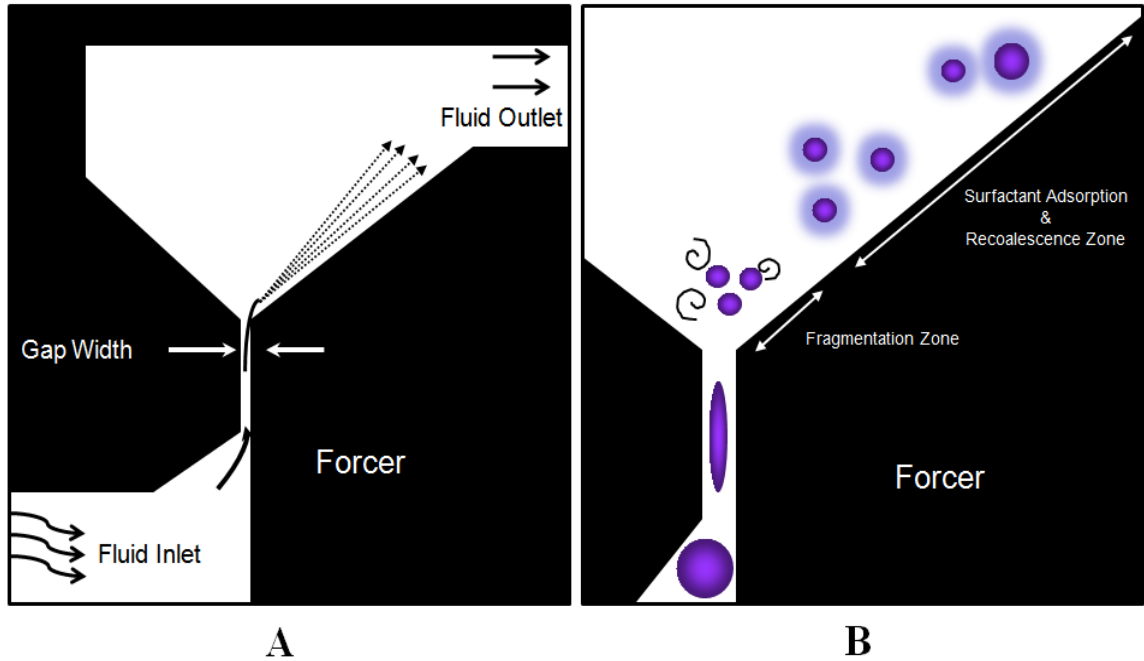
To prevent degradation or premature polymerisation of the newly formed droplets, the heat generated in the system needs to be quickly removed, typically using an ice-water bath. On this note, the suitability of ultrasonication for the generation of composite and hybrid miniemulsions becomes questionable, as the high shear inherent to the technique may rupture the droplets and release their contents.



**Figure 2.6 Branson VC 750 Vibra-Cell Ultrasonic Processor.**

### 2.3.2 HIGH PRESSURE HOMOGENISERS

Another device widely used in the dairy industry for the homogenisation of milk and milk products is the high pressure homogeniser (HPH). In HPH devices, a coarse emulsion is forced through a narrow gap(s), resulting in velocities of up to hundreds of m/s at high pressure ratings (5 - 500 MPa) and flow rates (10 – 10000 L/h).<sup>[46]</sup> Velocity is driven by a pressure gradient dependent on the gap size of the flow channel and the pump (Figure 2.7A).



**Figure 2.7 A - Cross section of a HPH outlining the flow path. B - Droplet elongation, fragmentation and recoalescence process.**

It has been computationally simulated that droplets travelling through the gap are initially elongated at the entrance of the gap but experience some degree of relaxation along the length of the gap.<sup>[47]</sup> Upon exiting the gap, the droplets are jetted out and fragment at a region near the outlet known as the active region (Figure 2.7B).<sup>[47]</sup> It has been predicted that cavitation, turbulent and laminar shear cause droplet breakage in the active region. However, a deeper understanding of the dominant mechanism(s) is difficult to ascertain with confidence due to the high flow velocities within the narrow gap, which makes accurate measurements and models which estimating the velocity flow fields very difficult.<sup>[48]</sup> For a more in-depth discussion, the reader is referred to work contributed by Hakansson *et al.*<sup>[47, 48]</sup> and references therein. As the jet travels further downstream, the newly generated droplets enter regions of lower shear, cease fragmenting and are said to have entered the recoalescence zone.<sup>[47]</sup> The recoalescence zone is much longer than the fragmentation zone. The rate of coalescence, as previously mentioned (see section 2.2.2),

is dependent on the surfactant concentration, the frequency of surfactant collision, the rate of surfactant adsorption and volume fraction of the oil phase.<sup>[47]</sup> Even in the presence of stabilised droplets, recoalescence is still very likely to occur after droplets have been stabilised because the pressure to aggregate in turbulent conditions is predicted to be approximately 100 times stronger than the stabilising force due to the presence of surfactants.<sup>[47]</sup> Correspondingly, the rate of droplet recoalescence increases with increasing operating pressure. The droplets are recycled through the high shear fragmentation and recoalescence zones several times until an equilibrium droplet size is reached. It has been shown that the time scale to reach a stable system can be significantly reduced if the pre-emulsified mixture were pre-homogenised, reducing the droplets to micron size range and hence reducing the exposure time within the HPH.<sup>[49]</sup>

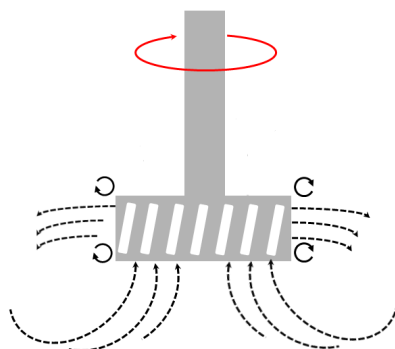
Because the use of HPH in the preparation of miniemulsions has been investigated elsewhere, more attention is directed towards rotor-stators and static mixers. They have not been extensively investigated at the laboratory scale for the generation of miniemulsions until recently and therefore they are the main focus of the present investigation.

### 2.3.3 ROTOR-STATORS

Rotor-stators (RS) are utilised in the food, cosmetic, chemical and biochemical industries as homogenisation units in the preparation of dispersion products such as latices, adhesives, pesticides, personal care items and dairy products.<sup>[50]</sup> RS are made up of rotating blades encased by a stationary stator with perforations. They are commonly referred to as high shear mixers because they generate an increased amount of shear ( $10^4$ -

$10^5 \text{ s}^{-1}$ ) compared to conventional stirred tanks ( $< 10^3 \text{ s}^{-1}$ ).<sup>[50]</sup> RS range from 1 to  $> 1000 \text{ L}$  in volume and operate from 50 to  $> 20\,000 \text{ RPM}$  depending on the process and the scale of operation.

Typically, mixing in the RS is initiated when energy imparted by the rotating blades pushes the coarse emulsion up the mixing head and forces the emulsion through narrow clearances between the rotor blades and stator. The mixture is pushed axially from the rotating blades towards the gaps in the stator, where it is subjected to a chaotic environment and a number of stresses such as turbulence, cavitation, shear and elongational, causing droplet breakage (Figure 2.8).<sup>[44]</sup>



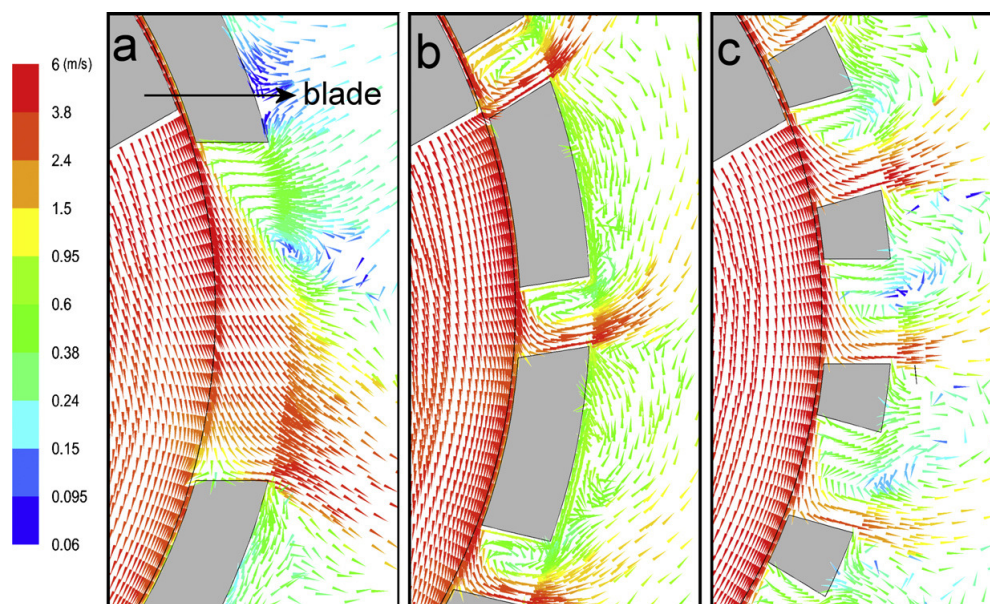
**Figure 2.8** Flow paths through a rotor-stator mixing head. Mixture is pushed up through the mixing head and ejected axially from the rotating blades, through the gaps of the stator and into a chaotic environment.

It has been proposed that a droplet located between the rotor and stator will travel along with the rotating blade until it reaches an opening in the stator. According to Megias-Alguacil *et al.* the originally ellipsoidal droplet is elongated to a tear drop shape and then either cut at the edge of the stator slit, generating two droplets or it is thinned out and eventually breaks generating a few smaller droplets.<sup>[51]</sup> Once droplets are formed, they are expelled through the open slots and sent back out into the bulk emulsion. It was believed that the average droplet diameters generated with RS are on the order of



microns<sup>[50]</sup>, however previous work has shown that it is possible to generate polymerisable miniemulsion droplets as small as  $\sim 200$  nm (Chapter 5).<sup>[44]</sup> Little work has been done in assessing and predicting performance of rotor-stators, and hence very little is understood as to the fundamentals of droplet formation in RS when considering droplets of micron size and smaller. Discussion concerning droplet formation possessing greater complexity on the scale of 100's of nanometers, typical of polymer latices, is even more rare.

Commercially available mixing heads vary in geometric design. They differ in the number and angle of rotating blades, the width of the mixing head and the design of perforations along the stator. Flow patterns and shearing intensity may differ slightly from one device to the next (Figure 2.9) but the basic principles of operation are the same.<sup>[52]</sup>



**Figure 2.9** Flow patterns of the jets emerging from different stators: (a) disintegrating head (circular slots) (b) slotted head (vertical slots) and (c) square hole head.<sup>[52]†</sup>

<sup>†</sup> Reprinted from Chemical Engineering Research and Design, 87, Utomo, A.; Baker, M.; Pacek, A. W. The Effect of Stator Geometry on the Flow Pattern and Energy Dissipation Rate in a Rotor – Stator, 533-542, 2009, with permission from Elsevier.

Determining appropriate RS dimensions and operating parameters is often based on trial and error and even then mixing profiles cannot be reported with absolute certainty, as the fluid flow through the mixing head is a complex and dynamic process. Understanding local velocity and shear gradients becomes increasingly difficult as they quickly vary from one point to the next. It has been observed through simulations that the most intense flow regimes and shear rates are located within the vicinity of the mixing head and slowly decay in intensity as they move into the bulk area (Figure 2.9).<sup>[52]</sup> Basic information is usually gathered through advanced computational fluid dynamics (CFD). A number of studies have shown that the mass flow rates through the slots fluctuate depending on the location of the blades and whether the flow is being impeded.<sup>[50,53]</sup> Since experimental validation of the above observations is difficult, parameters such as the shear rate are estimated to be a function of the tip speed ( $V_{tip}$ , m/s) and the width of the gap ( $\delta$ , m) between the rotor and stator:

$$\dot{\gamma} = V_{tip} / \delta \quad (3)$$

Where,  $V_{tip} = \pi DN$ , where  $D$  is the diameter of the stator head (m), and  $N$  is the revolutions per minute.

Emulsification with the rotor stator requires constant recirculation in the high shearing zones and the efficiency of recirculation is a fundamental problem that has received plenty of attention. Because mixing heads are typically small in diameter with respect to the vessel diameter, circulation through the mixing head and tank is usually very poor, creating stagnant zones. Therefore, it has always been speculated that a significant amount of energy needs to be imparted in order to re-circulate fluids in the distant parts of the tank.<sup>[50]</sup> However, this mixing approach comes at a cost of increased

shear. CFD simulations have shown that varying the location of the mixing head within the vessel varies the mixing profile. Mixing heads located centrally in a round vessel tend to form cavities within and around the mixing head region, impeding mixing; cavity size depends on the rotations per minute and fluid properties.<sup>[54, 55]</sup> For this reason, the heads can be placed off-centre and often, on larger scales, a second impellor is installed to induce additional circulation.<sup>[50]</sup> Due to the physical constraints within our set-up, relocating the mixing head off centre was not an option. Upon mixing, a vortex would form, inhibiting the two phases from mixing. Therefore, to eliminate the vortex, baffles were inserted to break the flow and induce additional circulation near the mixing head.

Even with these improvements, it is very difficult to control the time scale to which a droplet resides in the high shearing zone. Irregular circulation of the fluid through the mixing head typically results in longer emulsification time scales (~ hours) and wider droplet size distributions (Chapter 3). However, it has been shown that the time to reach a stable system in the RS can be improved if the pre-emulsified mixture were pre-homogenised, reducing droplets down to microns in size.<sup>[43]</sup> The breadth of the distribution can be reduced by including a recirculation loop around a batch RS unit, simulating a semi-continuous process.<sup>[56]</sup> In the case of continuous processes, the mixing head is encased in a much smaller volume with inlet and outlet ports. However the use of continuous processes in the production and preservation of composite droplet systems is unreliable as small volumes are exposed to tremendously high shear rates, compromising the quality of the droplet. Additionally, it is important to maintain an appropriate flow rate so that the mean residence time matches the required mixing time for the process.

Continuous emulsification processes demonstrate greater control and accuracy for

generating reproducible droplet sizes/distributions compared to RS batch systems (Chapter 3 & 7). Given the additional economic and operational advantages of continuous over batch processes, there is considerable motivation towards investigating continuous emulsification devices. It has been found that static (or motionless) mixers (SM), installed in a recirculation loop in line with a pump, generated droplets comparable in size to those generated with US or RS.<sup>[44]</sup> Additionally, the SM generated narrower droplet size distributions and imposed less shear in comparison to the US and RS (Chapter 5).

#### 2.3.4 *STATIC MIXERS*

Homogenisation through the use of in line static mixers (SM) is another commercially-proven emulsification technique. It has received much more attention in the last two decades in dispersion applications as replacements to mechanical agitators, generating droplets on the order of 10  $\mu\text{m}$  in diameter. Static mixers are in fact motionless elements inserted in tubes or pipes. They induce flow in the radial direction creating plug flow conditions with very little back mixing. The elements are very compact and they range in size from a few millimeters up to meters in diameter depending on the application. The only power required is that supplied by a pump (to offset the pressure drop across the elements); therefore cost and maintenance of the unit are inexpensive which is industrially favorable. A number of static mixers are commercially available, some of which are shown in Figure 2.10. They mostly differ in geometry, but operate in a relatively similar fashion. As multiphase streams pass through the elements, they are split into layers, divide and recombine along the length of the mixing elements. Similarly,

irrespective of the element used, the pressure drop along the length of the bed increases with flow rate; the higher the pressure drop, the better the emulsification (Chapter 7).

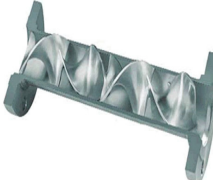
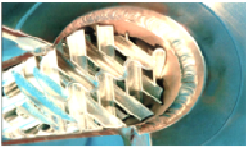



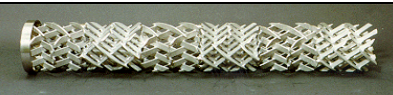
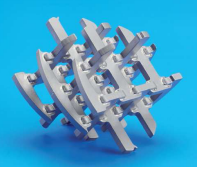

<i>Chemineer</i>	  Kenics      KMX
<i>Charles Ross &amp; Son</i>	 LPD
<i>Lightnin</i>	 Inliner
<i>Komax</i>	
<i>Sulzer</i>	   SMX      SMX Plus      SMV

Figure 2.10 Commercially available static mixers, differing in design and material.

Zalc *et al.* ran numerical simulations to assess the mixing performance of SMX (Sulzer ChemTech) mixers and compared them to experimental results.<sup>[57]</sup> Each SMX element consists of X-shaped cross bars aligned at  $45^\circ$  to the axis of the pipe, with each additional element angled at  $90^\circ$  relative to the previous element. They examined the

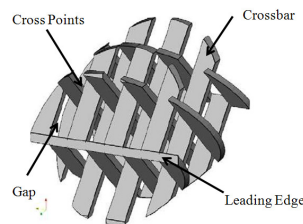
evolution of the mixing patterns of flow within the laminar regime.<sup>[57]</sup> Computational simulations identifying variations in pressure, velocity and shear rates along the length of the element for flow in the laminar regime have also been reported.<sup>[58]</sup> Rauline *et al.* examined tracer distributions and compared numerical to experimental mixing efficiencies of SMX and Kenics (helical elements by Chemineer) mixers.<sup>[59]</sup> Separately, Heniche *et al.* compared SMX to KMX (curved crossbars by Chemineer) mixers.<sup>[60]</sup> They examined the effects of parameters such as pressure drops, intensity of segregation, stretching, shear rates and residence times for a number of elements. It was found that SMX elements were superior in mixing performance and generated droplets 2-3 times faster than Kenics mixers.<sup>[59]</sup> However, KMX elements create a larger amount of secondary flow compared to SMX elements because of their curved blades; imposing a higher shear rate and inducing additional mixing at a cost of higher pressure drop.<sup>[60]</sup> We have chosen to examine SMX mixers manufactured by Sulzer Chemtech based on these simulations presented as they show that SMX mixing elements are efficient, create reasonably low shear rates and have the lowest segregation intensity.<sup>[61]</sup> Similar to the case of RS, understanding local velocity and shear gradients becomes increasingly difficult as they quickly fluctuate from one point to the next. It has been observed through simulations that the most intense flow regimes and shear rates are located at the intersection of two crossbars and along their perimeters.<sup>[57]</sup> Experimental validation of flow and shear rates is a difficult and intrusive process, therefore parameters such as the shear rate are estimated to be a function of the overall fluid velocity and tube diameter:

$$\dot{\gamma} = K_s \frac{V}{D_s} \quad (4)$$

Where,  $K_s$  is determined using the Metzner and Otto approach as explained by Arzate *et*

*al.*,<sup>[62]</sup>  $V$  is the fluid velocity (m/s) and  $D_s$  is the tube diameter (m). A closer examination of shear rate using static mixers will be addressed in Chapter 5.

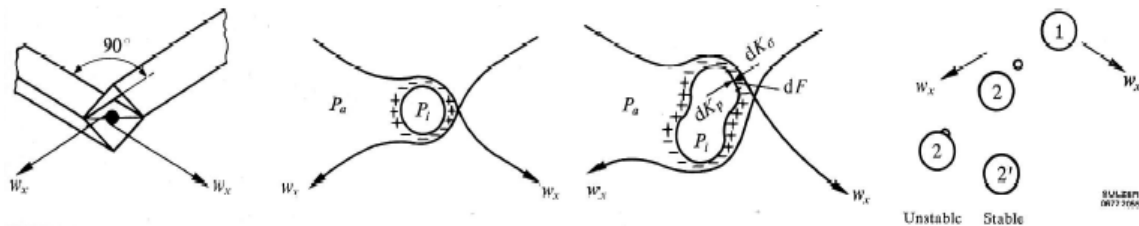
Liu *et al.* investigated various element configurations and observed mixing performances. They concluded that an element with 10 cross bars across the axis performed the best.<sup>[63]</sup> However, Singh *et al.* used mapping methods to predict that 6 cross bars initiated a more uniform distribution of striations compared to 4 cross bars which caused under-stretching of the striations, while anything more than 6 crossbars over-stretched the striations, altering the uniformity across the axis.<sup>[64]</sup> Additionally, they varied the number of parallel plates and the angle between the blades and found that reducing the number of parallel crossbars or increasing the angle between two bars reduced the pressure drop across the bed and subsequently the mixing efficiency.<sup>[64]</sup> Models of droplet breakage were also developed in order to predict droplet sizes in different flow regimes. Liu *et al.* developed a droplet breakage model simulating the breakage evolution along the length of an element in the laminar regime and validated their findings experimentally. They identified three locations in the mixing element where the droplets could break: the cross points (intersection of the cross bars), the leading edge (the first cross point), and the gap between the crossbars (Figure 2.11).<sup>[65]</sup>



**Figure 2.11 Breaking positions in and SMX mixing element.**

The observations made by Liu *et al.* concluded that droplets on the order of

millimeters were more likely to break at the leading edge and at the cross point and less likely to break in the gaps between the crossbars as it is highly probable that droplets will flow around the cross bars then collide and break on impact.<sup>[65]</sup> As the droplet approaches the leading edge with sufficient amount of force, the droplet will fold with the neck located at the leading edge and the two bulbous ends entering the gap between the crossbars, assuming the flow is injected at the centerline (injection off the centerline causes channeling and mixing begins downstream). As the two bulbous ends move forward, the neck begins to stretch into a long thread. The thread will eventually thin out and break creating two larger sister droplets and smaller satellite droplets. The mechanism of droplet breakage at the cross point was found to be the same as that of the leading edge.<sup>[65]</sup> Liu *et al.* concluded that droplet breakage occurring in an SMX mixing element is a two step process. The droplets are stretched by extensional flow and then folded around a crossbar or a leading edge. Droplet breakage will subside when the cohesive forces are stronger than the disruptive forces. A similar description was given by Streiff *et al.* of Sulzer Chemtech.<sup>[66]</sup> As the droplet approaches the cross point, the velocity fields are shifted 90° causing velocity and pressure fluctuations which ultimately induce breakage (Figure 2.12).



**Figure 2.12** Droplet deformation in an SMX mixing element as described by Streiff *et al.*<sup>[66]</sup>

Upon droplet breakage, droplets of similar surface areas are formed along with a small population of satellite droplets. Streiff *et al.* stated that satellite droplets can either



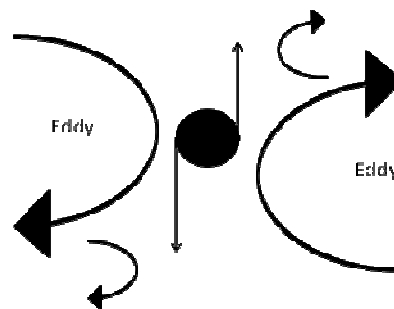
recombine with larger droplets due to the reunion of separate streams or can remain stable if  $D_D < D_{\max}$ .<sup>[66]</sup> Furthermore, large droplets will continue to break so long as  $D_D > D_{\max}$ , where:

$$D_{\max} \propto K We^n Re^m \quad (5)$$

Where,  $K$  is a constant, the Weber ( $We$ ) number is the ratio of destructive to cohesive forces and Reynolds ( $Re$ ) number is the ratio of inertial to viscous forces. A number of empirical correlations similar to that of Equation 2 have been developed, for a number of mixing elements, where typical values of  $n$  range from -0.2 to -0.6 and  $m$  from -0.02 to 0.2.<sup>[26, 67, 68]</sup> However, It should be noted that these correlations are not entirely complete as some do not take into account the physico-chemical properties of the two phases such as: the concentration of the dispersed phase, the viscosity ratio of the dispersed to aqueous phase, porosity of the elements and more specifically local velocity gradients, which as previously stated, are very difficult to estimate without advanced computational methods. Additionally, the majority of the correlations developed predict droplet sizes of micron size and larger, thus are not entirely valid for droplets in our size range. The situation is somewhat more complicated as there is no unique way to describe the way a droplet breaks as it travels through a mixing element because each commercial mixing element is different.

The mixing process in SMX mixers in a turbulent regime can be considered a hybrid of two mechanisms. Initially, upon entering the mixing elements, the multiphase streams are split into layers and the layers are divided into striations which are reoriented, redistributed and recombined and subjected to more separation.<sup>[58]</sup> However, as stated by

Hinze, this mechanism fails to describe the disintegration of a droplet in a chaotic environment.<sup>[69]</sup> Kolmogorov's theory (as described by Walstra<sup>[26]</sup>) characterises turbulent flow as chaotic random motion with pressure and velocity fluctuations and eddies of assorted sizes; the largest eddies containing most of the kinetic energy in the system.<sup>[26]</sup> The energy is cascaded down through smaller and smaller eddies until it reaches the Kolmogorov length scale; the smallest eddy. Only droplets larger in size than any eddy length scale are capable of being deformed and broken up. Droplets smaller than the Kolmogorov length scales are not affected and are transported throughout the system by eddy motions (Figure 2.13).<sup>[26]</sup>



**Figure 2.13 Droplet deformation in turbulent flow.**

Generating droplets with SMX static mixers is not difficult. The challenge lies in making the droplets small enough, within the miniemulsion size range and obtaining a narrow droplet size distribution. Therefore, is it reasonable to assume that the breakage mechanisms proposed by Liu *et al.*<sup>[65]</sup> and Streiff *et al.*<sup>[66]</sup> in combination with the Kolmogorov's theory<sup>[26]</sup> are applicable to droplets on the order of a 100 nm, or would they simply flow around the leading edges and cross points?

Ouzineb *et al.* showed that they were able to create ~300 nm styrene and butyl methacrylate droplets separately within 400 minutes using two polyacetal (PAC, manufactured by Bioblock) static mixers (similar in form to Kenics mixers) in series.<sup>[44]</sup>

Within the first 100 minutes through the static mixers the droplets decreased  $\sim 400$  nm in size and another  $\sim 100$  nm over the next 300 minutes.<sup>[44]</sup> The asymptotic drop in droplet size suggests that larger droplets are more likely to encounter breaking points along the length of the mixing elements than smaller droplets. Therefore, when reaching a certain droplet size (400 nm in the case of Ouzineb *et al.*) it becomes harder and requires more time to break the droplets further as they are less likely to come across a breaking point along the length of the elements due to their smaller size. It was later found that the PAC mixers were less efficient than the SMX mixers, generating smaller droplets under similar operating conditions.<sup>[70]</sup>

The majority of the previously cited literature, report sizes of micron range or larger. Within the last 5 years, it was found that the minimum attainable droplet size decreased from  $\sim 400$  nm to as small as  $\sim 100$  nm, by making slight improvements to the process set up and formulations (Chapters 4, 5 & 7). In the following chapters we discuss how varying surfactant type, surfactant concentration and the pump flow rate, will affect the droplet size and distribution.

## 2.4 CONTINUOUS POLYMERISATION

Reactor selection is important for miniemulsion processes, and while many options are available, the use of continuous stirred tank reactors (CSTR) is not recommended as they exhibit wide residence time distributions, which would lead to the inclusion of unpolymerised droplets in the exit stream. However, they are advantageous for copolymerisation systems where control on the copolymer composition is essential. For this reason, either (semi-)batch reactors or continuous tubular reactors seem to be better

choices since all of the particles in the reactor will have the same residence time; exploiting the benefits of miniemulsions by nucleating a large fraction of the droplets within a small time frame.

The ability to continuously generate miniemulsions that could be immediately polymerised has a number of advantages, such as eliminating the need to store and transport intermediate emulsions. Additionally, operating a continuous process improves product consistency and increases product throughput. From an economical standpoint, linear tubular reactors are simple to design and construct and can operate for an extended period of time with very little maintenance. Tubular reactors also offer many advantages such as: high heat removal due to a large surface area to volume ratio, conversion-time profiles similar to that in a batch process and extremely rapid grade changes with respect to continuous stirred tank reactors. The main drawbacks in operating in a continuous tubular reactor are potential fouling and plugging problems. These can be overcome with use of special anti-fouling treatments, or, as is the case of this work, through the use of polymer materials for the tube.

Previous studies have demonstrated successful polymerisation of miniemulsions in a continuous process.<sup>[71, 72, 73, 74, 75]</sup> Samer *et al.* prepared miniemulsions in two separate stages.<sup>[73]</sup> They emulsified in a batch unit using ultrasonication or the rotor-stator. Their emulsification unit contained a recycle loop which re-circulated the miniemulsion system until a desired size range was reached, at which point it was transferred to a CSTR for polymerisation. Ouzineb *et al.* were one of the first to demonstrate successful polymerisation of a high solids content (60%) methyl methacrylate miniemulsion system and the preparation of methyl methacrylate and butyl acrylate copolymer, in a tubular

reactor.<sup>[74]</sup> Their process consisted of two separate stages where they emulsified in a batch unit and then transferred their system to be polymerised in a tubular reactor. They were able to control both the size and the number of polymer particles. Their results demonstrated that problems such as insufficient mixing, separation and clogging that are typically associated with continuous emulsion polymerisation could be eliminated when using miniemulsion technology. Rusum *et al.* developed a continuous process whereby an ultrasonic dismembrator (with a recycle loop) was placed in line with a series of tubular reactors.<sup>[75]</sup> However, as previously mentioned, the large energy consumption per unit volume limits the use of an ultrasonicator to bench scale operations. Nonetheless, based on these results, we believe that there is tremendous potential for polymerising high solids content miniemulsions in a continuous manner if a low energy alternative for emulsification can be found. As such, investigating the combination of an energy efficient, scalable emulsification device in line with a linear tubular reactor will be addressed in Chapter 7.

## 2.5 LITERATURE CITED

1. Thickett, S. C.; Gilbert, R. G. Emulsion Polymerisation: State of the Art in Kinetics and Mechanisms. *Polymer*. **2007**, *48*, 6965-6991.
2. Chern, C. S. Emulsion Polymerisation Mechanisms and Kinetics. *Prog. Polym. Sci.* **2006**, *31*, 443-486.
3. De la Cal, J.C.; Leiza, J.R.; Asua, J.M.; Buttè, A.; Storti, G.; Morbidelli, M. In Handbook of Polymer Reaction Engineering. Ed: Meyer, T.; Keurentjes, J. **2005**, Wiley-VCH: Weinheim, pg. 249-322.
4. Gilbert, R. G. Emulsion Polymerisation: A Mechanistic Approach. **1996**. Academic Press: London.
5. Harkins, W. D. Theory of the Mechanism of Emulsion Polymerisation. *J. Am. Chem. Soc.* **1947**, *69*, 1428-1444.
6. Priest, W. J. Particle Growth in the Aqueous Polymerisation of Vinyl Acetate. *J. Phys. Chem.* **1952**, *56*, 1077-1082.
7. Smith, W. V.; Ewart, R. H. Kinetics of Emulsion Polymerisation. *J. Chem. Phys.* **1948**, *16*, 592-599.
8. Fitch, R. M.; Tsai, C. H. Homogeneous Nucleation of Polymer Colloids. Role of Soluble Oligomeric Radicals. *Polym. Prepr. (Am. Chem. Soc., Div. Polym. Chem.)*. **1970**, *11*, 811-816.
9. Ugelstad, J.; Hansen, F. K. Kinetics and Mechanism of Emulsion Polymerisation. *Rubber Chem. Technol.* **1976**, *49*, 536-609.
10. Autran, C.; De la Cal, J. C.; Asua, J. M. (Mini)emulsion Polymerisation Kinetics Using Oil - Soluble Initiators. *Macromolecules*. **2007**, *40*, 6233-6238.
11. Luo, Y.; Schork, F. J. Emulsion and Miniemulsion Polymerisations with an Oil-Soluble Initiator in the Presence and Absence of an Aqueous-Phase Radical Scavenger. *J. Polym. Sci., Part A: Polym. Chem.* **2002**, *40*, 3200-3211.
12. Reimers, J. L.; Schork, F. J. Lauroyl Peroxide as a Cosurfactant in Miniemulsion Polymerisation. *Ind. Eng. Chem. Res.* **1997**, *36*, 1085-1087.
13. Alduncin, J. A.; Forcada, J.; Asua, J. M. Miniemulsion Polymerisation Using Oil-Soluble Initiators. *Macromolecules*. **1994**, *27*, 2256-2261.
14. Higuchi, W.I.; Misra, J. Physical Degradation of Emulsions via the Molecular Diffusion Route and the Possible Prevention Thereof. *J. Pharm. Sci.* **1962**, *51*, 459-466.

15. Ugelstad, J.; El-Aasser, M. S.; Vanderhoff, J. W. Emulsion Polymerisation. Initiation of Polymerisation in Monomer Droplets. *J. Polym. Sci., Part C: Polym. Lett.* **1973**, *11*, 503-513.
16. Taylor, P. Ostwald Ripening in Emulsions. *Adv. Colloid Interface Sci.* **1998**, *75*, 107-163.
17. Schork, F. J.; Luo, Y.; Smulders, W.; Russum, J. P.; Butte, A.; Fontenot, K. Miniemulsion Polymerisation. *Adv. Polym. Sci.* **2005**, *175*, 129-255.
18. Asua, J. M. Miniemulsion Polymerisation. *Prog. Polym. Sci.* **2002**, *27*, 1283-1346.
19. Tang, P. L.; Sudol, E. D.; Silebi, C. A.; El-Aasser, M. S. Miniemulsion Polymerisation – A Comparative Study of Preparative Variables. *J. Appl. Polym. Sci.* **1991**, *43*, 1059-1066.
20. Miller, C. M.; Sudol, E. D.; Silebi, C. A.; El-Aasser, M. S. Polymerisation of Miniemulsions Prepared from Polystyrene in Styrene Solutions. 1. Benchmarks and Limits. *Macromolecules.* **1995**, *28*, 2754-2764.
21. Reimers, J. L.; Schork, F. J. Predominant Droplet Nucleation in Emulsion Polymerisation. *J. Appl. Polym. Sci.* **1996**, *60*, 251-262.
22. Wang, S.; Schork, F. J. Miniemulsion Polymerisation of Vinyl Acetate with Nonionic Surfactant. *J. Appl. Polym. Sci.* **1994**, *54*, 2157-2164.
23. Chern, C. S.; Chen, T. J. Effect of Ostwald Ripening on Styrene Miniemulsion Stabilised by Reactive Cosurfactants. *Colloids Surf., A.* **1998**, *138*, 65-74.
24. Chern, C. S.; Chen, T. J. Miniemulsion Polymerisation of Styrene Stabilised by Nonionic Surfactant and Reactive Cosurfactant. *Colloid. Polym. Sci.* **1997**, *275*, 1060-1067.
25. Chern, C. S.; Chen, T. J. Miniemulsion Polymerisation of Styrene Using Alkyl Methacrylates as Reactive Cosurfactants. *Colloid. Polym. Sci.* **1997**, *275*, 546-554.
26. Walstra, P. Principles of Emulsion Formation. *Chem. Eng. Sci.* **1993**, *48*, 333-349.
27. Landfester, K.; Bechthold, N.; Tiarks, F.; Antonietti, M. Miniemulsion Polymerisation with Cationic and Nonionic Surfactants: A Very Efficient Use of Surfactants for Heterophase Polymerisation. *Macromolecules.* **1999**, *32*, 2679-2683.
28. Urbina-Villalba, G. An Algorithm for Emulsion Stability Simulations: Account of Flocculation, Coalescence, Surfactant Adsorption and the Process of Ostwald Ripening. *Int. J. Mol. Sci.* **2009**, *10*, 761-804.

29. McBain, J. W.; Woo, T. Spontaneous Emulsification and Reactions Overshooting Equilibrium. *Proc. R. Soc. London, Ser. A.* **1937**, *163*, 182-188.
30. McBain, J. W.; Sierichs, W. C. The Solubility of Sodium and Potassium Soaps and the Phase Diagrams of Aqueous Potassium Soaps. *J. Am. Oil Chem. Soc.* **1948**, *25*, 221-225.
31. Lawrence, A. S. C. Soap Films and Colloidal Behavior. *J. Phys. Chem.* **1930**, *34*, 263-272.
32. McBain, J. W.; Field, M. C. The Equilibria Underlying the Soap-Boiling Processes. The System Potassium Laurate-Potassium Chloride-Water. *J. Phys. Chem.* **1926**, *30*, 1545-1563.
33. McBain, J. W.; Hoffman, O. A. Lamellar and Other Micelles, and Solubilisation by Soaps and Detergents. *J. Phys. Colloid Chem.* **1949**, *53*, 39-55.
34. Lawrence, A. S. C. Soap Micelles. *Trans. Faraday Soc.* **1935**, *31*, 189-200.
35. Ogino, K.; Ichikawa, Y. The Solubilities and Krafft Points of Fatty Acid Soaps of Odd Carbon Numbers. *Bull. Chem. Soc. Jpn.* **1976**, *49*, 2683-2686.
36. Chatterjee, J.; Wasan, D. T. A Kinetic Model for Dynamic Interfacial Tension Variation in an Acidic Oil / Alkali / Surfactant system. *Chem. Eng. Sci.* **1998**, *53*, 2711-2725.
37. Liu, Q.; Dong, M.; Yue, X.; Hou, J. Synergy of Alkali and Surfactant in Emulsification of Heavy Oil in Brine. *Colloids Surf., A.* **2006**, *273*, 219-228.
38. Lawrence, A. S. C.; Mills, O. S. Kinetics of the Coagulation of Emulsions. *Discuss. Faraday Soc.* **1954**, *18*, 98-104.
39. Niraula, B. B.; Seng, T. N.; Misran, M. Vesicles in Fatty Acid Salt-Fatty Acid Stabilised O/W Emulsion - Emulsion Structure and Rheology. *Colloids Surf., A.* **2004**, *236*, 7-22.
40. Prokopov, N. I.; Gritskova, I. A. Characteristic Features of Heterophase Polymerisation of Styrene with Simultaneous Formation of Surfactants at the Interface. *Russ. Chem. Rev.* **2001**, *70*, 791-800.
41. Saygi-Arslan, O.; Sudol, E. D.; Daniels, E. S.; El-Aasser, M.S.; Klein, A. *In Situ* Surfactant Generation as a Means of Miniemulsification? *J. Appl. Polym. Sci.* **2009**, *111*, 735-745.
42. Landfester, K.; Eisenblaetter, J.; Rothe, R. Preparation of Polymerisable Miniemulsions by Ultrasonication. *J. Coat. Technol. Res.* **2004**, *1*, 65-68.



43. Lopez, A.; Chemtob, A.; Milton, J. L.; Manea, M.; Paulis, M.; Barandiaran, M. J.; Theisinger, S.; Landfester, K.; Hergeth, W. D.; Udagama, R.; McKenna, T.; Simal, F.; Asua, J. M. Miniemulsification of Monomer - Resin Hybrid Systems. *Ind. Eng. Chem. Res.* **2008**, *47*, 6289-6297.
44. Ouzineb, K.; Lord, C.; Lesauze, N.; Graillat, C.; Tanguy, P. A.; McKenna, T. Homogenisation Devices for the Production of Miniemulsions. *Chem. Eng. Sci.* **2006**, *61*, 2994-3000.
45. Richardson, E.S.; Pitt, W.G.; Woodbury, D.J. The Role of Cavitation in Liposome Formation. *Biophys J.* **2007**, *93*, 4100-4107.
46. Innings, F.; Traegaardh, C. Analysis of the Flow Field in a High - Pressure Homogeniser. *Exp. Therm Fluid Sci.* **2007**, *32*, 345-354.
47. Hakansson, A.; Traegaardh, C.; Bergenstaahl, B. Studying the Effects of Adsorption, Recoalescence and Fragmentation in a High Pressure Homogeniser Using A Dynamic Simulation Model. *Food Hydrocolloids.* **2009**, *23*, 1177-1183.
48. Hakansson, A.; Traegardh, C.; Bergenstahl, B. Dynamic Simulation of Emulsion Formation in a High Pressure Homogeniser. *Chem. Eng. Sci.* **2009**, *64*, 2915-2925.
49. Manea, M.; Chemtob, A.; Paulis, M.; De la Cal, J. C.; Barandiaran, M. J.; Asua, J. M. Miniemulsification in High - Pressure Homogenisers. *AIChE J.* **2008**, *54*, 289-297.
50. Calabrese, V.; Atiemo-Obeng, V. A. In Handbook of Industrial Mixing: *Science and Practice*; Ed: Paul, E. L.; Atiemo-Obeng, V. A.; Kresta, S. M., **2004**, Wiley & Sons: New Jersey, pg. 479-506.
51. Megias-Alguacil, D.; Windhab, E. J. Experimental Study of Drop Deformation and Breakup in a Model Multitoothed Rotor - Stator. *J. Fluids Eng.* **2006**, *128*, 1289-1294.
52. Utomo, A.; Baker, M.; Pacek, A. W. The Effect of Stator Geometry on the Flow Pattern and Energy Dissipation Rate in a Rotor - Stator Mixer. *Chem. Eng. Res. Des.* **2009**, *87*, 533-542.
53. Utomo, A. T.; Baker, M.; Pacek, A. W. Flow Pattern, Periodicity and Energy Dissipation in a Batch Rotor - Stator Mixer. *Chem. Eng. Res. Des.* **2009**, *86*, 1397-1409.
54. Doucet, L.; Ascanio, G.; Tanguy, P. A. Hydrodynamics Characterisation of Rotor - Stator Mixer With Viscous Fluids. *Chem. Eng. Res. Des.* **2005**, *83*, 1186-1195.
55. Barailler, F.; Heniche, M.; Tanguy, P. A. CFD Analysis of a Rotor - Stator Mixer with Viscous Fluids. *Chem. Eng. Sci.* **2006**, *61*, 2888-2894.
56. Maa, Y. F.; Hsu, C. Liquid - Liquid Emulsification by Rotor / Stator Homogenisation.

*J. Controlled Release.* **1996**, 38, 219-228.

57. Zalc, J.M.; Szalai, E. S.; Muzzio, F.J. Characterisation of Flow and Mixing in an SMX Static Mixer. *AIChE J.* **2002**, 48, 427-436.

58. Fradette, L.; Li, H.Z.; Choplin, L. 3D Finite Element Simulation of Fluid Flow Through a SMX Static Mixer. *Comput. Chem. Eng.* **1998**, 22, S759-S761.

59. Rauline, D. Le Blévec, J. M.; Bousquet, J.; Tanguy, P. A. A Comparative Assessment of the Performance of the Kenics and SMX Static Mixers. *Trans IChemE.* **2000**, 78, 389-396.

60. Heniche, M.; Tanguy, P. A.; Reeder, M.F.; Fasano, J.B. Numerical Investigation of Blade Shape in Static Mixing. *AIChE J.* **2005**, 51, 44-58.

61. Rauline, D.; Tanguy, P. A.; Le Blévec, J. M.; Bousquet, J. Numerical investigation of the performance of several static mixers. *Can. J. Chem. Eng.* **1998**, 76, 527-535.

62. Arzate, A.; Réglat, O.; Tanguy, P.A. Determination of In-Line Process Viscosity Using Static Mixers. *Flow Meas. Instrum.* **2004**, 15, 77-85.

63. Liu, S.; Hrymak, A. N.; Wood, P. E. Design Modifications to SMX Static Mixer for Improving Mixing. *AIChE J.* **2006**, 52, 150-157.

64. Singh, M. K.; Anderson, P. D.; Meijer, H. E. H. Understanding and Optimizing the SMX Static Mixer. *Macromol. Rapid Commun.* **2009**, 30, 362-376.

65. Liu, S.; Hrymak, A. N.; Wood, P. E. Drop Breakup in an SMX Static Mixer in Laminar Flow. *Can. J. Chem. Eng.* **2005**, 83, 793-807.

66. Streiff, F. In-Line Dispersion and Mass Transfer Using Static Mixing Equipment. *Compressors and Process Engineering.* **1977**, 3, 108-113.

67. Legrand, J.; Morancais, P.; Carnelle, G. Liquid - Liquid Dispersion in an SMX - Sulzer Static Mixer. *Chem. Eng. Res. Des.* **2001**, 79, 949-956.

68. Das, P. K.; Legrand, J.; Morancais, P.; Carnelle, G. Drop Breakage Model in Static Mixers at Low and Intermediate Reynolds Number. *Chem. Eng. Sci.* **2005**, 60, 231-238.

69. Hinze, J. O. Fundamentals of the Hydrodynamic Mechanism of Splitting in Dispersion Processes. *AIChE J.* **1955**, 1, 289-295.

70. Farzi, G. Ph.D. Thesis, Université Claude Bernard Lyon 1, **2008**.

71. Poehlein, G. W.; Schork, J. Continuous Emulsion and Miniemulsion Polymerisation Reaction Systems. *Trends in Polymer Science.* **1993**, 1, 298-302.

72. Schork, F. J.; Guo, J. Continuous Miniemulsion Polymerisation. *Macromol. React. Eng.* **2008**, 2, 287-303.
73. Samer, C. J.; Schork, F. J. The Role of High Shear in Continuous Miniemulsion Polymerisation. *Ind. Eng. Chem. Res.* **1996**, 4, 173-176.
74. Ouzineb, K.; Graillat, C.; McKenna, T. F. Continuous Tubular Reactor as a Seed Reactor in Miniemulsion Polymerisation. *DECHEMA Monographien.* **2001**, 137, 293-301.
75. Russum, J. P.; Jones, C. W.; Schork, F. J. Continuous Reversible Addition - Fragmentation Chain Transfer Polymerisation in Miniemulsion Utilizing a Multi - Tube Reaction System. *Macromol. Rapid Commun.* **2004**, 25, 1064-1068.

# 3

## ***POLYMERISABLE MINIEMULSIONS USING ROTOR-STATOR HOMOGENISERS***

---

The use of a rotor-stator mixer as a homogenisation device to make miniemulsion droplets with industrially pertinent solids content was investigated. Methyl methacrylate/butyl acrylate (50:50 w/w ratio) miniemulsions with droplet diameters from 2  $\mu\text{m}$  to 300 nm and polydispersity indices from 1.2 to 3.6 were prepared. Only the miniemulsions of three different mean droplet diameters (300, 400, 600 nm) were polymerised and the evolution of particle size was observed. When 300 nm droplets were polymerised they yielded particles of similar diameter to the original droplets, whereas particle coalescence of the growing particles with a loss of control over the particle size distribution was observed for the 400 and 600 nm droplets.

The influence of costabiliser, agitation speed, solids content, colloidal protectors and surface coverage on the evolution of the droplet size and distribution, as well as on the evolution of the average particle size and distribution were examined. It was observed that changing the above parameters had no impact on the evolution of the particle size, suggesting we have a very robust miniemulsion system.

### 3.1 EXPERIMENTAL

#### 3.1.1 MATERIALS

Deionised water was used for all experiments. The monomers used were methyl methacrylate (MMA) (Aldrich, 99%) and butyl acrylate (BA) (Aldrich, 99%). The surfactants used were sodium dodecylbenzene sulphonate (SDBS) (Acros, 88% technical grade) and Disponil® A 3065 (graciously supplied by Cognis). Disponil® A 3065 is a mixture of linear ethoxylated fatty acids with an average molecular weight of 1 022 g/mol.<sup>[1]</sup> The costabilisers used were octadecyl acrylates (ODA) (Aldrich, 97%) and n-hexadecane (HD) (Acros, 99%). The oil-soluble initiators used were dilauryl peroxide (LPO) (Acros, 99%), dibenzoyl peroxide (BPO) (Acros, 75%), and 2,2'-azobis(2-methylpropionitrile) (AIBN) (Acros, 98%). The water solubilities and dissociation rate constants of these initiators are given in Table 3.1. Protective colloidal dispersants used were poly(vinyl alcohol) (PVOH) (Acros, 88% hydrolysed, MW = 22 000 g/mol) and Acacia Powder (Gumme Arabicum) (Aldrich). All materials were used as received.

**Table 3.1** Dissociation rate constants at 70 °C and solubility in water constants of AIBN, BPO and LPO.

	AIBN	BPO	LPO
$k_d (s^{-1})$ 70°C <sup>[2]</sup>	$3.2 \times 10^{-5}$	$1.4 \times 10^{-5}$	$2.9 \times 10^{-5}$
Water solubility <sup>[3]</sup> (g / 100g of H <sub>2</sub> O)	0.4	$3.0 \times 10^{-4}$	$2.0 \times 10^{-9}$

### 3.1.2 HOMOGENISATION

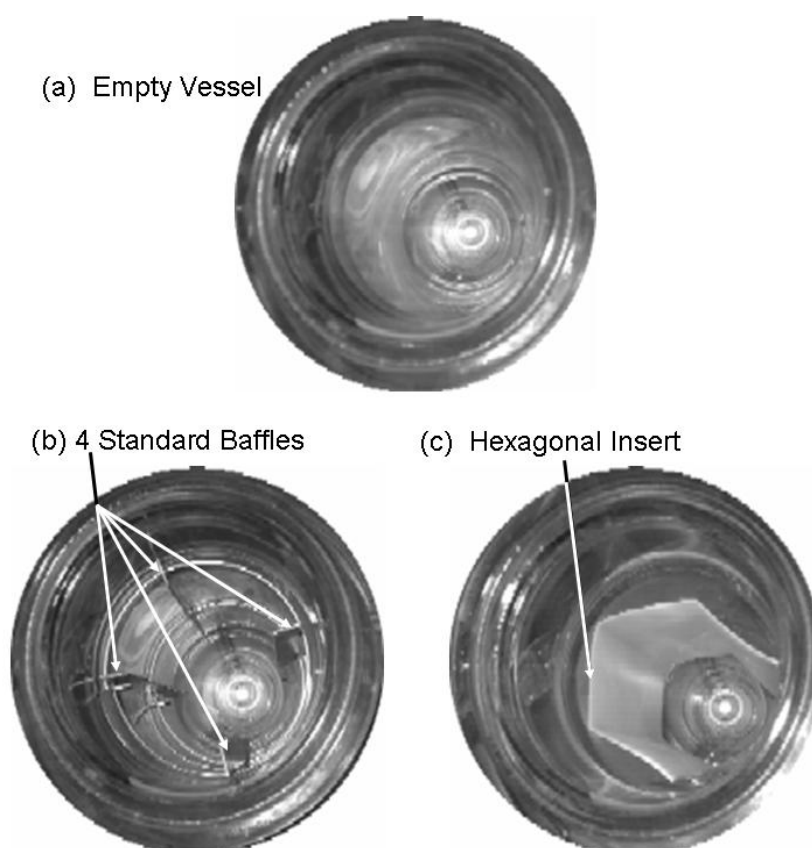
Miniemulsions were made using 50:50 w/w MMA/BA, with 10 wt% costabiliser based on monomer, 0.4 – 1.2 wt% surfactant based on monomer and 0.14 wt% initiator based on monomer. Total solids content (volume fraction of the dispersed phase in the emulsion) was approximately  $50 \pm 4\%$  unless otherwise stated. Monomers, costabilisers and oil-soluble initiators were prepared as one phase, and the surfactants were dissolved in the deionised water and prepared as a second phase. The two phases (combined total 500 grams) were then combined in a 2 L glass reactor and subjected to high shear using a Turbotest® rotor - stator (RAYNERI) with digital display. The rotor-stator assembly was an H30 Form B; the stator head measured 5.5 cm in diameter and was equipped with four blades. The stator head had 19 vertical slits along the side and 12 circular slots along the top. Maximum rotational speed of the rotor-stator is 3300 RPM, however we operated between 2000 and 3000 RPM.

In order to evaluate the performance of the baffles, we did a series of emulsifications using recipe R1 (c.f. Table 3.2) and an agitation rate allowing us to operate in a turbulent flow regime. Reynolds number was found to be  $> 10^5$  (equation 6)

$$\text{Re} = \frac{\rho N D^2}{\eta} \quad (6)$$

Where,  $\rho$  is the density,  $N$  is the revolutions per minute,  $D$  is the diameter of the stator head and  $\eta$  is the viscosity. Without baffles (Figure 3.1A) we obtained droplets with an average size greater than 300 nm, and a wide, bimodal droplet size distribution (DSD). We also observed significant vortex formation which could be inhibiting the two phases from mixing. To eliminate the vortex we inserted a standard set of baffles (Figure 3.1B) and a custom-made (Figure 3.1C) hexagonal baffle. Both the standard and custom-made

baffles yielded similar results. The average droplet sizes were 334 nm and 330 nm, respectively. Subsequent emulsifications were performed using the custom-made vessel since with the standard baffles we observed deposits of the organic phase on the trailing edge of each blade. Finally, in order to verify that no droplets were caught behind the baffles, droplet size measurements were taken in the centre of the vessel in Figure 3.1C and the clearance between the reactor wall and the custom-made hexagonal baffle. In both locations the droplet sizes were found to be similar.



**Figure 3.1** Top view of 2L vessels used during emulsification with the rotor-stator. (A) Simple circular vessel. (B) Baffled vessel. (C) Custom made hexagonal baffle layout.

### 3.1.3 POLYMERISATION

Polymerisations were carried out in a 2 L glass unbaffled, jacketed reactor equipped with

a reflux condenser, a nitrogen inlet, an anchor stirrer and a sampling device. All polymerisations were carried out at 70°C. Temperature was controlled using a thermostatted bath. Impeller speed of the reactor was set to 300 RPM. Initially, the homogenised mixture was purged with nitrogen for approximately 25 minutes to remove any dissolved oxygen. Once purged, the temperature of the bath was increased to 70°C from room temperature. The time at which the reaction was said to begin (i.e.  $t = 0$ ) was defined as the moment where the temperature in the reactor reached 70°C. Samples were taken every 10 minutes for the first half an hour and then every half hour for the remainder of the experiment. Since the temperature rise took only a few minutes, it is assumed that no significant quantity of polymer formed during the heating period. Most reactions were run for approximately four to five hours.

#### 3.1.4 CHARACTERISATION

Complete droplet and particle size distributions were measured by Static Light Scattering using a Beckman-Coulter LS-230. Full droplet and particle size distributions included number average ( $D_N$ ) and volume average ( $D_V$ ) values and the polydispersity index (PDI) was defined as  $D_V/D_N$ . Conversion was measured gravimetrically (See Appendix A1).

#### 3.1.5 CONDUCTIVITY MEASUREMENTS

Conductivity of the emulsion was monitored with a Copenhagen CDM 83 conductivity meter equipped with platinum cells. Samples were allowed to cool to room temperature before the measurement was taken. Vale and McKenna showed that the value of  $A_s$ , the specific surface area, of the SDBS surfactant molecules, varied by ~ 10% (from 47 to 54  $A^2$ ) on PVC particles between 20 and 50 °C. <sup>[4]</sup> Since we are working in a comparable



temperature range we used an average  $A_s$  value of  $50 \text{ A}^2$  in all of our calculations. Therefore our measurements in Figures 3.6, 3.7, 3.9 and Table 3.6 are not exact in terms of the true partitioning values in the reactor at reaction temperature. Nevertheless, these measurements can be taken as representative of the evolution of the system.

In a latex, the conductivity will mostly reflect the amount of surfactant located in the aqueous phase (since we are using oil-soluble initiators that do not decompose to yield charged radicals, the contribution from the initiator will be negligible). Therefore, the difference between the total amount of surfactant and that in the aqueous phase is the amount of surfactant located at the oil-water interface. Using the percentage of surfactant located at the oil-water interface, we refer to equation 7 to calculate the actual percentage surface coverage:

$$\%Coverage = \frac{(\% \times \frac{m_{SDBS}}{M_{SDBS}}) \times A_s \times N_A}{\frac{6 \times M_{pol}}{d_{pol} \times D_p}} \quad (7)$$

where,  $m_{SDBS}$  (g) is the amount of SDBS used,  $M_{SDBS}$  (g/mol) is the molecular weight of SDBS,  $A_s$  ( $\text{m}^2$ ) is specific surface area,  $N_A$  is Avogadro's number (1/mol),  $M_{pol}$  (g) is the mass of polymer,  $d_{pol}$  ( $\text{kg/m}^3$ ) is the density of the polymer and  $D_p$  (m) is the diameter of the particle ( $D_V$ ).

## 3.2 RESULTS AND DISCUSSION

### 3.2.1 HOMOGENISATION AND POLYMERISATION

By varying the rotational speed and the amount of surfactant, miniemulsion droplets with volume average diameters ranging from  $2 \text{ }\mu\text{m}$  to  $300 \text{ nm}$  with PDI's ranging from 1.2 to

3.6 were prepared (Table 3.2). PDI is defined as the volume average diameter divided by the number average diameter. During emulsification with the rotor-stator, the mixture was kept in an ice bath to prevent a measurable temperature increase from the heat generated by the homogenisation. Average DSDs were measured every hour for up to 6h and were found to not change. None of the emulsified solutions showed visual evidence of phase separation within 2 weeks.

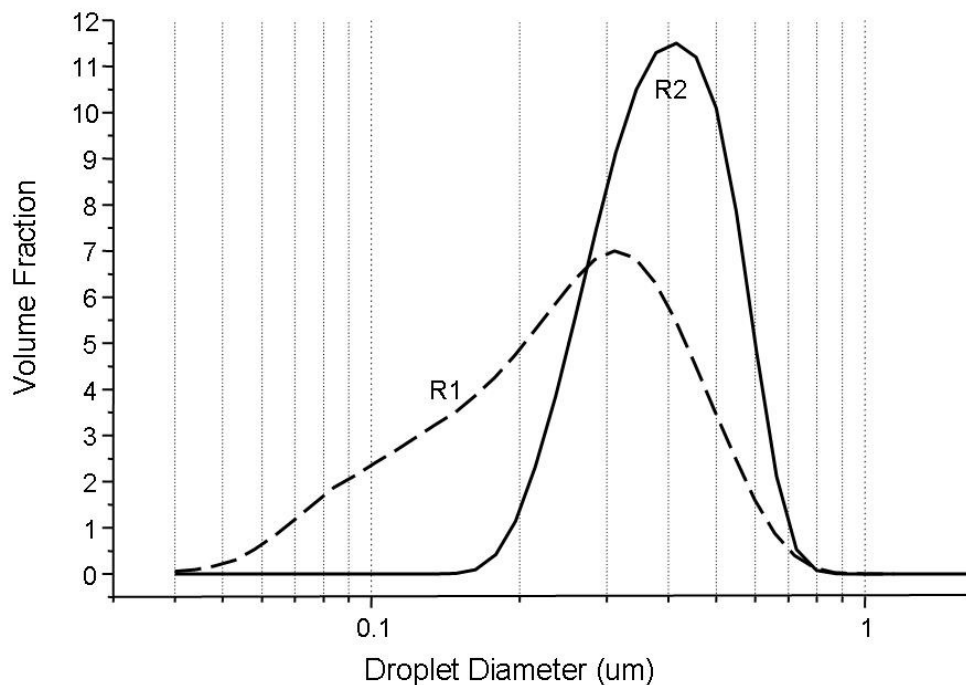
**Table 3.2 Effect of surfactant concentration (SDBS) and rotational speed on mean droplet diameter by volume ( $D_v$ ) and polydispersity (PDI).**

Expt Number	Speed (RPM)	Time (mins)	SDBS (wt %)*	PDI ( $D_v/D_N$ )	$D_v$ (nm)
R1	3000	95	1.2	AIBN: 3.6	322
				LPO: 2.6	298
R2	3000	90	0.8	AIBN: 1.3	426
				BPO: 1.3	411
				LPO: 1.2	418
R3	3000	80	0.8	AIBN: 1.4	544
R4	2500	75	0.6	AIBN: 1.7	644
				BPO: 1.6	595
R5	2500	65	0.4	AIBN: 2.3	933
R6	2000	50	0.4	AIBN: 1.9	1930

\* Weight percent with respect to total monomer mass ( $M_{TOT} = 500$  grams).

The PDI for the ~ 300 nm droplets (Figure 3.2) prepared with AIBN and 1.2 wt% of SDBS (R1) was wider than that of the droplets from run R2 (3.6 vs. 1.2 respectively) due to the presence of a larger fraction of small droplets in R1. It is possible that the larger quantity of small droplets in R1 was due to a combination of the mechanism of rupture of the large droplets and the higher surfactant concentration (relative to the other experiments). In fact, if the rotor-stator is capable of breaking larger droplets into smaller sister droplets, the breakage process might also produce a number of smaller satellite droplets. Typically, if the droplets are not stabilised fairly quickly, they will recoalesce regenerating larger droplets. Therefore, it is quite possible that with such a

high surfactant concentration, the satellites and sister droplets are being stabilised. In the other runs, the surfactant concentration is lower so the smaller droplets would not be stabilised if this interpretation is correct. A deeper investigation of this aspect is outside the scope of the current paper, but merits further investigation.



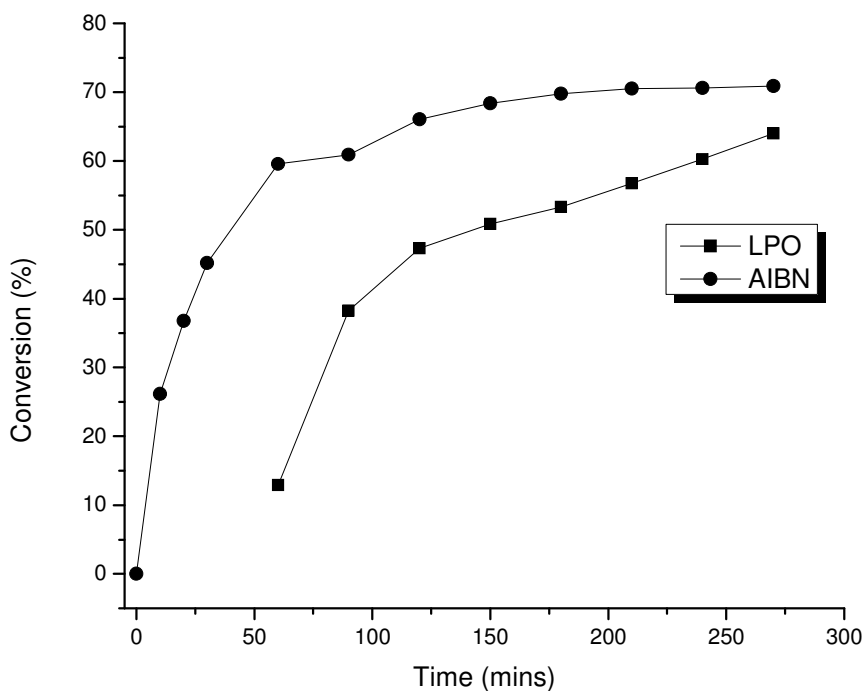
**Figure 3.2** Droplet diameter distribution of ~ 300 nm (R1) and ~ 400 nm (R2) droplets generated using the rotor-stator.

It should also be noted that the largest particles in Table 3.2 have diameters on the order of 2  $\mu\text{m}$ . It is possible that these particles are too large to be considered as “emulsion” or “mini-emulsion” particles *per se* since the swelling behaviour will be quite different for droplets of 2  $\mu\text{m}$  and for those of 300 nm. Typically, the range of particle/droplet sizes considered to be miniemulsions is  $50 > D_p > 500 \text{ nm}$ ; therefore, for the remainder of the investigation presented herein, we will only focus on the

polymerisation of 300, 400 and 600 nm sized droplets.

### 3.2.1.1 POLYMERISATION OF 300 NM MINIEMULSIONS (R1)

Miniemulsions with mean droplet diameters of ~300 nm (based on formulation R1 (50:50 w/w ratio of MMA/BA, 10 wt% ODA and 1.2 wt% SDBS)) were polymerised using either AIBN or LPO. Table 3.3 shows the evolutions of the particle size by volume and number, the PDI, the conversions and the evolution of the number of particles ( $N_p$ , which is an absolute value, calculated using  $D_v$  (Appendix A3)) for the two different initiators as a function of time. The evolution of conversion as a function of time is shown in Figure 3.3, where we can see that the rate of polymerisation (slope of the curve) is initially much higher for the run with AIBN than LPO.



**Figure 3.3** Conversion profile for ~ 300 nm droplets (R1) polymerised initiated at 70°C using AIBN and LPO.

As seen in Table 3.3, particles polymerised with AIBN remained relatively constant in size ( $D_V$  and  $D_N$  did not exhibit much change) throughout the reaction, whereas in the case of LPO there was coalescence in the system. In this second case, the smaller particles seemed to disappear; whether by coalescence or Ostwald ripening is not clear. Nevertheless, the PSD narrowed as the reaction progressed. It is possible that no new particles were formed during the polymerisation. However AIBN is somewhat soluble in the aqueous phase (cf. Table 3.1) rendering the initiation system more complex. Despite the presence of the initiator in the oil phase, a significant number of chains can be initiated by radicals coming from the aqueous phase. Given that AIBN is more soluble in the water phase than LPO, we could have faster initiation of particles with AIBN than with LPO. The rapid initial rate of polymerisation (Figure 3.3) could be attributed to radicals present in both the aqueous and oil phase, and eventually to the creation of new particles via secondary nucleation which is also supported by an increase in  $N_p$  (Table 3.3) at the beginning of the polymerisation. This can be seen by a decrease in the value of  $D_V$  as the reaction progresses. Clearly there is an accumulation of smaller particles as the reaction progresses when using AIBN, an effect which was not observed when polymerizing with LPO.

**Table 3.3 Evolution of the conversion, droplet diameters ( $D_V$  &  $D_N$ ) and PDI during polymerisation as a function of the initiator (AIBN or LPO) used for ~ 300 nm miniemulsions (R1). T=70°C.**

Time (mins)	AIBN					LPO				
	Conv (%)	$D_V$ (nm)	$D_N$ (nm)	PDI	$N_P$ ( $10^{16}$ ) (abs.)	Conv (%)	$D_V$ (nm)	$D_N$ (nm)	PDI	$N_P$ ( $10^{16}$ ) (abs.)
0	0.0	330	91	3.6	3.2	0.0	298	114	2.6	4.3
10	26.1	320	92	3.5	3.3	0.0	311	120	2.6	3.8
20	36.7	299	90	3.3	4.0	12.9	311	125	2.5	3.8
30	45.2	294	93	3.2	4.1	38.3	302	140	2.2	4.2
60	59.6	304	86	3.5	3.6	12.9	343	156	2.2	2.8
90	60.9	311	86	3.6	3.4	38.3	390	266	1.5	1.8
120	66.1	319	91	3.5	3.1	47.3	385	241	1.6	1.8
150	68.4	297	86	3.5	3.8	50.8	363	257	1.4	2.2
180	69.8	299	87	3.4	3.8	53.3	377	257	1.5	1.9
210	70.5	306	94	3.3	3.5	56.7	366	260	1.4	2.1
240	70.6	281	89	3.2	4.5	60.3	352	265	1.3	2.3
270	70.9	280	91	3.1	4.6	64.0	385	263	1.5	1.8

### 3.2.1.2 POLYMERISATION OF 400 NM MINIEMULSIONS (R2)

Miniemulsions with mean droplet diameters of ~ 400 nm were made using formulation R2 (50:50 w/w ratio of MMA/BA, 10 wt% ODA and 0.8 wt% SDBS). The evolution of the particle size by volume and number, the PDI, the conversions and  $N_P$  (See Appendix A3) are shown in Table 3.4 for all three initiators.

**Table 3.4** Evolution of the conversion and droplet diameters ( $D_V$  &  $D_N$ ) during polymerisation as a function of the initiator (AIBN, BPO and LPO) used for ~ 400 nm miniemulsions (R2). T=70°C.

Time (mins)	AIBN					BPO					LPO				
	Conv (%)	$D_V$ (nm)	$D_N$ (nm)	PDI	$N_p$ ( $10^{16}$ ) (abs.)	Conv (%)	$D_V$ (nm)	$D_N$ (nm)	PDI	$N_p$ ( $10^{16}$ ) (abs.)	Conv (%)	$D_V$ (nm)	$D_N$ (nm)	PDI	$N_p$ ( $10^{16}$ ) (abs.)
0	0.0	402	313	1.2	1.7	0.0	392	294	1.3	1.9	0.0	410	321	1.3	1.6
10	4.3	426	324	1.3	1.4	0.0	400	286	1.4	1.8	0.0	418	337	1.2	1.5
20	9.7	432	270	1.6	1.4	0.5	392	294	1.3	1.9	2.5	420	321	1.3	1.5
30	15.9	462	100	4.6	1.1	1.5	411	315	1.3	1.6	5.8	452	319	1.4	1.2
60	42.2	505	105	4.8	0.8	10.4	412	300	1.4	1.6	15.0	447	337	1.3	1.2
90	63.5	484	94	5.1	0.9	16.6	438	327	1.3	1.3	25.1	559	331	1.7	0.6
120	77.6	545	102	5.3	0.6	25.4	511	297	1.7	0.8	37.5	618	331	1.9	0.4
150	83.5	547	105	5.2	0.6	36.2	502	294	1.7	0.8	53.5	622	354	1.8	0.4
180	87.3	542	114	4.6	0.6	49.3	555	308	1.8	0.6	65.2	693	353	2.0	0.3
210	87.9	543	100	5.4	0.6	60.6	582	321	1.8	0.5	74.1	740	370	2.0	0.2
240	89.9	587	110	5.5	0.4	70.7	584	343	1.7	0.5	80.7	718	340	2.1	0.2
270	89.1	555	98	5.6	0.5	75.9	658	352	1.9	0.3	83.3	747	372	2.0	0.2

It can be seen that, similar to the case of the 300 nm miniemulsion droplets, the formulation with AIBN polymerised faster during the initial stages than did those initiated with LPO or BPO (Figure 3.4). This is due to nucleation of new particles since  $D_N$  decreases significantly throughout the reaction (Table 3.4). In addition, the larger particles grow larger during the reaction as manifested by a 37% increase in the value of  $D_V$ . This formulation is not optimal if we wish to retain control over the average particle size and to obtain a roughly 1:1 mapping of droplets into particles.

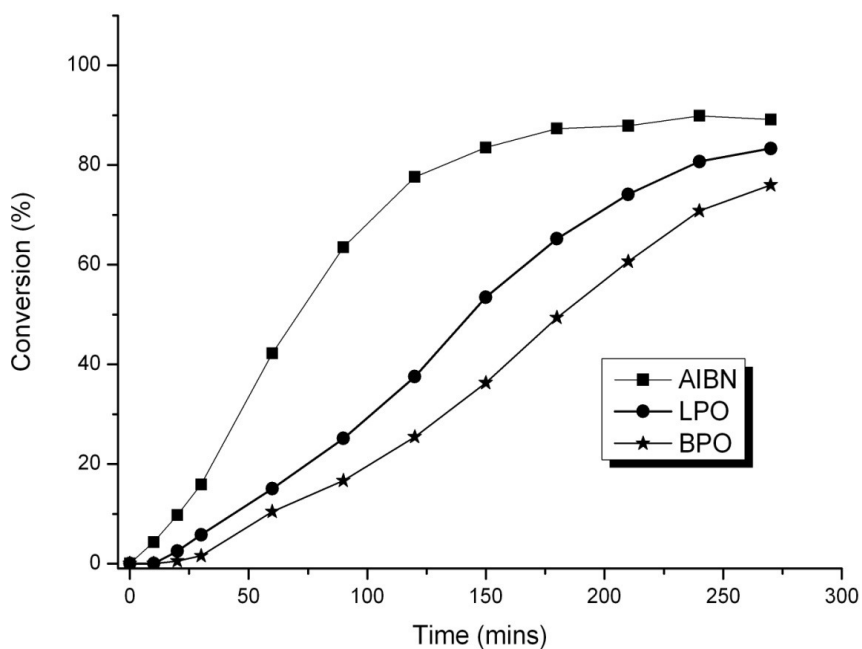


Figure 3.4 Conversion profiles of ~ 400 nm droplets (R2) initiated with AIBN, LPO and BPO at 70°C.

On the other hand, the miniemulsions polymerised with LPO and BPO evolved in a similar manner throughout the reaction, but differently than those using AIBN. With both BPO and LPO, the droplet diameter by volume and by number increased. Droplet diameters by volume increased from ~ 400 nm to ~ 700 nm and the droplet diameters by



number increased from ~ 300 nm to ~ 370 nm, resulting in an increased, yet reasonably low PDI (1.3 to 2.0). The increase in the diameters is an indication that there is little or no secondary nucleation in the system (or if there is, the resulting particles are clearly not stabilised), but rather there is some coalescence occurring throughout the reaction. These observations support prior observations made by Alduncin *et al.*,<sup>[3]</sup> who performed work on styrene miniemulsions and evaluated the use of the same three initiators. They found that initiation in the water phase is expected when AIBN is used but is less pronounced with BPO and almost negligible with LPO. In our case, water phase nucleation appears to be negligible for both BPO and LPO but evident with AIBN.

#### 3.2.1.3 POLYMERISATION OF 600 NM MINIEMULSIONS (R4)

Miniemulsions with mean droplet diameters of ~ 600 nm were made using formulation R4 (50:50 w/w ratio of MMA:BA, 10 wt% ODA, and 0.64 wt% SDBS). The evolution of the particle size by volume and number, the PDI, the conversions and the evolution of the  $N_p$  for the polymerisations initiated with AIBN and BPO are shown in Table 3.5.

**Table 3.5 Evolution of the conversion and droplet diameters ( $D_V$  &  $D_N$ ) during polymerisation as a function of the initiator (AIBN and BPO) used for ~ 600 nm miniemulsions (R4). T=70°C.**

Time (mins)	AIBN					BPO				
	Conv (%)	$D_V$ (nm)	$D_N$ (nm)	PDI	$N_P$ ( $10^{15}$ ) (abs.)	Conv (%)	$D_V$ (nm)	$D_N$ (nm)	PDI	$N_P$ ( $10^{15}$ ) (abs.)
0	0.0	644	390	1.7	4.3	0.0	640	384	1.7	4.4
10	0.0	656	394	1.7	4.1	0.0	652	409	1.6	4.2
20	0.0	624	356	1.8	4.7	0.0	636	372	1.7	4.5
30	5.8	666	332	2.0	3.8	0.0	646	375	1.7	4.2
60	20.1	757	229	3.3	2.5	8.6	696	398	1.8	3.3
90	42.5	726	117	6.2	2.7	15.7	737	417	1.8	2.8
120	65.3	791	118	6.7	2.0	27.1	776	414	1.9	2.3
150	81.5	851	130	6.5	1.6	45.6	906	407	2.2	1.4
180	88.9	828	150	5.5	1.7	63.2	952	402	2.4	1.1
210	93.2	909	192	4.7	1.2	68.8	1020	356	2.9	0.9
240	94.9	910	164	5.6	1.2	71.2	937	360	2.6	1.2
270	95.9	957	134	7.1	1.1	72.7	1020	416	2.4	0.9

Once again it appears that there is a combination of secondary nucleation of particles and coagulation of the larger particles in the system initiated with AIBN. As mentioned above, this is consistent with the argument that this is due to the partial solubility of AIBN in the water phase, which can begin to polymerise the soluble fraction of MMA.

The miniemulsions initiated with BPO behaved in the same manner as seen previously for the 400 nm miniemulsions; particle size increased from 640 nm to ~ 1  $\mu\text{m}$ , while the particle diameter by number remained relatively constant. From the results

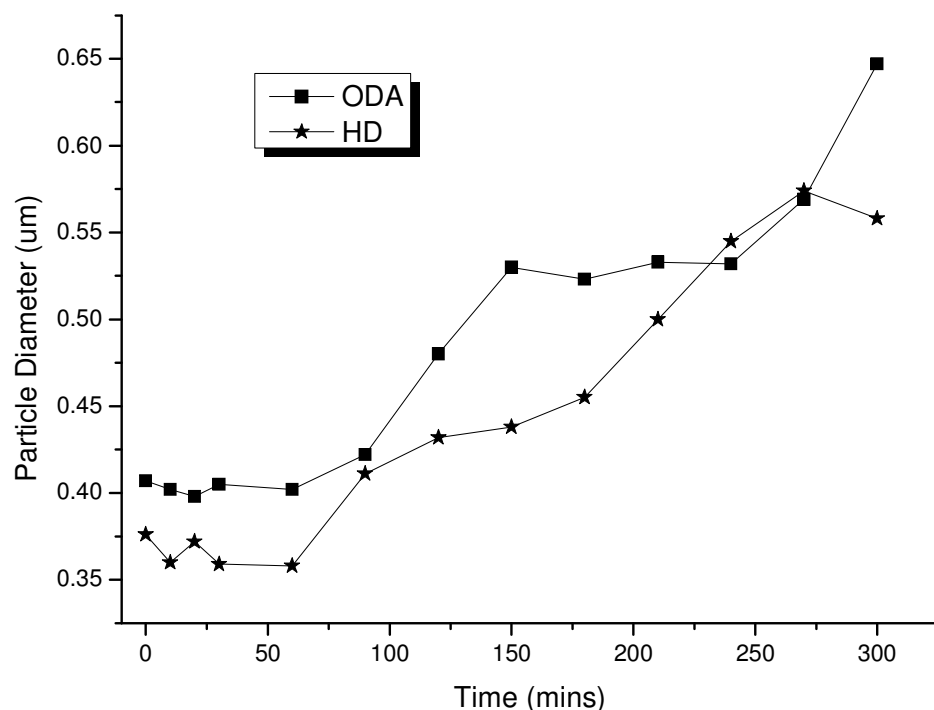
presented in this section, we can conclude that AIBN is not well-suited as an initiator for miniemulsions with our formulations. It is less hydrophobic than the other two initiators, and its presence in the aqueous phase is correlated with an increase in the number of small particles in the reactor. The other two initiators, LPO and BPO behave in a similar manner. Upon polymerisation with either initiator the volume average particle size increased by roughly 40-60%, whereas the number average diameter increased slightly. While not ideal in the sense that there is not a 1:1 mapping of droplets into particles, this situation is preferable to one where we experience a renucleation of new particles, as this gives us better control over the composition of the particles (i.e. in a composite material, a dispersion with renucleation would contain particles with AND without the second material, whereas in a miniemulsion with limited coagulation and no renucleation all of the final particles would contain the second material). In the following sections, we report the role of several different parameters (using the 400 nm miniemulsions) in order to understand why the particle size increases, including the costabiliser type, impeller speed in the reactor, solids content, protective colloid dispersants and surface coverage. All reactions were initiated with BPO.

### 3.2.2 POLYMERISATION OF 400 NM DROPLETS

#### 3.2.2.1 PREPARATION OF MINIEMULSION WITH DIFFERENT COSTABILISERS

As mentioned above, all of the formulations tested to this point consisted of ODA as the costabiliser. It is ideally suited for this purpose (ODA has a low molecular weight of MW 324.54 g/mol and very low water solubility) and it is a monomer which means that it reacts during the polymerisation and becomes incorporated in the final product (i.e. it

does not have to be removed). The costabiliser is crucial in miniemulsion droplets as it prevents or delays Ostwald ripening. Its presence enhances the osmotic pressure of the species within the droplets and helps counteract the Laplace pressure created by the presence of surfactant.<sup>[5]</sup> In order to test whether the consumption of ODA during the polymerisation caused the osmotic pressure to drop, thereby provoking a rearrangement of the particle size distribution, we replaced ODA by HD, another very well-known hydrophobe for miniemulsion applications. The evolution of particle size for formulations of R2 as a function of time for the two costabilisers is shown in Figure 3.5.



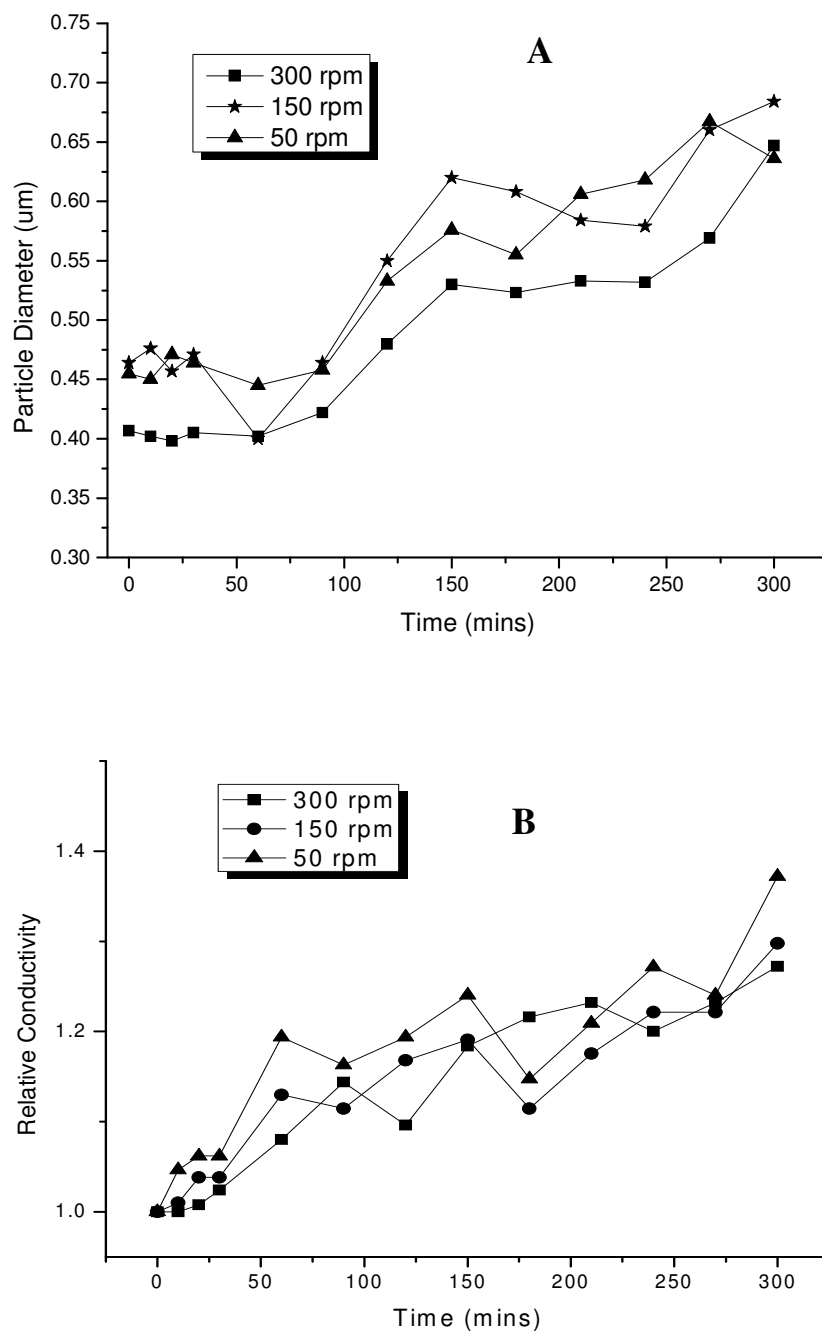
**Figure 3.5** Evolution of the particle diameter ( $D_v$ ) over time as a function of the costabilisers ODA and HD for  $\sim 400$  nm miniemulsions polymerised at  $70^\circ\text{C}$  using BPO.

As can be seen from this figure, the particle size evolved in essentially the same manner for polymerisations with HD and ODA. This means that increased diffusional

degradation due to the consumption of ODA is not the reason for the increase in particle size in this system. These results are comparable to those observed by Alduncin *et al.*<sup>[3]</sup> who ran miniemulsion polymerisations using BPO as initiator. They compared results with and without HD and observed an increase in particle size and a loss in particle number, regardless of whether or not HD was present. Overall, these results suggest that the miniemulsion system is not suffering diffusional degradation due to the consumption of ODA.

#### 3.2.2.2 POLYMERISATION OF MINIEMULSIONS WITH DECREASING AGITATION SPEED IN THE REACTOR

Agitation speed is a major contributor to the rate at which droplets break and coalesce in polymerising systems. At higher impeller speeds, particles collide with greater energy possibly causing aggregation if there is insufficient stabilisation at the surface of the particles. Our standard agitator speed was 300 RPM. We lowered the impeller speed to observe the effect it would have on the particle size. Recipe R2 was polymerised at stirring speeds of 300, 150 and 50 RPM. The evolution of the average particle size and the relative conductivity as a function of polymerisation time are shown in Figure 3.6.



**Figure 3.6 A - Evolution of the particle diameter ( $D_v$ ) and relative conductivity with time as a function of the reactor impeller speeds: 300, 150 and 50 RPM for ~ 400 nm droplets polymerised at 70°C using BPO. B - The relative conductivity is the conductivity as a function of time divided by the conductivity at time  $t=0$  for each experiment.**

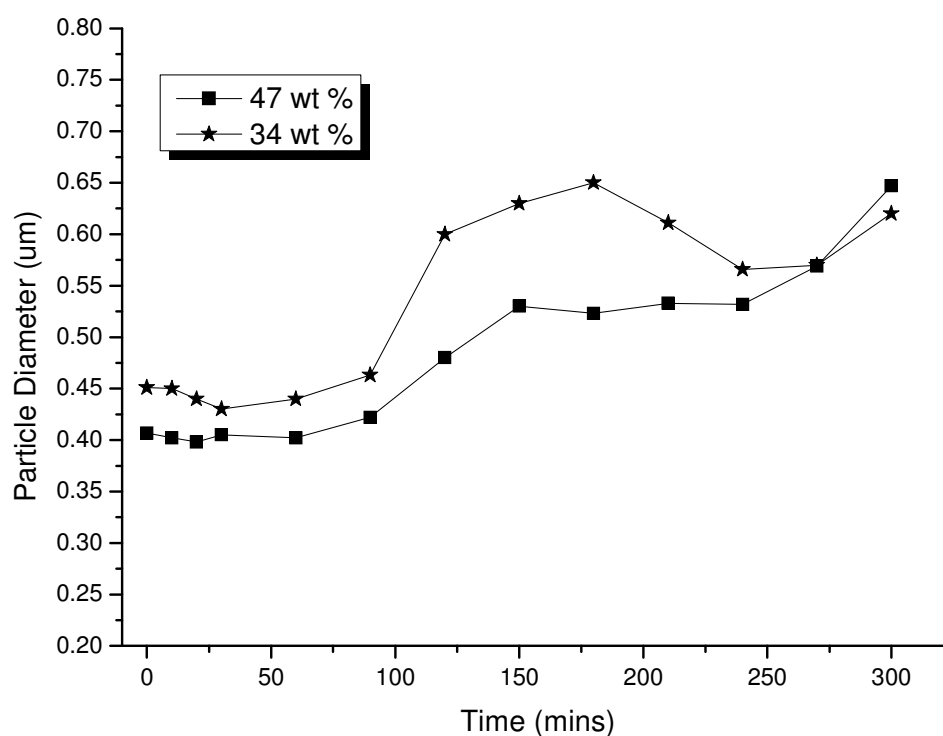
It can be seen that lowering the impeller speed within the limits defined here had

no visible effect on the evolution of the volume average particle size, nor on the PDI. Relative conductivity measurements performed at each interval of time show the quantity of surfactant that is being desorbed as the particles grow. From Figure 3.6, there does not seem to be any discernible difference between the three rotation speeds suggesting that the agitation speed does not affect particle size. However, surface coverage calculations (based on emulsion conductivity measurements) reported a different conclusion. It was found that at lower impeller speeds, more surfactant desorbed from the oil-water interface into the aqueous phase (i.e. increasing relative conductivity readings suggesting that particles formed at lower agitation rates desorbed more surfactants). Calculations reveal that at 50 RPM, 32 % of the surfactant located at the oil-water interface was desorbed throughout the polymerisation. This value is compared to 26 % desorbed at 150 RPM and 23 % at 300 RPM. A second set of polymerisations were carried under similar conditions using LPO as the initiator. The particle sizes and conductivity measurements evolved in a similar manner (as seen in Figure 3.6) at all three agitation speeds. However, surface coverage calculations reported that 7, 27, and 34% of the surfactant located at the oil-water interface desorbed throughout polymerisations agitated at 300, 150, and 50 RPM respectively. In all cases we continue to observe an increase in both  $D_V$  and  $D_N$  and an increase in percentage of surfactant desorbed with decreasing agitation speeds. This suggests that the energy from the impellor is required to keep the particles apart from one another to prevent surfactant desorption.

### 3.2.2.3 POLYMERISATION OF MINIEMULSIONS WITH A LOWER SOLID CONTENT

Making high solid content latexes (> 45 wt %) is important if miniemulsions are to be commercialised, and for this reason the formulations used so far consisted of 46-54%

solids. A disadvantage of using high solids is that stabilisation is more difficult since the likelihood of particle-particle interaction is enhanced. Such interactions can cause particles to agglomerate if they are not well-stabilised. To evaluate the influence of high solids content on the rate of coagulation of the particles we examined a similar system but with a reduced solids content (34 wt %) keeping the wt % of the costabiliser and surfactant constant relative to monomer mass.



**Figure 3.7** Evolution of the particle diameter ( $D_v$ ) over time as a function of the solid contents 47 and 34 wt % for ~ 400 nm miniemulsions polymerised at 70°C using BPO.

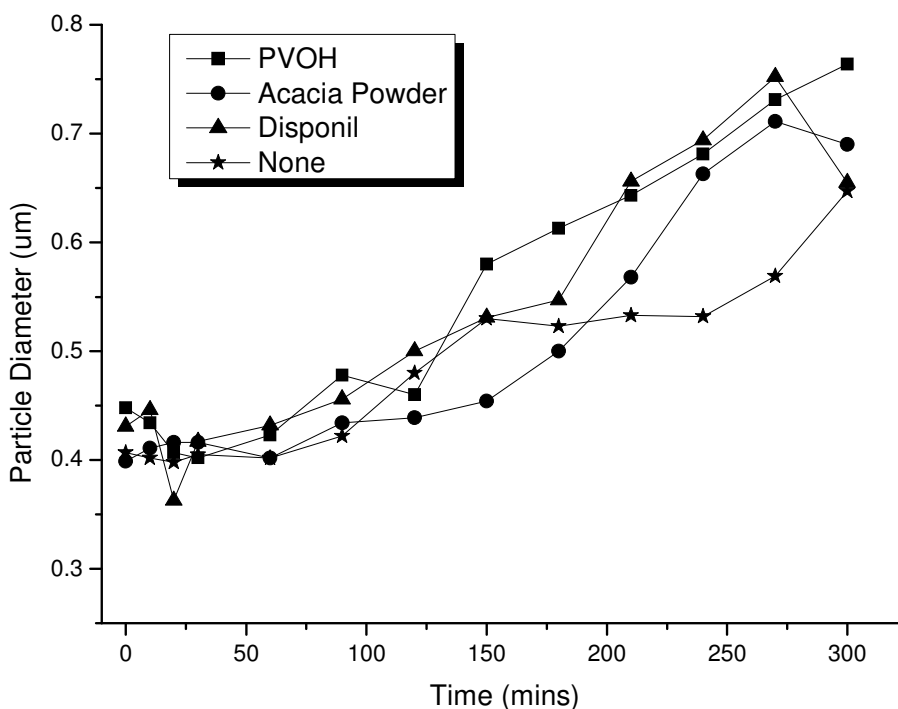
Based on the similar increasing trends observed in Figure 3.7 (and in replicate runs not shown for the sake of brevity), the evolution of the particle size throughout the polymerisation is independent of the solids content. Conductivity measurements



increased by  $\sim 27\%$  throughout both polymerisations. Overall, between 23 – 27 % surfactant initially located at the oil–water interface desorbed into the aqueous phase for both solid content systems as the particle sizes were evolving.

#### 3.2.2.4 POLYMERISATION OF MINIEMULSIONS WITH THE ADDITION OF PROTECTIVE COLLOID DISPERSANTS

Miniemulsions in which the polymerisation takes place inside the droplets are sometimes likened to suspension polymerisations, although the droplet size in suspension systems is typically an order of magnitude higher and the stabilisation system is usually different than in miniemulsions.<sup>[6]</sup> In suspension systems, protective colloid dispersants are used to stabilise the polymerising droplets. The protective colloid (for instance PVOH) forms a film at the droplet/particle interface<sup>[6]</sup> and 0.1 wt % protective colloid appears to be sufficient to prevent (or reduce) agglomeration.<sup>[7]</sup> It is also common practice in the emulsion polymerisation industry to make latexes using a combination of both steric and electrostatic stabilisation.<sup>[8]</sup> We used two different protective colloids and a non-ionic surfactant to observe any effect they have on particle aggregation. The protective colloids were PVOH or Acacia Powder. In these experiments, 2.8 wt % of one of the protective colloids (based on monomer mass) in 100 ml of DIW was added to the reactor along with the emulsified mixture. The non-ionic surfactant used was Disponil® A 3065. It was added in the same weight percent (0.8 wt %) as the anionic surfactant SDBS, but as a separate solution in a similar fashion as the colloidal protectors. The effects that PVOH, Acacia power and Disponil had on particle size can be seen in Figure 3.8.



**Figure 3.8** Evolution of the particle diameter ( $D_v$ ) over time as a function of the protective colloids PVOH, Acacia Powder and the non-ionic surfactant Disponil for  $\sim 400$  nm miniemulsions polymerised at  $70^\circ\text{C}$  using BPO.

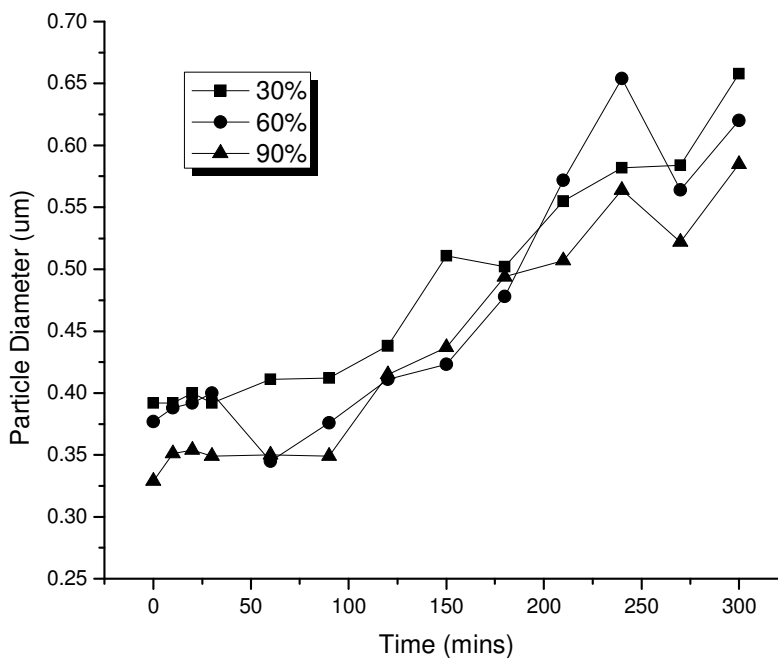
It can be seen here that the addition of non-ionic Disponil, and the protective colloids PVOH and Acacia powder did not have a significant impact on the particle size system. We still observed a measurable particle size increase in comparison to a system with no added stabiliser even though we have introduced the combination of steric and electrostatic stabilisation.

#### 3.2.2.5 PREPARATION OF MINIEMULSION WITH INCREASED SURFACE COVERAGE

Varying the costabiliser, agitation speed, solids content and stabilisation system did not show any effect on the evolution of the average particle size. Based on equation 7, our system (R2) has a maximum possible surface coverage of 30% at the end of

homogenisation if we assume that all the surfactant is located at the oil-water interface (however, in reality a certain portion of the surfactant will be partitioned between the interface and the aqueous phase, and some surfactant might even be buried in the droplets). We therefore decided to increase the surface coverage of the droplets to observe the effect it would have on particle size evolution.

We prepared three separate systems: the original R2 system with theoretical surface coverage of 30 % (i.e. assuming all surfactant is present at the interface), and two other systems with two and three times the original quantity of surfactant, resulting in theoretical surface coverage's of 60 and 90 %. Particle size during polymerisation for all three systems was measured and the results are shown in Figure 3.9.



**Figure 3.9** Evolution of the particle diameter ( $D_v$ ) over time as a function of the 30, 60, and 90% surface coverage for ~ 400 nm miniemulsions polymerised at 70°C using BPO.

During polymerisation, the particles continued to increase in size without any

clear evidence of renucleation. Doubling and tripling the amount of surfactant in the system, we obtained greater initial surface coverage but despite this we were still unable to reduce particle coalescence throughout the polymerisation.

Interestingly enough, even with excess surfactants in our system we do not observe secondary nucleation. This is supported by an increase in both  $D_V$  and  $D_N$  and a decrease in the number of particles  $N_P$  (Table 3.6). If any small particles did form, they were probably not stabilised for a long period of time.

**Table 3.6** Evolution of the  $N_p$  and droplet diameters ( $D_V$  &  $D_N$ ) during polymerisation as a function of the surfactant coverage (30, 60, and 90%) used for ~ 400 nm miniemulsions (R2). T=70°C. All polymerisations initiated with BPO.

Time (min)	30 %				60 %				90 %			
	$D_V$ (nm)	$D_N$ (nm)	PDI	$N_P$ ( $10^{16}$ ) (abs.)	$D_V$ (nm)	$D_N$ (nm)	PDI	$N_P$ ( $10^{16}$ ) (abs.)	$D_V$ (nm)	$D_N$ (nm)	PDI	$N_P$ ( $10^{16}$ ) (abs.)
10	392	294	1.3	1.9	388	266	1.5	2.0	351	242	1.5	2.7
20	400	286	1.4	1.8	392	293	1.3	1.9	354	257	1.4	2.6
30	392	294	1.3	1.9	400	276	1.4	1.8	349	221	1.6	2.8
60	411	315	1.3	1.6	345	253	1.4	2.8	350	253	1.4	2.7
90	412	300	1.4	1.6	376	255	1.5	2.1	349	245	1.4	2.7
120	438	327	1.3	1.3	411	247	1.7	1.7	415	291	1.4	1.6
150	511	297	1.7	0.8	423	244	1.7	1.5	437	299	1.5	1.3
180	502	294	1.7	0.8	478	261	1.8	0.9	494	247	2.0	0.9
210	555	308	1.8	0.6	572	280	2.0	0.6	507	286	1.8	0.8
240	582	321	1.8	0.5	654	299	2.2	0.4	564	321	1.8	0.6
270	584	343	1.7	0.5	564	281	2.0	0.6	522	310	1.7	0.7
300	658	352	1.9	0.3	620	317	2.0	0.4	585	300	2.0	0.5

### 3.3 CONCLUSIONS

The application of a rotor-stator to prepare miniemulsions at industrially relevant solids content was examined. By increasing the rotational speed and the surfactant quantity we were able to produce droplets ranging between 300 nm to 2  $\mu\text{m}$ . Although the rotor-stator does require more time to generate these droplets than, for example, ultrasonication, the major advantage is that it can be applied to industrial scale reactors. The droplets generated with the rotor-stator were polymerised to evaluate particle size evolution. We found that droplets below 300 nm were stable throughout the polymerisation, whereas those above 300 nm increased in size during polymerisation. After changing important process parameters such as costabiliser, solids content, adding colloidal protectors and increasing surface coverage, we were not able to directly show the cause for the particle size growth. As the droplets evolve into particles, the hydrophobicity of the particles increases as the monomers are consumed and polymer is produced. The initial stabilisation system that kept the droplets stable for hours ( $\pm$  5-10% change in  $D_v$ ) appears to be less effective in stabilising polymer-containing particles, resulting in coagulation.

In all of the situations presented above we have shown that changing these industrially important process parameters had no effect on controlling the particle size evolution during the polymerisation. This suggests that our droplet system is very robust, in the sense that imposing these process variations at the droplet stage has no effect on the outcome of our droplets. This also suggests that at the industrial level, the polymerisation process is less likely to be affected by operator error.

## 3.4 LITERATURE CITED

1. Schneider, M.; Graillat, C.; Guyot, A.; McKenna, T. F. High Solids Content Emulsions. II. Preparation of Seed Latexes. *J. Appl. Polym. Sci.* **2002**, *84*, 1897-1915.
2. Brandrup, J.; Immergut, E.H. Polymer Handbook. **1989**, Wiley Interscience: New York.
3. Alduncin, J. A.; Forcada, J.; Asua, J. M. Miniemulsion Polymerisation Using Oil-Soluble Initiators. *Macromolecules*. **1994**, *27*, 2256-61.
4. Vale, H. M.; McKenna, T. F. Adsorption of Sodium Dodecyl Sulfate and Sodium Dodecyl Benzenesulfonate on Poly(Vinyl Chloride) Latexes. *Colloids Surf., A*. **2005**, *268*, 68-72.
5. Taylor, P. Ostwald Ripening in Emulsions. *Adv. Colloid Interface Sci.* **1998**, *75*, 107-163.
6. Capek, I. On the Role of Oil-Soluble Initiators in the Radical Polymerisation of Micellar Systems. *Adv. Colloid Interface Sci.* **2001**, *91*, 295-334.
7. Vivaldo-Lima, E.; Wood, P. E.; Hamielec, A. E.; Penlidis, A. An Updated Review on Suspension Polymerisation. *Ind. Eng. Chem. Res.* **1997**, *36*, 939-965.
8. Colombie, D.; Sudol, E. D.; El-Aasser, M. S. Role of Mixed Anionic-Nonionic Systems of Surfactants in the Emulsion Polymerisation of Styrene: Effect on Particle Nucleation. *Macromolecules*. **2000**, *33*, 7283-7291.

## ***EMULSIFICATION FOR LATEX PRODUCTION: COMPARING IN LINE MIXERS TO ROTOR-STATORS***

---

Early laboratory studies extensively used ultrasonication for the generation of polymerisable droplets of a reasonable size (<300 nm). As an alternative means of generating miniemulsions, we have demonstrated the capability of the rotor-stator to produce droplets ranging from 300 nm to 2  $\mu\text{m}$  (Chapter 3). However, previous work by Ouzineb *et al.* showed that the static mixers were more efficient and required less energy than the rotor-stator to generate styrene miniemulsions.<sup>[1]</sup> Therefore, building on Ouzineb *et al.*'s results we investigated the use of in line static mixers for the generation of miniemulsion droplets. Up to now we have been able to generate < 200 nm droplets of



MMA/BA (50:50 wt%) at 44% solids content within ~ 45 minutes. Our set up consisted of 7, 7mm SMX mixers fitted flush with the surface of a Teflon tube located at the exit of the pump. The water and oil phases were pumped through at a flow rate of 114 g/s. The efficiency of the static mixer in terms of droplet size evolution and distribution and the homogenisation time were compared with that of the rotor-stator. All formulations were emulsified for the same length of time. The devices were not compared in terms of power/energy requirements as the focus was to get a general idea of the operating performance of each device. However, a more in-depth comparison will be presented in Chapter 5.

## 4.1 EXPERIMENTAL

### 4.1.1 MATERIALS

Deionised water was used for all experiments. The monomers used were methyl methacrylate (MMA) (Aldrich, 99%) and butyl acrylate (BA) (Aldrich, 99%). The surfactants used were sodium dodecylbenzene sulphonate (SDBS) (Acros, 88% technical grade) and Disponil® FES 32 (Cognis). The costabiliser used was octadecyl acrylate (ODA) (Aldrich, 97%) and the oil-soluble initiator used was 2,2'-azobisisobutyronitrile (AIBN) (Acros, 98%). (AIBN was used, despite the broad PDI's obtained in Chapter 3, in order to minimize the effect of secondary nucleation in the aqueous phase).

### 4.1.2 HOMOGENISATION

Miniemulsions were prepared with the formulations shown in Table 4.1 unless otherwise stated. Monomers, costabiliser and oil-soluble initiator were prepared as one phase, and

the surfactant dissolved in deionised water as a second phase. The two phases were then combined and subjected to a homogenisation process. Two different homogenisation devices were used: a Turbotest® rotor - stator (RAYNERI) and 7-SMX static mixers of 7mm in diameter by Sulzer Chemtech, which had a length to diameter ratio (L/D) of 1.4.

The rotor-stator assembly was an H30 Form B and the stator head measured at 5.5 cm in diameter and equipped with four blades. The maximum rotational speed of the rotor-stator was 3300 RPM. The stator head had 19 vertical slits along the side and 12 circular slots along the top. The oil and aqueous phases were combined in a baffled vessel and subjected to a speed of 3000 RPM for 44 minutes, with samples removed ever 7 ½ mins. For the static mixers, the 7 SMX elements were fitted flush with the surface of a Teflon tube and connected to a gear pump from Micropump® which had a maximum flow rate of 5.4 L/min and a maximum pressure drop of 8.7 bars. The mixing elements were installed in a closed loop system consisting of a pump, tubing, reservoir tank and temperature bath. All emulsifications were run at flow rates of 114 g/s unless otherwise stated and samples were removed every 7 ½ minutes.

**Table 4.1 Formulations prepared to be used in the static mixer and the rotor-stator.**

Expt Number	MMA (wt%)	BA (wt%)	Costabiliser* ODA(wt%)	Surfactant* SDBS(wt%)	Surfactant* DP(wt%)	Initiator* AIBN(wt%)
S1	50	50	9.0	2.5	--	0.4
S2	50	50	7.5	1.2	--	0.4

\* Weight percent with respect to total monomer mass ( $M_{TOT} = 166.7$  grams)

#### 4.1.3 POLYMERISATION

Polymerisations were carried out in a 2 L glass unbaffled, jacketed reactor equipped with a reflux condenser, a nitrogen inlet, an anchor stirrer and a sampling device. All polymerisations were carried out at 70°C. Temperature was controlled using a

thermostatted bath. Agitator speed was set to 300 RPM. Initially the homogenised mixture was purged with nitrogen at room temperature for ~ 25 minutes to remove any dissolved oxygen. Droplet size measurement was taken after purging to verify that no coalescence took place during purging. Once purging was done, the temperature of the bath was increased to 70°C. The reaction was considered to begin the moment when the reactor reached 70°C ( $t = 0$ ). Samples were taken every 10 minutes for the first half an hour and then every half hour for the remainder of the experiment. Most reactions were run for approximately two to three hours.

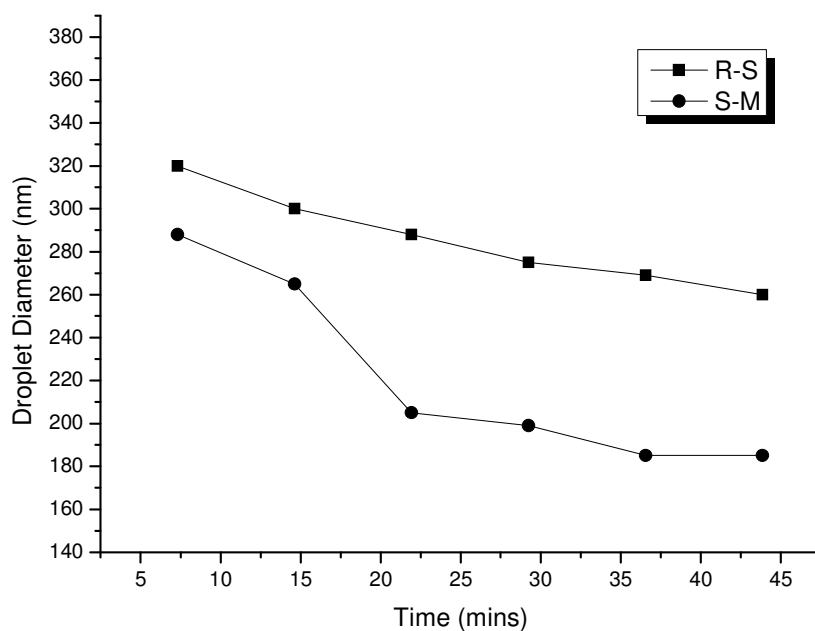
#### 4.1.4 CHARACTERISATION

Complete droplet and particle size distributions were measured with a Beckman-Coulter LS-230. Full droplet and particle size distributions included number average ( $D_N$ ) and volume average ( $D_V$ ) values, and the polydispersity index (PDI) was defined as  $D_V/D_N$ . Conversion was measured gravimetrically (See Appendix A1).

## 4.2 RESULTS AND DISCUSSION

### 4.2.1 HOMOGENISATION

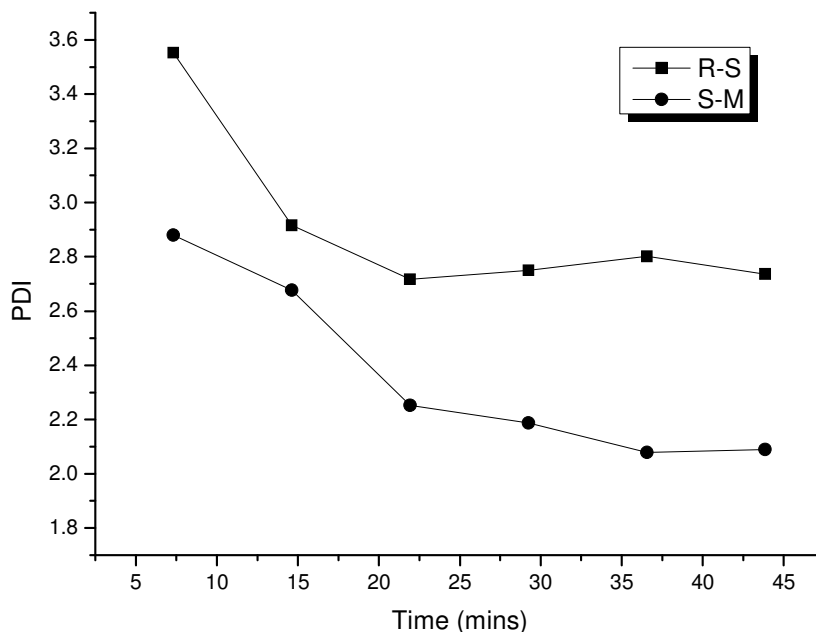
Formulation S2 was emulsified in the rotor-stator at 3000 RPM and with the static mixers separately in order to compare efficiency of each device with respect to the droplet size evolutions and homogenisation time (Figure 4.1).



**Figure 4.1** Evolution of droplet diameter ( $D_v$ ) over time for formulation S2 made using the static mixer and the rotor-stator.

As can be seen in Figure 4.1, applying the same formulation (S2) to two different homogenisation devices generated two different final droplet sizes. All results were found to be reproducible, however, for the sake of brevity, only one set of results are presented here. Figure 4.1 shows within the first few minutes, droplets prepared with the static mixers are smaller than those prepared with the rotor-stator. After  $\sim 44$  minutes of homogenisation, we obtained  $\sim 260$  nm droplets with the rotor-stator whereas  $\sim 260$  nm sized droplets were prepared after only  $\sim 15$  minutes using the static mixer. Further shearing of the droplets with the static mixers ( $\sim 44$  minutes) generated  $\sim 190$  nm sized droplets. Along with a smaller droplet size, the static mixer produced a much narrower PDI (Figure 4.2). Similar PDI's were observed by Ouzineb *et al.* who prepared styrene and butyl methacrylate miniemulsion droplets (separately) with the rotor-stator and the

static mixer.<sup>[1]</sup> They generated droplets ranging from ~ 300 to ~ 400 nm, within 200 minutes, using both devices separately. Styrene produced slightly larger droplets than butyl methacrylate due to its more hydrophobic nature (i.e. its higher interfacial tension (Equation 2)).

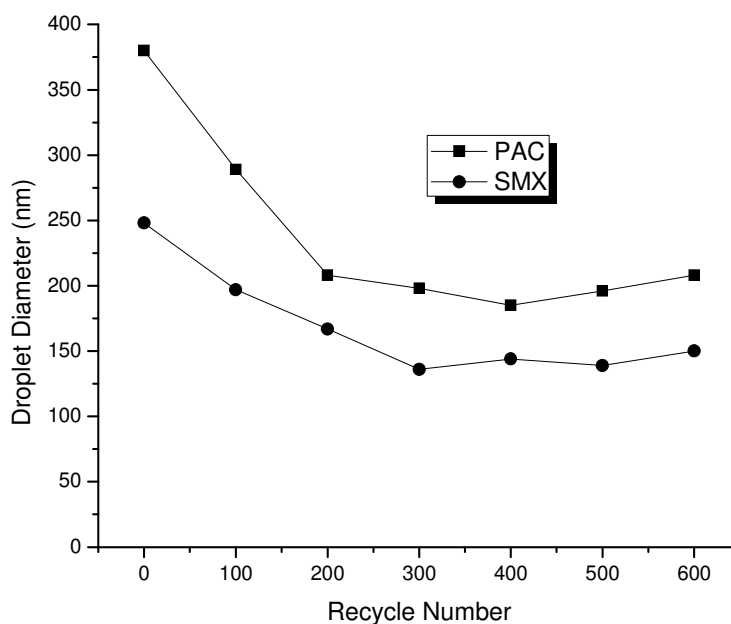


**Figure 4.2** Evolution of the PDI for S2 droplets generated using the static mixer and the rotor-stator.

The polydispersity obtained with the rotor-stator remained relatively wide (~2.8) and leveled out quite early (t=20 minutes) during homogenisation. On the other hand, that of the static mixer continued to improve, resulting in a narrower distribution (~2.1) of droplets. We understand that these results are specific to this static mixer set up and that this is not a generalisation for all static mixer systems. The preliminary results shown in Figure 4.1 & 4.2 demonstrate that the rotor-stator configuration used does not enable us to obtain droplets as narrowly dispersed as those obtained with the static mixer set up. It is stipulated that the primary cause of this is due to the length of time that the droplets are

exposed to the high shear zone. When emulsifying in the rotor-stator, the emulsion needs to be constantly recirculated around the high shear zone; a recirculation process which cannot be controlled in batch operations. On the other hand, when emulsifying with the static mixers, the emulsion is uniformly exposed to the high shearing zone along both the axis and the length of the mixing bed, resulting in narrower distributions.

At this point we can conclude that applying the same formulation (S2) to both devices produced different results, suggesting that the makeup of the formulation plays to a certain extent a role in the droplet breakup. Farzi *et al.*<sup>[2]</sup> compared the same formulation to two different static mixers (SMX vs. PAC). Farzi *et al.* compared the emulsification of an MMA system with the 7 mm SMX to that obtained by a bank of polyacetal (PAC) in line mixers with geometry similar to that of a Kenic's mixer, using the same formulation and flow rate.



**Figure 4.3** Evolution of droplet sizes ( $D_v$ ) for a 38 % solids content MMA miniemulsion system homogenised with SMX and PAC separately at 114 g/s.<sup>[2]</sup>

It can be seen from Figure 4.3 that one formulation emulsified with two different mixers (see Figure 4.3), generated two different final droplet sizes; strongly suggesting that the geometry of the mixers plays a role, especially in determining the plateau of limiting droplet size. Additionally, the time to reach steady droplet size is approximately the same for both mixers, but that the droplets obtained with the polyacetal mixer are about 35% larger than those obtained with the SMX. The reason for the smaller droplet sizes obtained with the SMX mixers is mostly due to their basic geometry. SMX elements are compact elements with ample droplet breakage locations; inducing a higher pressure drop across the bed. The PAC mixers are helical in shape, larger void fraction (i.e. lower pressure drop) and for the most part, simply separate the two phases into progressively smaller striations. Due to the encouraging results obtained with the SMX mixers, we further investigated their emulsification efficiency by varying the surfactant concentration.

Miniemulsions with droplet diameters of ~110 and ~190 nm were prepared using formulations S1 and S2 respectively. The formulations were pumped through the SMX static mixers at a flow rate of 114 g/s and samples were taken from the reservoir every 7.5 minutes. Figure 4.4A shows the evolution of droplet size over time as a function of the SDBS concentration. Once the emulsification was complete, the miniemulsions were transferred and polymerised in a batch process (Figure 4.4B).

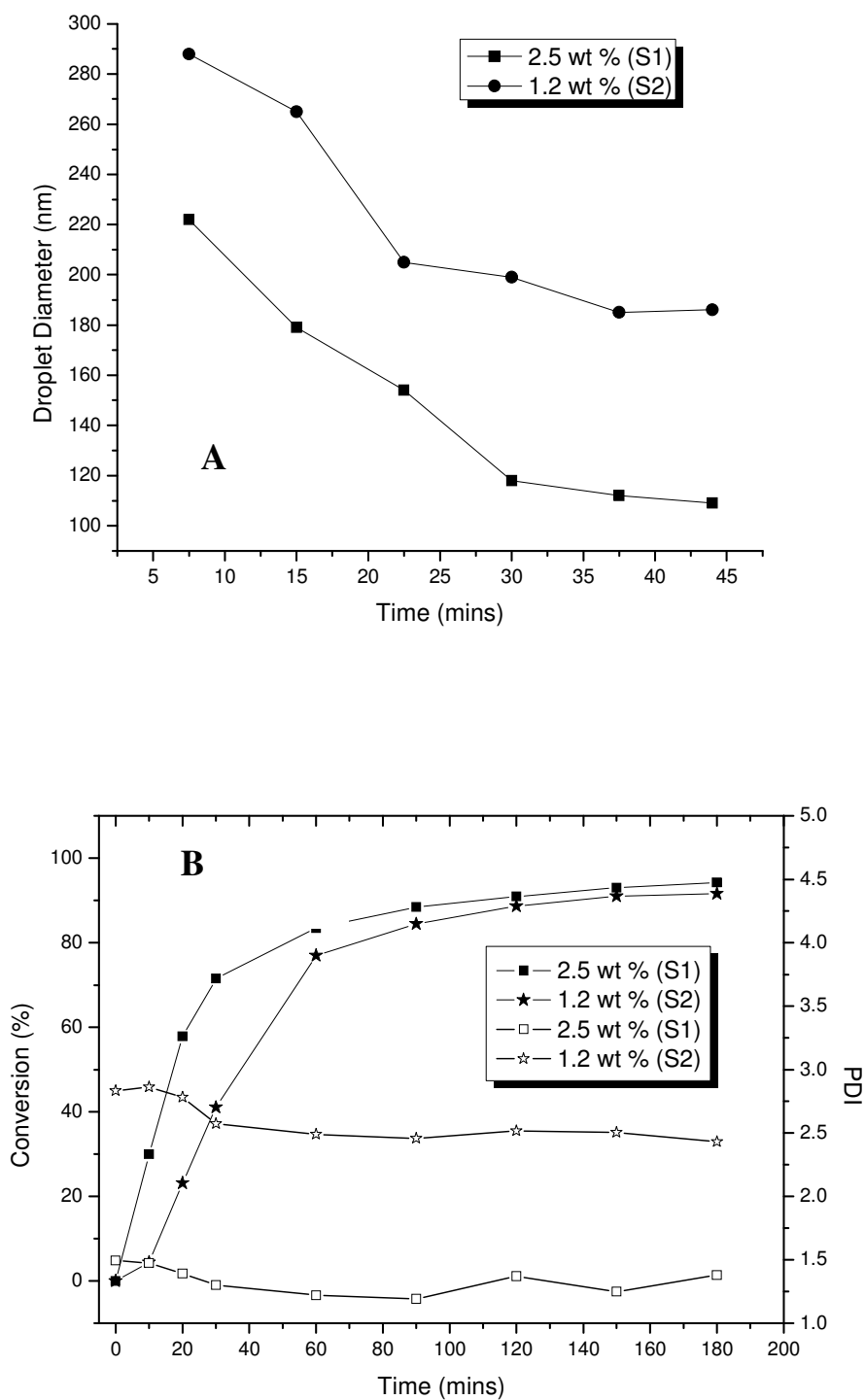
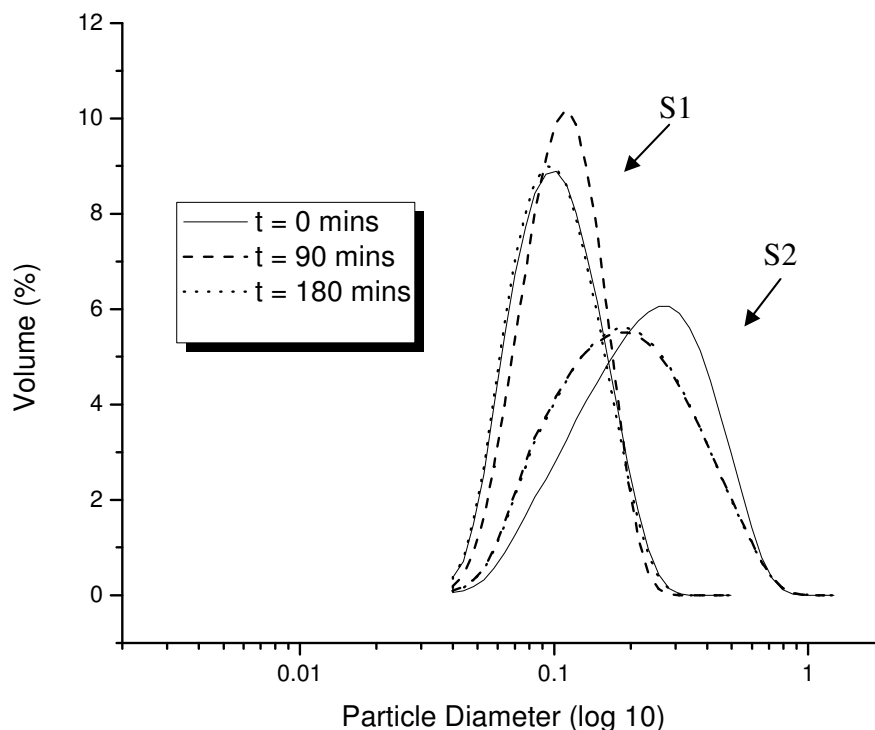


Figure 4.4 A - Evolution of droplet diameter ( $D_v$ ) over time as a function of the surfactant quantity.  
 B - Evolution of conversion and PDI as a function of time for formulations SM 1 and SM 2.



As Figure 4.4A shows, doubling the amount of surfactant in the system (while maintaining a constant flow rate of 114 g/s), generates smaller droplets (80 nm) with a narrower PDI (1.5 vs. 2.5; by static light scattering). The formulation consisting of 2.5 wt% SDBS produced ~ 110 nm droplets whereas the formulation with 1.2 wt% SDBS produced ~190 nm droplets after 45 minutes. The more the mixtures pass through the static mixers, the smaller the average droplet size. However, after a certain point (30 minutes) it becomes increasingly difficult to further reduce the droplet size, as can be observed by a mere 10 nm drop in droplet size in the last 15 minutes compared to ~100 nm drop in the first 30 minutes.

In both cases the non-polymerised droplet systems were found to be stable (little variation in the droplet diameter) for up to 6 hours. The miniemulsion systems were polymerised in a 2L batch reactor at 70°C using AIBN. The evolutions of conversions and PDI are shown in Figure 4.4B. In both cases we obtained ca. 90% conversion after 2 hours and maintained fairly constant PDI. The constant PDI suggests that nearly every droplet was converted to a polymer particle. The PDI (~1.5) is smaller for the system containing 2.5 wt% SDBS. However, even with less surfactant (SM 2) and consequently a wider distribution (PDI = 2.5), we managed to polymerise stable droplets as indicated by the fairly constant particle size distributions in the course of the polymerisations (Figure 4.5).



**Figure 4.5** Particle size distributions at 0, 90, and 180 minutes for the polymerised S1 and S2 formulations.

In Figure 4.5, we see the particle size distribution in the course of polymerisation of systems SM 1 and SM 2. There is little variance in the distributions at 90 and 180 minutes compared to the unpolymerised droplets at  $t = 0$  minutes suggesting predominant droplet nucleation. If any particles were created through secondary nucleation, they were not stable for a time period long enough to be observed. Overall, on the basis of preliminary results obtained using the SMX static mixers, it can be concluded that smaller droplets are generated in the SMX compared to the PAC and that adjusting surfactant concentration can lead to very good control of both droplet and particle size distributions.

### 4.3 CONCLUSIONS

The major focus of this work was to demonstrate the feasibility of using industry techniques to generate polymerisable dispersions of droplets. Using the static mixers it was possible to generate nano-sized droplets and polymerise them to obtain a nearly 1:1 mapping of droplets to particles for droplets as small as 110 nm at industrially relevant solids content. It was found that the average droplet size could be varied by changing the surfactant concentration. As was expected, the droplet size decreases as the surfactant concentration increases.

Based on preliminary results obtained using the SMX static mixers, it can be concluded that smaller droplets are generated in the SMX compared with the PAC and that adjusting the surfactant concentration can lead to very good control of both droplet and particle size distributions. Although these results are still preliminary, they demonstrate the potential of static mixers as miniemulsification devices. A further investigation for improving the emulsification process in terms of flow rates and formulations is required. A future topic will focus on the optimisation of the emulsification process by shortening the mixing time scale and developing a polymerisation process in line with the emulsification step.

#### 4.4 LITERATURE CITED

1. Ouzineb, K.; Lord, C.; Lesauze, N.; Graillat, C.; Tanguy, P. A.; McKenna, T. Homogenisation Devices for the Production of Miniemulsions. *Chem. Eng. Sci.* **2006**, *61*, 2994-3000.
2. Farzi, G. Ph.D. Thesis, Université Claude Bernard Lyon 1, **2008**.

## ***COMPARISON OF EMULSIFICATION DEVICES FOR THE PRODUCTION OF MINIEMULSIONS***

---

Droplets generated using ultrasonication, the rotor-stator and static mixers have been investigated in terms of power and energy consumption, droplet distributions and shear rates. It was observed that with energy costs being of similar orders of magnitude, the static mixers imposed less shear on the system making them the optimal choice for miniemulsification. Similarly, the absolute widths of the distributions for droplets generated with the sonicator and rotor-stator were larger than those generated with the static mixers and during polymerisation underwent secondary nucleation.

## 5.1 EXPERIMENTAL

### 5.1.1 MATERIALS

Deionised water was used for all experiments. The monomers used are methyl methacrylate (MMA) (Aldrich, 99%) and butyl acrylate (BA) (Aldrich, 99%). The surfactant used was sodium dodecylbenzene sulphonate (SDBS) (Acros, 88% technical grade). The costabiliser used was octadecyl acrylate (ODA) (Aldrich, 97%). The initiator used was 2,2'-azobisisobutyronitrile (AIBN) (Acros, 98%) and was added directly to the organic phase. AIBN was used throughout all polymerisation in order to minimize the amount of secondary nucleation which is typical of common water-soluble initiators (e.g., persulfates). For all runs, the same formulations and volume were used (see Table 5.1).

**Table 5.1 Formulation used for emulsifications using the RS, SM and US.**

Component	Amount (g)
Methy Methacrylate	84
Butyl Methacrylate	84
Octadecyl Acrylate	18
Sodium Dodecylbenzene sulphonate	3.6
2,2'-Azobisisobutyronitrile	0.6
Deionised Water	250

### 5.1.2 HOMOGENISATION

#### 5.1.2.1 ULTRASONICATION

The oil and aqueous phase were combined in an 800 mL beaker with a magnetic stir bar. The mixture was kept cool in a large ice bath placed on a magnetic stir plate set at 10 Hz. The coarse emulsion was sonicated using a VC 750 Vibra-Cell Ultrasonic Processor with a fixed frequency of 20 kHz using a 0.025 m solid high gain probe. The sonication probe

was immersed into the coarse emulsion and set approximately 0.03 m from the bottom of the beaker. The amplitude of the sonicator was set at 80%, equivalent to an amplitude of 28  $\mu\text{m}$  that is delivered to the tip. Samples were removed every minute for 4 minutes. Emulsifying beyond 4 minutes did not generate smaller sized stable droplet systems. Only a small region near the sonication tip is affected by these ultrasonic waves, therefore, the emulsion was circulated using a stir bar to ensure homogeneous exposure to the sonication tip.

#### 5.1.2.2 ROTOR-STATOR

The bench top mixer used in this study was a VMI Rayneri TURBOTEST rotor-stator. It features a digital display, speed range of 1-55 Hz (50-3300 RPM), and a mixing capacity ranging from 200 mL up to 20 L. The mixing unit also includes a beaker clamp and a height sensor for safety purposes. Two rotor-stator heads were used for emulsifications. The first stator head measured at 5.5 cm in diameter and was equipped with four blades angled at 90°. The stator head had 23 vertical slits along the side and 8 circular slots along the top. The second stator head measured at 7.5 cm in diameter and was equipped with six blades angled at 30°. The stator head had 30 vertical slits along the side and 8 circular slots along the top.

The aqueous and organic phases to be emulsified were combined in a 2 L polycarbonate vessel with baffles. Baffles were required as it was realized in previous work that they prevent vortex formation and force the phases to combine (see Chapter 3). Both emulsification processes were operated at 50 Hz (3000 RPM), and the solution vessels were chilled with ice baths to prevent excessive heating and potential degradation

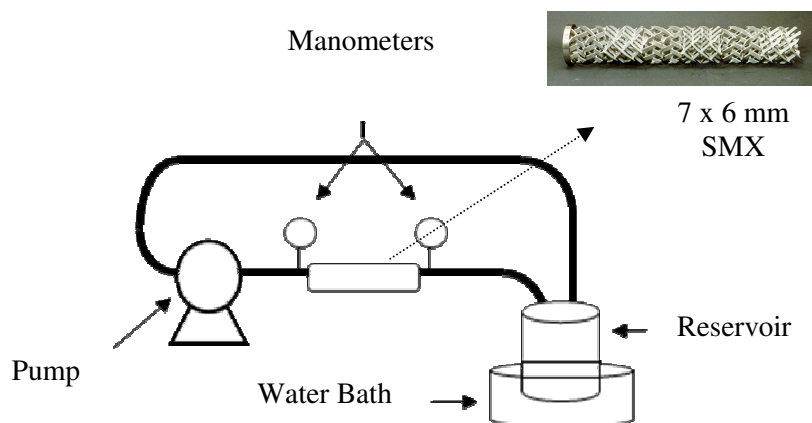
of the miniemulsions. Samples were removed every 10 min. The emulsification process was completed when very little change in droplet size, in successive measurements, was observed. The cleaning procedure included the following: removing and emptying the mixing vessel contents and immersing the mixing heads in cleaning solvent so that the slits and the blades are thoroughly cleaned.

#### 5.1.2.3 STATIC MIXERS

The SMX static mixers used throughout the work presented here were supplied by Sulzer Chemtech Ltd. Seven 6 mm SMX mixers were bound together with each element rotated 90° from the previous. Each element contained six cross bars aligned at 45° to the axis of the pipe. Each element has a length to diameter ratio of one.

The elements were fitted flush within a stainless steel pipe. The mixing elements were installed in a closed loop system consisting of a pump, tubing, reservoir tank, and water bath (Figure 5.1). The pump used was a positive displacement gear pump from Viking Pump. The aqueous and organic phases were combined in a 2 L reservoir vessel. The mixture was pumped through at a flow rate of ~ 0.05 kg/s and samples were removed from the reservoir vessel every 7.5 minutes. The pressure drop over the mixing elements was measured using manometers placed at both the entry and exit of the tubing. Once the emulsification was complete, the miniemulsion was pumped through to the reactor.





**Figure 5.1 Homogenisation set up for the static mixers. A closed loop system consisting of a pump, tubing, product reservoir and temperature bath.**

### 5.1.3 POLYMERISATION

Polymerisations were carried out in a 1 L glass unbaffled, jacketed reactor equipped with a reflux condenser, a nitrogen inlet, an anchor stirrer, and a sampling port. All polymerisations were carried out at 70 °C. The temperature was controlled using a thermostatted bath. The agitator speed was set to 5 Hz. Initially the homogenised mixture was purged with nitrogen at room temperature for ~20 minutes to remove any dissolved oxygen. Droplet size measurements were taken after purging to verify that no droplet coalescence took place during purging. Once purging was complete, the temperature of the bath was increased to 70 °C. The reaction was considered to begin the moment when the reactor reached 70 °C ( $t = 0$ ). Samples were taken every 10 min for the first 30 min and then every 30 min for the remainder of the experiment. All reactions were run for 2.5 hours.

### 5.1.4 CHARACTERISATION

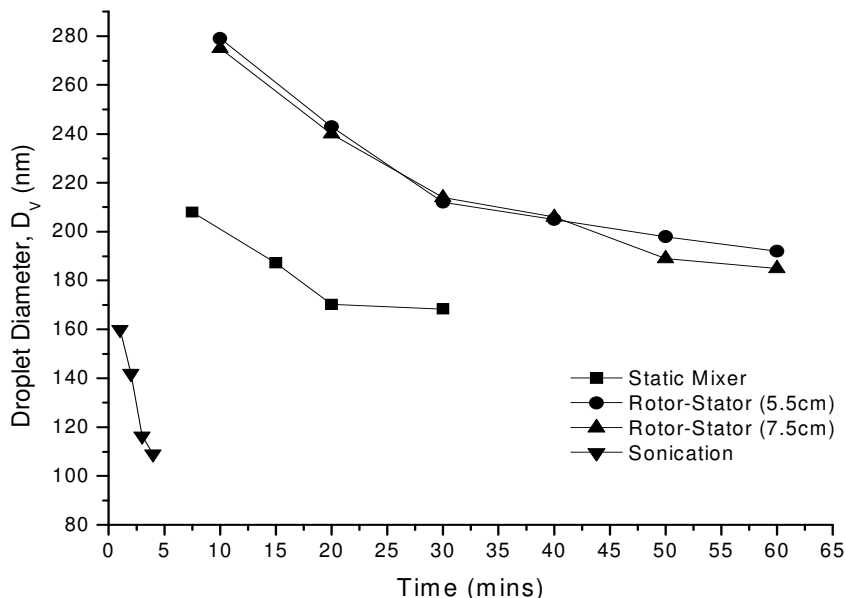
Droplet and polymer particle diameters were measured using the Malvern Zeta-Sizer

Nano ZS. Samples were diluted with deionised water plus surfactant in concentrations beyond the CMC (critical micelle concentration). The polydispersity index provided by the Malvern Zeta-Sizer was based on the  $z$ -average droplet diameter (mean diameter calculated from Brownian motion); values of 0.15 and less suggested a homogeneous distribution. For all runs, conversion was measured gravimetrically (See Appendix A1).

Light scattering is a very common technique for droplet and particle size measurements in emulsion and miniemulsion studies. Samples are typically diluted in saturated mediums in order to enhance their stability during measurements. Typically for the results presented throughout this thesis, a sample is analyzed several times and the averages of all the measurements are reported. Measurements are repeated several times over a period of a couple hours and when the droplet or particle sizes vary by  $\pm 5$  to 10 nm, the droplet or particle is reported to be 'stable'. For a more thorough and in-depth review of light scattering theory and standard operating procedures and parameters, the reader is referred to the online manual available at <http://www.malvern.com/>.

## 5.2 RESULTS AND DISCUSSION

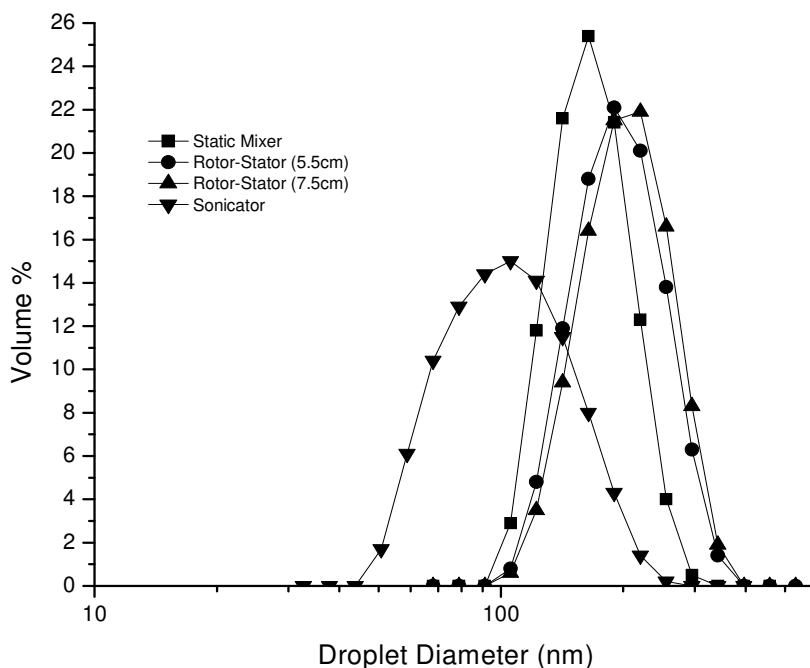
The ability of three emulsification devices to generate miniemulsions was assessed using a standard formulation (outlined in Table 5.1). The droplet size evolutions is reported in Figure 5.2, where it can be seen that the performance of the three devices varied, both in terms of required emulsification time (1 to 60 minutes) and final volume average droplet diameter (100-200 nm). The emulsification processes were considered complete, once very little change in stable droplet sizes, in successive measurements, was observed.



**Figure 5.2** Droplet diameter evolutions for miniemulsions generated using the rotor-stator (5.5 and 7.5 cm stator head), static mixer and sonicator

It is well known that the combination of a stabilisation system (surfactant and costabiliser) and the emulsification procedure influence droplet formation. However throughout the work presented here, the formulation remained the same in order to investigate the extent of emulsification and the effect of residence time in the emulsification/rupture zones of each device. The same formulation applied to three different devices produced different results. In the case of the rotor-stator there appears to be no difference in the evolution and final droplet size of miniemulsions generated using the 5.5 or 7.5 cm head at a constant rotational speed of 50 Hz. It can be seen that after 60 minutes of high speed shearing in the rotor-stator the smallest obtainable droplet diameter ranges from approximately 180 to 200 nm in size. The sonicator and static mixer produced smaller droplets. With the 6 mm SMX static mixers, 170 nm droplets were generated after 30 minutes of emulsification while the sonicator produced 110 nm

droplets in only 4 minutes. The final droplet size distributions for the miniemulsions created using the three different emulsification devices can be seen in Figure 5.3.



**Figure 5.3** Final volume average droplet size distribution for miniemulsions generated using the rotor-stator, static mixer and sonicator.

The polydispersity index was below 0.15 in all of the trials presented here. From visual analysis of the four distributions, the absolute widths of the distributions appear to be dissimilar (Figure 5.3). Final average droplet size distribution for miniemulsions generated using the rotor-stator range from 100 to 400 nm, for the sonicator they ranged from 40 to 300 nm, while those of the static mixer ranged from 100 to 300 nm. One striking point is that the sonicator generates a large population of very small droplets. Comparing the distributions of the static mixer and rotor-stator, they both start at similar points however there are much larger droplets generated with the rotor-stator than static

mixer, suggesting that the static mixers are more efficient at breaking larger droplets and generating tighter distributions.

What can be concluded from Figures 5.2 and 5.3 is that different homogenisation devices produce different results using the same formulation and volume, as expected. This is not simply a difference in the amount of work done on the system as was shown previously with the rotor-stator where the formulations were emulsified for an extended period of time to no avail (see Chapter 3); after a certain point droplet sizes do not change. This could be attributed to the amount of energy input and the method/conditions of droplet formation of each device (Table 5.2).

Larger droplets are produced with the rotor-stator than the static mixer, and larger droplets are generated with the static mixer than those generated with the sonicator, and from Figure 5.3 we can see that the tightest distribution is generated with the static mixers. The amount of power and energy required to generate the droplets varies a great deal from one device to the next. The power input needed by the rotor-stator is based on the torque and the frequency as follows:

$$P_w = 2\pi N\tau \quad (8)$$

Where,  $N$  is the revolutions per minute in Hz and  $\tau$  the torque in N·cm. The amount of power required for the static mixer is dependent on the pressure drop along the length of the mixing bed and the flow rate:

$$P_w = \Delta P \times Q \quad (9)$$

Where  $\Delta P$  is the change in pressure along the length of the 7 elements and  $Q$  is the flow rate (kg/s).

The amount of power required to generate droplets using the sonicator in this study is 80% of the maximum power output of the sonicator. The difference between the power inputs required for the three homogenisation devices is reported in Table 5.2. The total amount of energy required for emulsification and the amount of shear imposed is also reported. The energy required is a product of the power input and the respective time of emulsification in each device needed to generate droplets ranging between 160 to 200 nm.

**Table 5.2** Estimation of the amount of power and energy required by the rotor-stator, static mixer and sonicator to generate droplets ranging between 160-200 nm. The quantity used for all emulsifications was consistent throughout, totaling 0.42 kg.

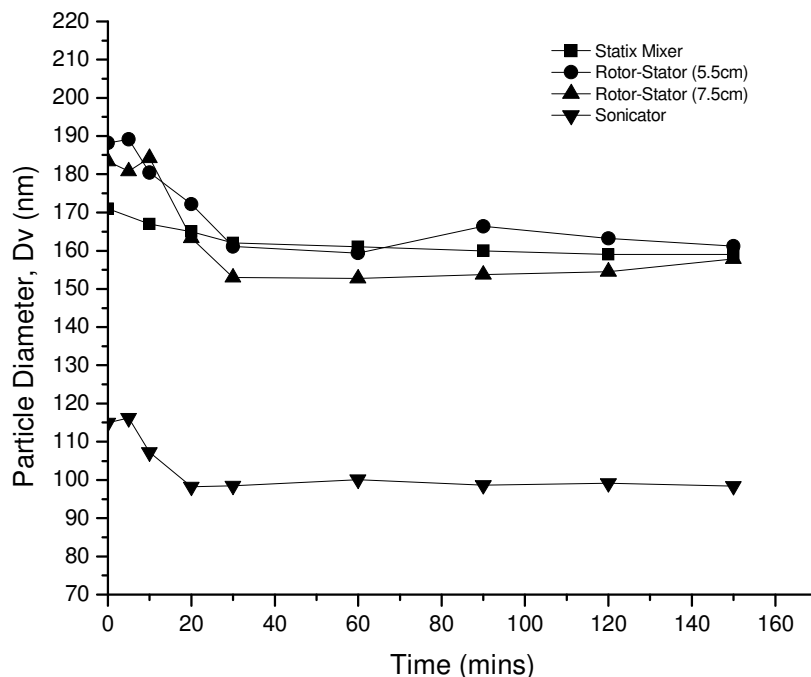
<b>Device</b>	$D_v$ (nm)	$N$ (Hz)	$\tau$ (Ncm)	$\Delta P$ (bar)	$Q$ (kg/s)	% Amplitude	$P_w$ (W)	Emulsification Time (min)	Energy (J/kg)	Magnitude of Shear ( $s^{-1}$ )
Static Mixer	170	--	--	6.7	0.051	--	37	30	$1.6 \times 10^5$	$10^3$
Rotor-Stator (5.5 cm)	192	50	22	--	--	--	69	60	$5.7 \times 10^5$	$10^4$
Rotor-Stator (7.5)	185	50	11	--	--	--	50	60	$4.3 \times 10^5$	$10^4$
Sonicator	156	--	--	--	--	80	600	1	$8.6 \times 10^4$	$10^6$ - $10^{7(5)}$

An exact comparison between each device may not be entirely suitable as the droplets generated vary by 50 nm in diameter. However with energy costs being of similar orders of magnitude or less compared to the rotor-stator or sonicator, the static mixers impose less shear on the system making them the optimal choice for miniemulsification. Improvements on the static mixer homogenisation process, including optimisation of the miniemulsion formulation, are the focus of future work.

It should be pointed out that similar droplet diameters are generated with the two different rotor-stator heads, yet when using the 5.5 cm stator head much more power (and energy) is required to homogenise the system, possibly due to the geometry of the 7.5 cm head. Furthermore, to generate droplets larger in size with the rotor-stator than those generated by the static mixer, the rotor-stator would need to run for approximately an hour compared to a residence time of 30 minutes with static mixer resulting in significant difference in energy consumption.

The miniemulsions generated with the various emulsification devices were polymerised in a one litre batch reactor. As can be seen in Figure 5.4, the miniemulsions generated with the more shear intensive emulsification devices underwent secondary nucleation supported by a decrease in particle size and a 30 to 50% increase in the number of particles relative to the number of droplets (See Appendix A2 & A3) at the beginning prior to polymerisation. Miniemulsions generated using the static mixers appeared to polymerise in a controllable manner with a nearly one to one mapping of droplets to particles supported by a relatively constant particle size and ratio of the number of particles to the number of droplets ( $\pm 5\%$ ).





**Figure 5.4** Particle diameter evolutions for miniemulsion prepared using the rotor-stator, static mixer and sonicator.

The reason for the renucleation is not entirely clear. The results would suggest that it is not necessarily the droplet size (and consequently the surfactant surface coverage) that determines whether the system will renucleate; as droplets both larger and smaller than those generated with the static mixer renucleated upon polymerisation (Figure 5.4). Rather, droplets that were generated using the more shear intensive devices underwent renucleation. A possible explanation could be that there are events occurring during the homogenisation process (using the more shear intensive rotor-stator and sonicator) that cannot be detected using light scattering techniques. During droplet breakage, the formation of satellite droplets in addition to small daughter droplets is very likely, however the ability to detect their presence using light scattering is questionable. There is a high probability that the population of satellite droplets is too small to detect

by number or volume fraction yet their presence is significant enough to veer the nucleation process from the desired droplet nucleation which is characteristic of miniemulsion polymerisation.

### 5.3 CONCLUSIONS

As can be seen from the results presented above, droplets ranging from 100 to 200 nm can be generated using a rotor-stator, static mixer and sonicator. However, there is a difference in the amount of shear imposed by each device and the amount of energy required to generate the droplets. As mentioned above, a commercially viable technique should be economically and energy efficient and from the results tabulated in Table 5.2, the static mixer requires the least amount of energy to operate and imposes the least amount of shear generating a narrower droplet distribution in a reasonable amount of time and are stable during polymerisation.

Static mixers offer the added advantages over the other homogenisation devices examined in this paper as they are cheaper to operate (power/energy costs), clean and install (not to mention to purchase). Rotor-stators present a viable option for manufacturers that already have existing equipment and do not want to invest in the equipment and infrastructure required for setting up a static mixer loop. Nevertheless, the installation of static mixers requires only basic engineering knowledge and the only power required is that of a pump. The process is simplified a great deal if they are installed in-line with existing pumps. Operating in a closed loop system eliminates the need for vessels, or agitators. They require very little maintenance as there are no moving parts, further strengthening their case as commercially viable miniemulsification devices.

## ***MINIEMULSIONS VIA IN SITU SURFACTANT GENERATION***

---

The preparation and stabilisation of miniemulsion systems using *in situ* generated surfactants is presented. Neutralizing a water-soluble base with an oil-soluble long chain acid almost instantaneously generates *in situ* surfactants at the oil-water interface, allowing a more rapid reproducible homogenisation/polymerisation process compared to using preformed conventional surfactants. As surfactant concentration (using either form of KSA) increases, the average droplet size decreased, with slightly larger droplets formed using preformed KSA. In addition, a limit in terms of solubility was encountered with preformed KSA, which was avoided when using *in situ* KSA. Furthermore, as

solids content increased (40 to 60%) the droplet size increased (100 to 185 nm). The role of *in situ* KSA functioning as both a surfactant and costabiliser was investigated. It was determined that *in situ* KSA is not capable of simultaneously serving the dual role but the presence of stearic acid (SA) in the droplets contributes to the stability of the droplets, reducing the rate of ripening. A variety of *in situ* generated surfactants were prepared with different carboxylic acids and bases. It was observed that the average droplet size decreased with decreasing hydrated radius of the surfactant counterions, as expected since more counterions collect at the interface for a smaller hydrated radius.

## 6.1 EXPERIMENTAL

### 6.1.1 MATERIALS

The monomers used were methyl methacrylate (MMA) (Aldrich, 99%) and butyl acrylate (BA) (Aldrich, 99%). The costabiliser used in all formulations was octadecyl acrylate (ODA) (Aldrich, 97%). Preformed surfactants used were sodium dodecylbenzene sulphonate (SDBS) (Acros, 88%) and potassium stearate (*p*KSA) (Acros, 95%). A number of carboxylic acids were used throughout the study presented (Table 6.1), including: behenic acid (docosanoic acid, DA) (Eastman Kodak), stearic acid (octadecanoic acid, SA) (Aldrich, 95%) and lauric acid (dodecanoic acid, LA) (Aldrich, >98%).

**Table 6.1 Formula and molecular weight of behenic, stearic and lauric acid.**

Carboxylic Acid	Linear Formula	Molecular Weight (g/mol)
Behenic Acid	$\text{CH}_3(\text{CH}_2)_{20}\text{COOH}$	340.58
Stearic Acid	$\text{CH}_3(\text{CH}_2)_{16}\text{COOH}$	284.48
Lauric Acid	$\text{CH}_3(\text{CH}_2)_{10}\text{COOH}$	200.32

The bases used were potassium hydroxide (KOH) (Aldrich,  $\geq 90\%$ ), sodium hydroxide (NaOH) (Aldrich, 97+%) and lithium hydroxide (LiOH) (Aldrich, 98+%); solubility data are given in Table 6.2. All polymerisations were initiated using 0.06 wt% (with respect to monomer mass) water-soluble potassium persulphate (KPS) (Acros, 98%). Water deionised with a Millipore® unit (resistivity of 18.5 M $\Omega$ ·cm at 25 °C) was used for all experiments. All materials were used as received.

**Table 6.2 Solubility and molecular weight data for potassium, sodium and lithium hydroxide.**

Base	Solubility in 0.1 L H <sub>2</sub> O (20 °C)	Molecular Weight (g/mol)
KOH	0.12 kg	56.11
NaOH	0.10 kg	39.99
LiOH	0.013 kg	23.95

Miniemulsions were prepared according to formulations listed in Table 6.3, unless otherwise indicated. In formulation FM 1, the surfactant was generated *in situ* whereby the organic phase consisted of monomer, costabiliser and carboxylic acid; the alkali base was dissolved in the aqueous phase. The phases were left to mix for approximately 5 minutes at room temperature to allow the neutralisation of acid and base to take place. For formulation FM 2, the organic phase consisted of the monomers and costabiliser and the preformed surfactants were dissolved in the aqueous phase. In the case of preformed KSA, the solution required elevated temperatures to dissolve the surfactant ( $> 50$  °C).

**Table 6.3 Miniemulsion formulations containing MMA and BA in a 50:50 w/w ratio, ODA and either *in situ* generated (FM 1) or preformed surfactant (FM 2).**

Sample	DIW (g)	MMA (g)	BA (g)	ODA (g)	Preformed surfactant (mmol)	Acid (mmol)	Base (mmol)
FM 1	250	84	84	11.6 (35 mmol)	--	9.0	13.5
FM 2	250	84	84	11.6 (35 mmol)	9.0	--	--

### 6.1.2 HOMOGENISATION

In the initial part of the investigation, a rotor-stator was used to demonstrate the efficiency of each stabilisation system used due to the longer time scales required to generate droplets. The rotor-stator was a VMI Rayneri TURBOTEST with a rotational speed range of 50 to 3300 RPM. The stator head was equipped with 4 blades angled at 90° and measured at 5.5 cm in diameter. The stator had 23 vertical slits along the side and 8 circular slots along the top. The aqueous and organic phases were combined in a 2 L glass jacketed vessel with baffles and homogenised. Appropriate sample volumes were withdrawn and periodically tested.

For the remainder of the investigation, droplets were generated using ultrasonication. The oil and aqueous phases were combined in an 800 mL beaker with a magnetic stir bar. The solution was cooled in a large ice bath on a magnetic stir plate set at 600 RPM. The emulsion was sonicated using a VC 750 Vibra-Cell Ultrasonic Processor with a 2.5 cm solid high gain probe at 80% amplitude (600 W) for 4 minutes; samples were taken every minute.

### 6.1.3 POLYMERISATION

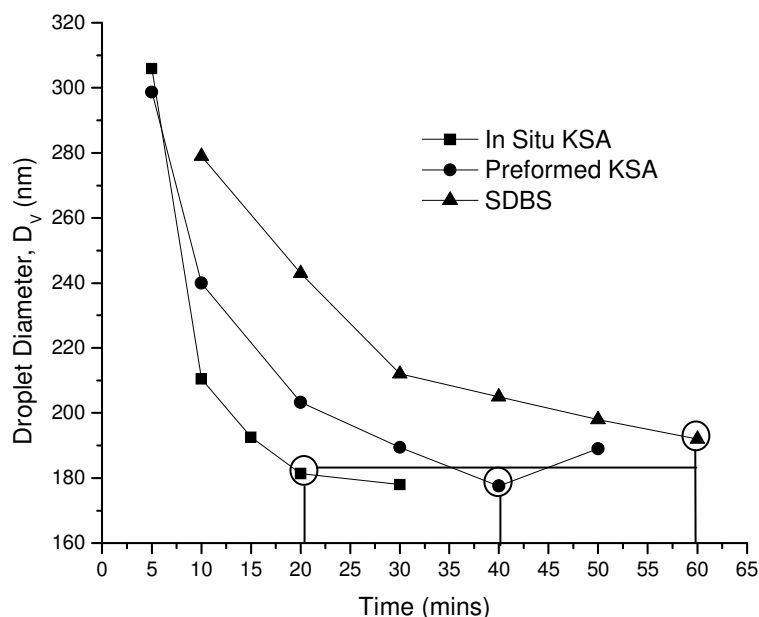
Polymerisations were carried out in a 1 L glass, unbaffled, jacketed reactor equipped with a reflux condenser, a nitrogen inlet, an anchor stirrer (set at 300 RPM) and a sampling port. All polymerisations were initially purged with nitrogen (25 minutes) and then heated to 70 °C, with temperature controlled using a thermostatted bath. The initiator solution was injected when the reactor reached 70 °C ( $t = 0$  min). Samples were withdrawn at  $t = 0, 5, 10, 20$  and 30 minutes and then every half hour for the remainder of the experiment. All reactions were run for 2 hours.

#### 6.1.4 CHARACTERISATION

Droplet and particle diameters were measured using a Malvern Zeta-Sizer Nano ZS (dynamic light scattering). Samples were diluted in an SDBS solution in concentrations above the CMC to maintain stability of droplets. Light scattering measurements showed no sign of micelles. The polydispersity index provided by the Malvern Autosizer is based on the z-average droplet diameter (mean diameter calculated from Brownian motion); values of 0.15 and less suggest a monomodal distribution. For all runs, conversion was determined gravimetrically.

### 6.2 RESULTS AND DISCUSSION

In the initial phase of the investigation, three emulsifications were performed using the rotor-stator and formulations FM 1 and 2 (Figure 6.1). Formulation FM 1 contained stearic acid in the organic phase and potassium hydroxide in the aqueous phase. It was assumed that if the entire amount of acid was neutralised then 9.0 mmol of potassium stearate (KSA) would have been produced at the interface. Two FM 2 formulations were prepared containing 9.0 mmol of the preformed equivalent potassium stearate (*p*KSA) and the commonly used surfactant SDBS, separately.



**Figure 6.1** Droplet size evolutions for droplets prepared with a rotor-stator (3000 RPM) using equal amounts (9.0 mmol) of preformed KSA, *in situ* KSA or SDBS. (○ = minimum droplet size)

The *in situ* case was run using a 2:3 mole ratio of stearic acid to potassium hydroxide. The amount of base was increased by approximately 50% over the stoichiometric requirement (FM 1 as listed in Table 6.1) to ensure near complete neutralisation of the acid. This simple change allowed us to generate a stable, monomodal distribution ( $D_v \sim 130$  nm) which could be polymerised successfully. Doubling the amount of base did not further decrease the droplet size or enhance the already sufficiently stable droplet system. Therefore for the remainder of the work presented here, miniemulsions were prepared using a 2:3 molar ratio of stearic acid to potassium hydroxide.

Figure 6.1 shows droplets prepared with *p*KSA (FM 2) decreased gradually in size with homogenisation time, eventually reaching a minimum droplet size ( $\sim 180$  nm) in approximately 40 minutes. When SDBS was used as the surfactant, the final droplet size



was slightly larger (~ 190 nm) and 50% more time was needed to achieve this result. The final droplet size for the *in situ* KSA is very close to that obtained using an equivalent amount of *p*KSA (~ 180 nm), however, the important difference is the emulsification time. It takes approximately half the time (20 minutes) to reach a steady droplet size distribution with the *in situ* KSA than with the *p*KSA. Furthermore, the fact that the droplets are of the same size for both formulations suggests that the same amount of surfactant is available on the surface of the droplets in both cases. For this reason, our earlier assumption that the bulk of the carboxylic groups on the surface of the particles is neutralised seems to be supported.

The results first suggest that either form of KSA required less time to reach minimum droplet size than the widely used SDBS and second, surfactants prepared *in situ* stabilise droplets faster than preformed surfactants. When homogenizing with the rotor-stator, surfactant molecules experience highly turbulent flows near the rotor-stator head. Moving farther away from the head, the flow regime can change to a transitional/laminar environment and as a result the rate at which the surfactant molecules travel to and collide with the new surfaces varies, ultimately varying the rate of adsorption of the surfactant molecules to the interface. When homogenizing with *in situ* generated surfactant, interfacial neutralisation leads to effective mixing on small length scales (even in the absence of external shear forces), stabilizing newly formed surfaces faster than is the case with the transport and adsorption of a preformed surfactant. The easy access to the interface, due to the short distance for travel, reduces the amount of coalescence during droplet breakage and the time to reach a minimum stable droplet size, ultimately improving the homogenisation process.

### 6.2.1 INCREASING SURFACTANT CONCENTRATION

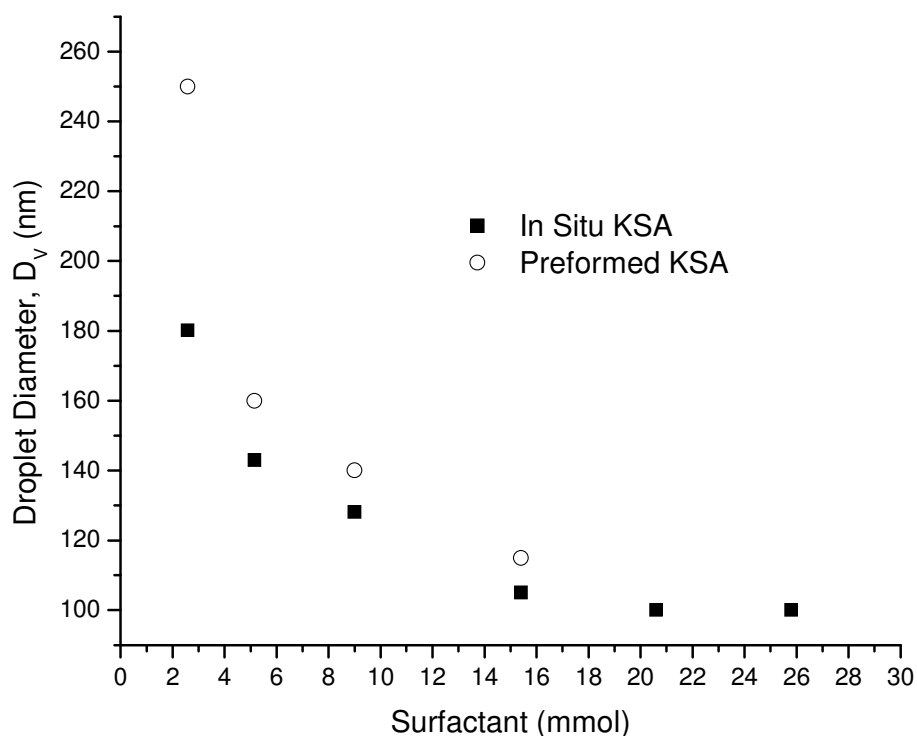
The use of the rotor-stator for the above investigation was ideal due to the longer time scales required to emulsify, clearly pointing out the differences between each stabilisation system. However, for the remainder of the investigation, emulsifications were performed using ultrasonication due to its simplicity and rapidity. We next investigated the effect of increasing the *in situ* and preformed KSA concentration on the droplet diameter for systems homogenised using ultrasonication (Figure 6.2). The stability of miniemulsion droplets is dependent on the mobility and adsorption/reaction efficiency of the surfactant molecules. However, the droplet sizes are also determined by the amount of surfactant available at the interface. Increasing the surfactant concentration lowers the interfacial tension ( $\gamma$ ) in the system resulting in an overall increased surface area ( $\Delta A$ ) and hence smaller droplets for systems exposed to the same amount of shear ( $W_{\text{Breakage}}$ ; the energy required to break/form an interface) (Equation 2).

$$W_{\text{Breakage}} = \gamma \times \Delta A \quad (2)$$

In the case of carboxylate anions, the interfacial tension is strongly dependent on the solution properties, which are dominated by the pH of the system and subsequently the carboxylate species formed.<sup>[1,2]</sup> As the pH of the system increases, carboxylic acids begin to form a range of molecular complexes such as protonated anions, dimers and soaps (if neutralised). Each complex contributes a certain surface activity and depending on the ratio of the species available, their presence strongly influences the interfacial properties.<sup>[2]</sup> Attempts were made to buffer the system and measure interfacial tension between the oil and water phase, in order to examine the extent of these non-idealities and to determine the CMC. However, the static interfacial tension measurements made

were inconsistent and could not be reported here with absolute confidence. Additionally, the hydrophobic character of KSA makes it virtually impossible to perform interfacial tension measurements at room temperature. Zacccone *et al.* heated the particle system to 65 °C and centrifuged the particles; surface tension measurements were then performed on the supernatant and the CMC was found to be  $\sim 10^{-5}$  M.<sup>[3]</sup>

Starting with formulations FM 1 and FM 2, the *in situ* and preformed surfactant concentration was varied. Formulations containing amounts ranging from 2.5 to 25.8 mmol of *in situ* KSA and 2.5 to 15.5 mmol of preformed KSA were sonicated at 600 W for 4 minutes (Figure 6.2).



**Figure 6.2** Droplet size evolutions for miniemulsions at 40 % solids content prepared with varying amounts of *in situ* and preformed potassium stearate (assuming 100% neutralisation) and emulsified using an ultrasonic dismembrator for four minutes.

As expected, droplet size decreased with surfactant concentrations to a lower limit of  $\sim 90$  nm. Droplets ranging in size from 180 to  $\sim 90$  nm were obtained when using *in situ* KSA; however, we were only able to go as small as  $\sim 110$  nm with preformed KSA. Overall, preformed KSA generated slightly larger droplets but the differences in droplet sizes at similar surfactant concentrations are negligible and can partially be attributed to small errors during dynamic light scattering measurements. Possible concerns with respect to the actual amount of carboxylic acid groups neutralised during the acid-base reaction has been addressed since similar droplet sizes were obtained at similar *p*KSA concentrations. Similarities in droplet size at similar surfactant concentrations suggest that the interfacial tension values would also be comparable. Similarly, surfactant surface coverage's were roughly estimated to range from  $\sim 5$  to  $\sim 30\%$ , for droplets prepared with 2 to 25.8 mmol respectively, using a surface per molecule value of  $26 \text{ \AA}^2$ ; a value which was estimated for a styrene-acrylate system.<sup>[3]</sup> Additionally, a limiting factor when using *p*KSA is that concentrations greater than 15.5 mmol were insoluble in the aqueous phase at elevated temperatures; an issue which was not encountered with *in situ* KSA dissolved at room temperature. All miniemulsions were stable (little change in droplet size) for up to several hours. Hydrophobic surfactants offer the added advantage of preferentially residing on the hydrophobic surfaces due to the low aqueous solubility, thus enhancing droplet stability. Miniemulsions prepared with *in situ* KSA were subsequently polymerised using the water-soluble initiator KPS (Figure 6.3).

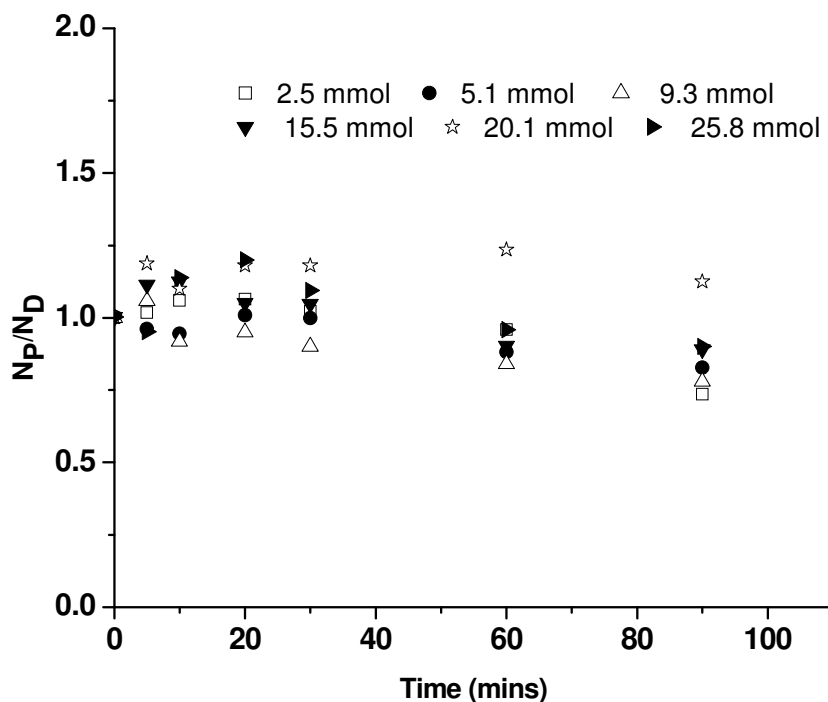


Figure 6.3 The ratios of the number of particles to the number of droplets throughout the polymerisations for systems prepared with *in situ* KSA ranging in amounts from 2.5 to 25.8 mmol.

In all cases, conversion reached 90 to 95% within two hours of polymerisation. No attempt was made to go higher than this in the current work as the major objective was to demonstrate that they can be polymerised in a controllable manner. Droplet diameters ( $D_V$ ) were measured and used to calculate the ratio of  $N_P/N_D$ . Miniemulsions consisting of up to 15.5 mmol of *in situ* KSA appeared to polymerise in a nearly one to one mapping of droplets to particles ( $N_P/N_D = 1$  within  $\pm 5$ -10% and with a relatively constant particle size). Systems containing 20.1 and 25.8 mmol *in situ* KSA underwent secondary nucleation, as evidenced by a 10 to 20% increase in the number of particles relative to the number of droplets. Whether the increased particle number is from micellar or homogeneous nucleation is unknown and remains to be answered in future

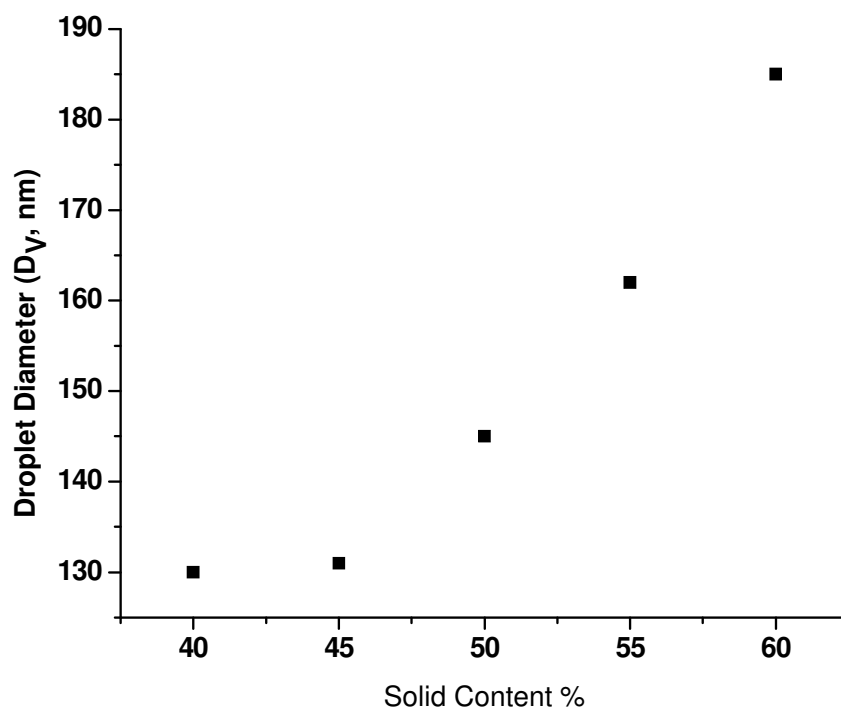
contributions. It should be pointed out that  $> 20$  mmol (with respect to monomer) of surfactant is excessive and the fact that there is some secondary nucleation when using MMA is not surprising. Typically, the aim is to incorporate  $\sim 2$  wt% (9.0 mmol) (with respect to monomer) in the formulation to avoid complications from secondary nucleation of new particles during the polymerisation step, or at least to avoid stabilizing them if they occur, in addition to undesirable properties such as foaming in the final product. Minimizing the free surfactant concentration in the reactor is one way to do this.

The hydrophilic nature of formulation FM 1 was also varied by adjusting the ratio of the monomers used for a given amount of work ( $W_{\text{Breakage}}$ ). Switching to MMA alone, a more hydrophilic monomer than BA, we were able to generate 80 nm droplets with sonication at 600 W for 4 minutes. By comparison, at the same sonication conditions, 130 nm droplets were generated for a system containing 50/50 MMA:BA and 160 nm droplets were generated for a system containing BA alone.

### 6.2.2 INCREASING SOLIDS CONTENT

The relationship between solids content and droplet size/stability is of particular interest for commercial applications. High solids content systems ( $\geq 45$ -50%) are desirable for industrial processes, due to reduction in transportation and storage costs as well as drying time. However, an increase in viscosity due to an increased number of particle-particle interactions can lead to problems during processing and application. Typically, a turbulent mixing environment is composed of eddies of assorted sizes. Kinetic energy contained within the larger eddies is cascaded down through to smaller and smaller eddies until it reaches the Kolmogorov length scale eddy. Droplets larger in size than any

eddy length scale are deformed and broken up, and droplets smaller than the Kolmogorov length scale travel unaffected throughout the system by eddy motion.<sup>[4]</sup> Increasing the solids content suppresses smaller turbulent eddies creating a broader distribution of the larger eddies, producing droplets larger in size.<sup>[4]</sup> Larger droplet diameter was observed when the dispersed volume fraction of formulation FM 1, using 9.0 mmol *in situ* KSA, was increased from 40 to 60% (Figure 6.4).



**Figure 6.4** Droplet size evolutions for systems prepared with increasing solids content (40-60%); keeping the weight percent of costabiliser (7.0 wt%) and *in situ* KSA (2.0 wt%) constant. All systems were emulsified using ultrasonication.

As the solids content increased from 40 to 60 %, the droplet diameter increased from 130 to 185 nm. Accordingly, the total surface area of the system decreased, pointing out certain limitations when using Equation 2. All systems, equal in formulation yet different in solids content, were sonicated at 600 W for 4 minutes and generated systems

differing in surface area. However, it should be pointed out that it was previously shown, by Ouzineb *et al.*, a large fraction of the energy inputted into the system is lost to heat (which is not accounted for here) and the difference works towards breaking the droplets.<sup>[5]</sup> Therefore, droplet sizes are not determined solely on the amount of work inputted or the quantity (and type) of surfactant available but rather a much more dynamic process involving a multitude of variables, such as: droplet breakage mechanism and efficiency and solids content, which affects the viscosity of the system and in turn the flow pattern in the vessel and the number of passes through the shearing zone. All miniemulsions were stable (small variation in droplet size) for several hours and were subsequently polymerised using KPS, reaching 90 to 95% conversion within two hours of polymerisation. The ratio of  $N_P/N_D$  was calculated and all systems appeared to polymerise with a nearly one to one copy of droplets to particles ( $N_P/N_D = 1$  within  $\pm 5$ -10 %).

### 6.2.3 ROLE OF SA AS SURFACTANT AND COSTABILISER

In miniemulsions, the presence of a costabiliser increases the hydrophobic nature (and solids content) of the system making it increasingly difficult to emulsify as the costabiliser concentration increases, typically resulting in slightly larger droplet sizes and/or an increase in the mechanical work required. The compound ODA used in our formulations is a reactive co-stabilizer, containing a hydrophobic  $C_{18}$  chain, which is covalently bound to the final polymer product. When generating surfactants *in situ*, carboxylate anions partition between the inside of the oil droplet (along with ODA), the interface and the aqueous phase (if heated above 65 °C). To assess whether or not the carboxylate anions can serve a dual purpose as both a surfactant (when neutralised) and a



costabiliser, three separate formulations were prepared and evaluated (Table 6.4).

**Table 6.4 Formulations prepared with varying amounts of *in situ* KSA to assess the roles of *in situ* KSA as costabiliser and surfactant.**

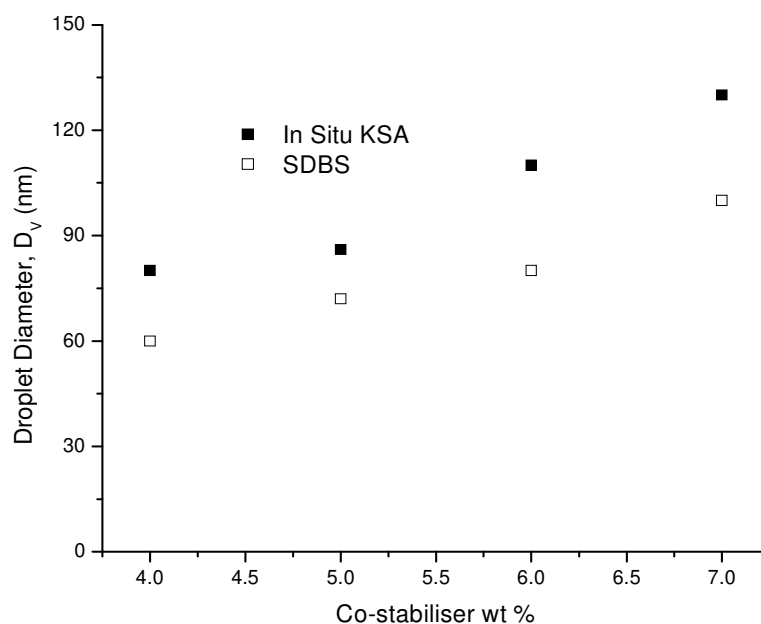
Sample #	ODA (mmol)	KOH (mmol)	SA (mmol)	SDBS (mmol)	D <sub>v</sub> (nm)	PDI
FM 1	35.0	13.5	9.0	--	131	0.06
FM 3	--	--	35.0	9.0	166	0.14
FM 4	--	52.5	35.0	--	Coarse Emulsion	

Formulation FM 1 is the standard formulation used in this work and contains 35 mmol of ODA as costabiliser and 9.0 mmol of *in situ* KSA as surfactant. To investigate the suitability of SA as the sole costabiliser (FM 3), an equivalent mole amount of SA in place of ODA was used. KOH was not added to avoid neutralizing the SA to the stearate ion. To prevent droplet coalescence, 9.0 mmol of SDBS was added to the aqueous phase. After sonicating for 4 minutes, light scattering results showed a monomodal distribution with an average diameter by volume (D<sub>v</sub>) of ~ 170 nm, approximately 40 nm larger than those generated after sonicating FM 1 for 4 minutes and comparable to the results in Figure 6.1 for SDBS. The droplets were relatively stable over a period of 2 hours suggesting that SA alone is suitable as a costabiliser. Formulation FM 4 contained 35 mmol of *in situ* KSA (equimolar amount to ODA in FM 1). Samples were taken after 4 minutes of sonication. Measured particle diameters were inconsistent, suggesting a coarse, unstable emulsion was prepared, and indicating that *in situ* KSA alone cannot serve as both a costabiliser and a surfactant for the stabilisation of miniemulsion droplets. It can however be used in the preparation of minisuspension/conventional emulsion systems as previously suggested by Propokov and Gistkova<sup>[6]</sup> and observed by Saygi-Arslan *et al.*<sup>[7]</sup> SA alone can stabilise the droplets against ripening if the droplets are stabilised against coalescence using a separate surfactant. SA can also serve as a

surfactant alone when neutralised with a base if the miniemulsion is stabilised against ripening with a separate costabiliser.

#### 6.2.4 REDUCING ODA CONCENTRATION

The combination of *in situ* KSA with ODA (FM 1) was further examined to determine if the amount of ODA required to maintain stable miniemulsions can be reduced. A similar examination was also performed with SDBS and ODA (FM 2). The amount of ODA was gradually reduced from 7 to 4 wt% with respect to monomer mass, keeping all other components constant (Figure 6.5).

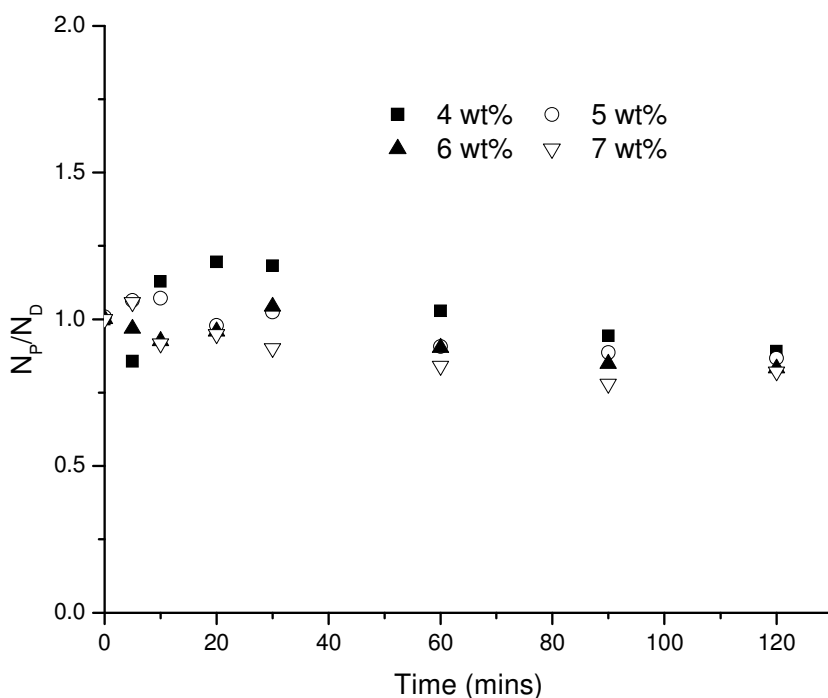


**Figure 6.5** Droplet diameters for miniemulsions prepared with *in situ* KSA and SDBS separately with varying amounts of ODA.

As the ODA content was reduced from 7 to 4 wt%, the average droplet diameter decreased from 130 to 80 nm for formulation FM 1 and from 100 to 60 nm for formulation FM 2 using SDBS. A possible explanation is that, as the hydrophobicity of

the droplet decreases, it becomes easier to generate smaller droplets when applying the same work per unit volume. Droplet sizes were measured over a period of two hours. Miniemulsions prepared with 6 and 7 wt% ODA and 2 wt% SDBS were found to be stable ( $\pm 2$ -8 nm) over the course of the measurements (2-3 hours). On the other hand, droplets prepared with 4 and 5 wt% ODA grew in average size, from  $\sim 60$  to 95nm and  $\sim 70$  to 95 nm respectively over a period of two hours. Below 6 wt% ODA with SDBS, the system is insufficiently stabilised against ripening. Conversely, systems prepared with 5 to 7 wt% ODA, using formulation FM 1 (*in situ* KSA), were found to be stable ( $\pm 5$ -10 nm) for two hours. Droplets prepared with 4 wt% ODA were found to be unstable (bimodal distribution) within an hour. Results suggest that when *in situ* KSA resides within the droplets along with ODA, the hydrophobic C<sub>18</sub> chains of the *in situ* generated surfactant help stabilise the system against ripening thus reducing the required costabiliser content slightly compared to systems prepared with preformed surfactants.

Droplets prepared with formulation FM 1 were polymerised in a batch process and initiated using KPS (Figure 6.6).



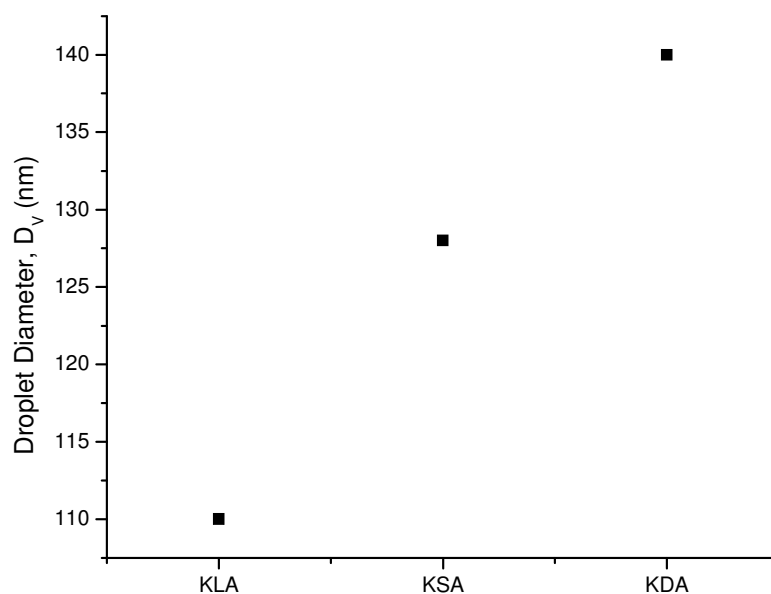
**Figure 6.6** The ratios of the number of particles to the number of droplets throughout the polymerisations for systems prepared with 9.0 mmol *in situ* KSA and 4-7 wt% ODA.

Miniemulsions prepared with 5 to 7 wt% costabiliser polymerised with a nearly 1 to 1 copy of droplet to particle. On the other hand, miniemulsions prepared with 4wt% costabiliser showed an increase in particle number of ~ 20% during the early stages of polymerisation, however these newly formed particles appear to coalesce with the existing particles by the end of the reaction. Further decreasing the concentration of costabiliser resulted in unstable (bimodal distributions) droplets systems.

#### 6.2.5 VARYING CARBOXYLIC ACID CHAIN LENGTH

Up to now, we have shown miniemulsion droplets stabilised with *in situ* KSA were robust to changes in process parameters such as solids content, surfactant and costabiliser concentration. The next parameter investigated was the carboxylic acid chain length used

for the *in situ* generated surfactants and how this effects miniemulsion droplet formation and stability. Starting with formulation FM 1, behenic ( $C_{22}$ ) and lauric acid ( $C_{12}$ ), which contain longer and shorter hydrocarbon chains compared to SA (Table 6.1) were neutralised with KOH to prepare equimolar amounts (9.0 mmol) of potassium behenoate (KDA) and potassium laureate (KLA) (Table 6.3). All formulations were sonicated for 4 minutes and droplet size was measured using dynamic light scattering (Figure 6.7).



**Figure 6.7** Droplet diameter by volume ( $D_v$ ) measurements for miniemulsions prepared with equimolar amounts (9.0 mmol) of potassium laurate (KLA), potassium stearate (KSA) and potassium behenoate (KDA).

Droplets prepared with equimolar amounts of potassium behenoate, stearate and laurate were found to be stable over a time span of a few hours. Miniemulsions prepared with potassium behenoate were slightly larger ( $\sim 10$  nm) than those prepared with potassium stearate which were also slightly larger ( $\sim 15$  nm) than those prepared with potassium laureate. A possible explanation for the change in droplet size could be due to

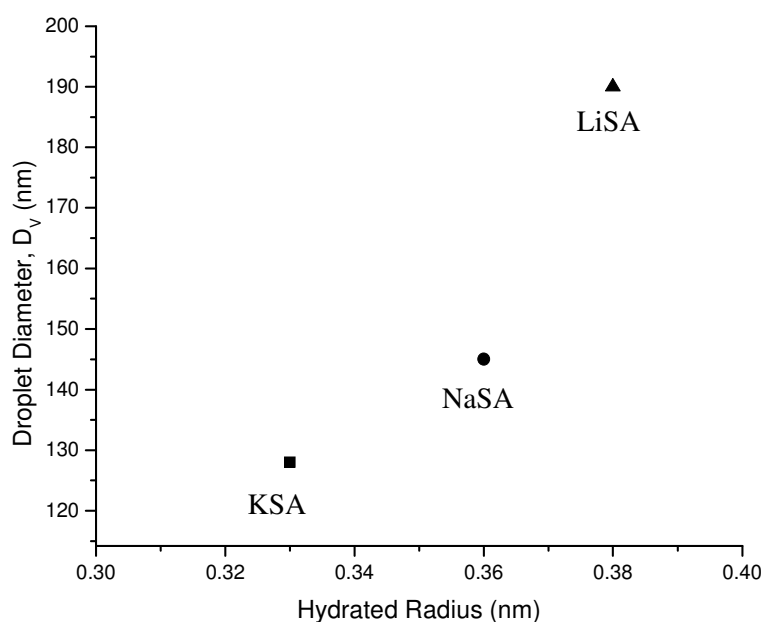
a number of contributing factors such as: increasingly hydrophobic environment with increasing hydrocarbon chain lengths ( $C_{12}$ - $C_{22}$ ) which ultimately affects the emulsification process and the final droplet size. Additionally, increasing or decreasing surfactant side reactions (i.e. dimerisation) would have an impact on the overall surfactant surface coverage and subsequently the final droplet size. However, as the fundamental factors behind the observed trends are still not fully understood, further work is being planned to investigate the underlying phenomenon. All systems were polymerised using KPS and reached over 90% conversion within two hours, with  $N_P/N_D = 1$  (within  $\pm 5$ -10%).

#### 6.2.6 VARYING SURFACTANT COUNTERION

Miniemulsion droplets can be prepared with *in situ* surfactants using different long chain carboxylic acids. However, we have not explored the potential role of the surfactant counterions and how varying their size and mobility may influence miniemulsion formation. Counterions dissolved in the aqueous phase, within the stern layer of the diffuse double layer, significantly affect the properties of the surfactant solution. The CMC, micelle size, and micellar activity are dependent on the degree of binding between the counterion and the carboxylate anion. The extent of binding is contingent on the polarisability, the valency and the hydrated radius of the counterion used, which subsequently affect the surfactant packing density at the droplet interface. The radius of non-hydrated counterions increases downwardly along group 1 metals in the order  $Li^+ < Na^+ < K^+$  (0.068, 0.095, 0.133 nm respectively).<sup>[8]</sup> However, due to ion-dipole interactions between water molecules and counterions, more water molecules bind to  $Li^+$ ,

compared to  $\text{Na}^+$  and  $\text{K}^+$ , so that the effective hydrated diameters are in the order of:  $\text{K}^+ < \text{Na}^+ < \text{Li}^+$  (0.33, 0.36, 0.38 nm respectively). Likewise, it was reported that the repulsive forces between similar ions increase as the hydrated radius increases.<sup>[8]</sup>

The larger hydrated radius of  $\text{Li}^+$  counterions requires larger area per surfactant molecule ( $A_s$ ) and therefore the  $\text{Li}^+$  ions are less densely packed at the interface compared to ionic surfactants stabilised with  $\text{Na}^+$  or  $\text{K}^+$  counterions.<sup>[8]</sup> Smaller hydrated radii equate to more surfactant molecules aligned at the interface and thus lower interfacial tension between the two insoluble phases, ultimately facilitating droplet breakage and resulting in smaller droplets. Using formulation FM 1, miniemulsions were prepared with equimolar amounts of potassium stearate (KSA), sodium stearate (NaSA) or lithium stearate (LiSA) separately. All formulations were sonicated at 600 W for 4 minutes and average droplet sizes were measured using dynamic light scattering (Figure 6.8).



**Figure 6.8** Droplet diameter by volume ( $D_v$ ) measurements for miniemulsions prepared with equimolar amounts (9.0 mmol) of lithium stearate (LiSA), sodium stearate (NaSA) and potassium stearate (KSA).

Droplets prepared with equimolar amounts of KSA, NaSA and LiSA resulted in droplets ranging in size from 130 to 190 nm. Counterions with a larger hydrated radius such as  $\text{Li}^+$  result in droplets larger in size at equal surfactant concentrations, compared to droplets prepared with  $\text{Na}^+$  and  $\text{K}^+$ . The droplets were found to be stable for several hours and polymerised with a nearly 1 to 1 copy of droplet to particle using KPS as initiator.

### 6.3 CONCLUSIONS

Based on the results presented here, it can be concluded that using an *in situ* generated surfactant results in a rapid, reproducible homogenisation/polymerisation process. Miniemulsions were prepared by generating a surfactant *in situ* at the interface of the monomer and water phases. *In situ* generation of KSA reduces the time required to reach a given droplet diameter compared to using preformed KSA or SDBS. Miniemulsions homogenised with a rotor-stator and stabilised with *in situ* KSA reached minimum droplet diameter within 20 minutes compared to 40 minutes for miniemulsions stabilised with a preformed KSA surfactant and 60 minutes for miniemulsions stabilised with SDBS. Smaller droplet sizes were also produced with the *in situ* KSA.

Surfactant concentration, solids content and costabiliser concentration were varied to determine the effect on droplet/particle size and stability. As the surfactant concentration (using either form of KSA) increased, the average droplet size decreased, with slightly larger droplets formed using preformed KSA. Increasing surfactant concentration from 2 to 25.8 mmol generated 180 to 90 nm sized droplets respectively. Droplets prepared with 15.5 mmol of *in situ* KSA or less, were polymerised with little contribution from secondary nucleation, supported by an  $N_p/N_D$  ratio of nearly one



(within  $\pm 5\%$ ). Moderate secondary nucleation (10-20%) was observed using higher amounts of KSA (20.1 and 25.8 mmol). In addition, a limiting solubility was encountered with preformed KSA, a limitation which was avoided when using *in situ* KSA. As solids content increased the droplet size increased.

It was determined that *in situ* KSA is not capable of serving the dual role of surfactant and costabiliser simultaneously. However, it was found that KSA is an effective surfactant when stabilised against ripening and SA can stabilise the droplets against ripening in the absence of KOH. As the costabiliser concentration decreased, the droplet size decreased. Droplets prepared with ODA and SDBS were unstable below 6 wt% ODA. However, droplets prepared with ODA and *in situ* KSA were stable up to a lower limit of 5 wt% ODA.

It has been demonstrated that a variety of *in situ* generated surfactants can be prepared with different carboxylic acids and bases. It was observed that the average droplet size decreased with decreasing hydrated radius of the surfactant counterion, an expected result since more counterions will be able to collect at the interface for a smaller hydrated radius.

## 6.4 LITERATURE CITED

1. Kanicky, J. R.; Poniatowski, A. F.; Mehta, N. R.; Shah, D. O. Cooperativity Among Molecules at Interfaces in Relation to Various Technological Processes: Effect of Chain Length on the pKa of Fatty Acid Salt Solutions. *Langmuir*. **2000**, *16*, 172-177.
2. Theander, K.; Pugh, R. J. The Influence of pH and Temperature on the Equilibrium and Dynamic Surface Tension of Aqueous Solutions of Sodium Oleate. *J. Colloid Interface Sci.* **2001**, *239*, 209-216.
3. Zacccone, A.; Wu, H.; Lattuada, M.; Morbidelli, M. Correlation Between Colloidal Stability and Surfactant Adsorption/Association Phenomena Studied by Light Scattering. *J. Phys. Chem. B*. **2008**, *112*, 1976-1986.
4. Walstra, P. Principles of emulsion formation. *Chem. Eng. Sci.* **1993**, *48*, 333-349.
5. Ouzineb, K.; Lord, C.; Lesauze, N.; Graillat, C.; Tanguy, P. A.; McKenna, T. Homogenisation Devices for the Production of Miniemulsions. *Chem. Eng. Sci.* **2006**, *61*, 2994-3000.
6. Prokopov, N. I.; Gritskova, I. A. Characteristic Features of Heterophase Polymerisation of Styrene with Simultaneous Formation of Surfactants at the Interface. *Russ. Chem. Rev.* **2001**, *70*, 791-800.
7. Saygi-Arslan, O.; Sudol, E. D.; Daniels, E. S.; El-Aasser, M.S.; Klein, A. *In Situ* Surfactant Generation as a Means of Miniemulsification? *J. Appl. Polym. Sci.* **2009**, *111*, 735-745.
8. Oh, S. G.; Shah, D. O. Effect of Counterions on the Interfacial Tension and Emulsion Droplet Size in the Oil/Water/Dodecyl Sulfate System. *J. Phys. Chem.* **1993**, *97*, 284-6.

## ***CONTINUOUS PRODUCTION OF MINIEMULSIONS USING IN LINE SMX ELEMENTS***

---

The preparation and stabilisation of miniemulsion systems using SMX static mixers (in line with a pump and reservoir tank) and *in situ* generated surfactants is presented. Neutralisation of a water-soluble base with an oil-soluble long chain acid, generating a *in situ* surfactant at the interface, results in rapid stabilisation and emulsification compared to preformed surfactant that must diffuse to, then absorb on the droplets.

As the flow rates (350 to 600 RPM) and number of mixing elements (7 to 21SMX mixers) in series increase, the emulsification time reduces by ~ 30 folds (14 vs. 0.5 min). The reduction in the emulsification time required to produce a stable emulsion at 600 RPM and 21 mixing elements more than compensated for the higher pressure in the emulsification loop, consuming 5 times less energy than what would be consumed

when working at 350 RPM and 7 SMX elements. Subsequently, with the rapid emulsification step, it was possible to test the feasibility of a continuous process for direct emulsification followed by polymerisation. Comparing this process with a batch process, similar results for the  $N_p/N_D$  ratio and conversion were obtained, but the continuous process was accomplished in a single step.

## 7.1 EXPERIMENTAL

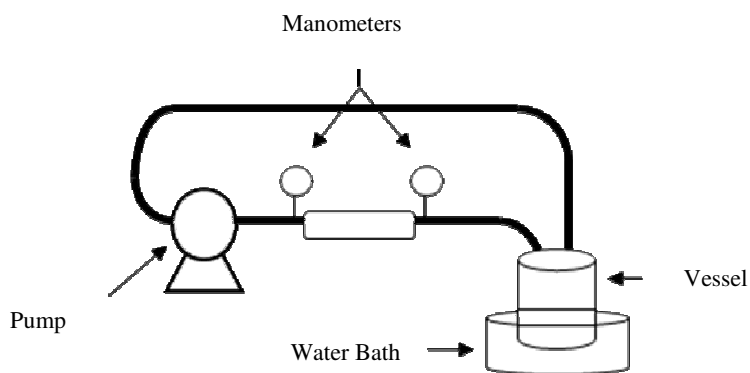
### 7.1.1 MATERIALS

The monomers used were methyl methacrylate (MMA) (Aldrich, 99%) and butyl acrylate (BA) (Aldrich, 99%). The costabiliser was octadecyl acrylate (ODA) (Aldrich, 97%). The *in situ* surfactant potassium stearate was prepared from reacting stearic acid (SA) (Aldrich, 95%) and potassium hydroxide (KOH) (Aldrich, 90%) in a 2:3 mole ratio to compensate for any hydrolysis of the stearate anion.<sup>[1]</sup> Deionised water and the water-soluble initiator, potassium persulphate (KPS) (Acros, 98%) were used for all experiments. All materials were used as received.

### 7.1.2 HOMOGENISATION

The SMX elements provided by Sulzer ChemTech Ltd were 6 mm in diameter with 6 crossbars aligned at 45° to the axis of the pipe with a pitch (length to diameter ratio) of 1.0. Each element was bound at 90° to the previous element, for a total of 7 elements fitted flush within a stainless steel pipe provided by Sulzer ChemTech Ltd. We will refer to 7 elements within a tube as a ‘bank’ of elements or mixers. A total of up to 3 banks of mixers (21 elements) were used at various points throughout our investigation. The banks

of mixers were installed in a closed loop system consisting of a pump, tubing, reservoir tank and a water bath (Figure 7.1).



**Figure 7.1** Homogenisation apparatus using static mixers, consisting of a closed loop system with a pump, tubing, product reservoir and temperature bath.

The pump used was a positive displacement gear pump from Viking Pump, controlled using a variable speed drive provided by 3M Technologies. The aqueous and organic phases were combined in a 2 L reservoir vessel and stirred for a few minutes to allow neutralisation of the acid and base (the reader is referred to reference 4 for more experimental details). The mixture was pumped through at various flow rates ranging from 50 to 75 g/s ( $Re: 10^3$ ) (see Table 7.1 for details). Small volumes of sample were removed from the reservoir intermittently. The pressure drop over the mixing bed was measured and recorded at timed intervals using manometers with  $\pm 0.5\%$  accuracy. The manometers were placed at the entry and exit of the banks. Data is reported in terms of time and passes required to emulsify the batch of emulsion solution. A single pass is defined as the entire volume of solution passing through the bank(s) of elements once. The mean time required for a single pass is based on the applied flow rate (Table 7.1) and

the volume (Table 7.2). A single pass is defined as the entire volume of miniemulsion passing through the mixing elements once.

**Table 7.1** Flow rates at varying RPM and the time required for a single pass through 1 bank of elements.

RPM	Calibrated Flow Rate (g/s)	Time for entire volume passing through the mixing elements once (s)
350	50	8.49
400	53	8.06
450	58	7.18
500	62	6.94
550	66	6.31
600	75	5.52

Miniemulsions were prepared according to the formulation FM 1 (Table 7.2). The organic phase contained monomer, costabiliser, and carboxylic acid. The alkali base was dissolved in the aqueous phase and KPS (0.06 wt% with respect to monomer mass) was added at the onset of the polymerisation.

**Table 7.2** Miniemulsion formulations containing MMA and BA monomer in a 50:50 w/w ratio, ODA and *in situ* generated KSA (FM 1)

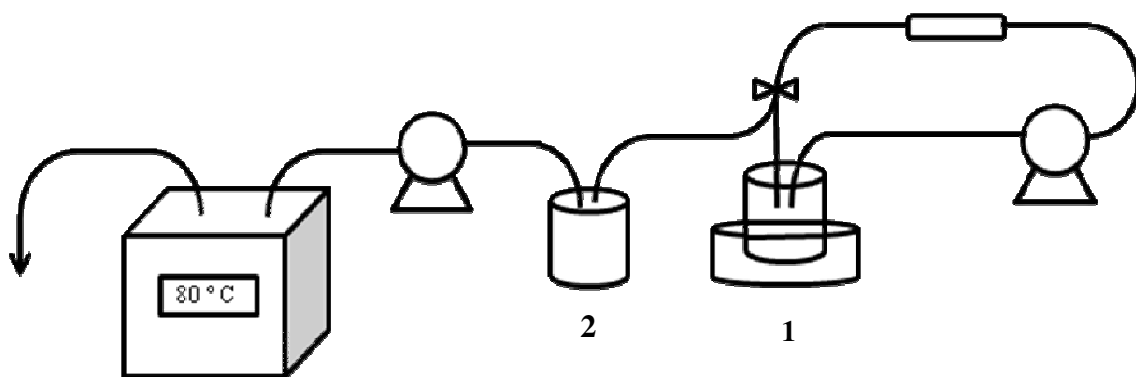
Sample	DIW (g)	MMA (g)	BA (g)	ODA (g)	SA (mmol)	KOH (mmol)
FM 1	250	84	84	11.6	9.0	13.5

### 7.1.3 POLYMERISATION

Batch polymerisations were carried out in a 1 L jacketed glass reactor equipped with a reflux condenser, a nitrogen inlet, an anchor stirrer (set at 300 RPM) and a sampling port. Dispersions were purged with nitrogen (25 minutes) and then heated to 70 °C, using a thermostatted bath. Droplet size measurements were taken after purging to verify that no droplet coalescence took place. The initiator solution was injected when the reactor reached 70 °C ( $t = 0$  min). Samples were taken every 10 minutes for the first half hour and then every half hour for the remaining 2 hours of the experiment.

In the last phase of the investigation, a batch reaction was run without a nitrogen purge, using 0.3 wt% initiator and polymerised at 80 °C. The purpose of the experiment was to simulate conditions for a continuous polymerisation process where purging with nitrogen was not done. Therefore, an excess of initiator (0.2 vs. 0.06 wt%) was used to compensate for initiator radicals terminating in the presence of oxygen.

The single step emulsification/polymerisation process was performed by combining the two steps (emulsification plus reaction) into an integrated process. Emulsifications were performed as previously described. After emulsification, the miniemulsions were discharged into a separate holding container (tank 2 of Figure 7.3) which was used as a feed storage for the tubular reactor. Emulsification continued and the valve between recipients 1 and 2 was opened as necessary to replace the feed consumed in the reactor. The initial batch of miniemulsions were quickly pumped through the tubular reactor (a step which took ~ 30 seconds) to fill the tubing and then the flow rate was dropped to desired flow rate using a driver with a cavity gear Micropump® head. The 200 ft of 4 mm ID PTFE tubing was arranged in several helical coils and submerged in a thermostatted bath preset to 80 °C. No significant temperature gradients were expected during polymerisation due to the large exposed surface area. Flow rate through the pump was set to ~ 12-13 g·min<sup>-1</sup>, to give a residence time of approximately 1 hour. An electronic balance located at the outlet was used to verify and ensure consistency in the flow rate. Samples were withdrawn at the end of the length of tubing every 10 mins for the first half hour and then every half hour for the remainder of the experiment. The continuous emulsification/polymerisation process was run for a total of 4 residence times (4 hours).



**Figure 7.2** Continuous emulsification/polymerisation process set up for the production of miniemulsions. Set up consists of the homogenisation unit as described in Figure 1 and a separate reservoir (tank 2), pump and water bath for the polymerisation process.

#### 7.1.4 CHARACTERISATION

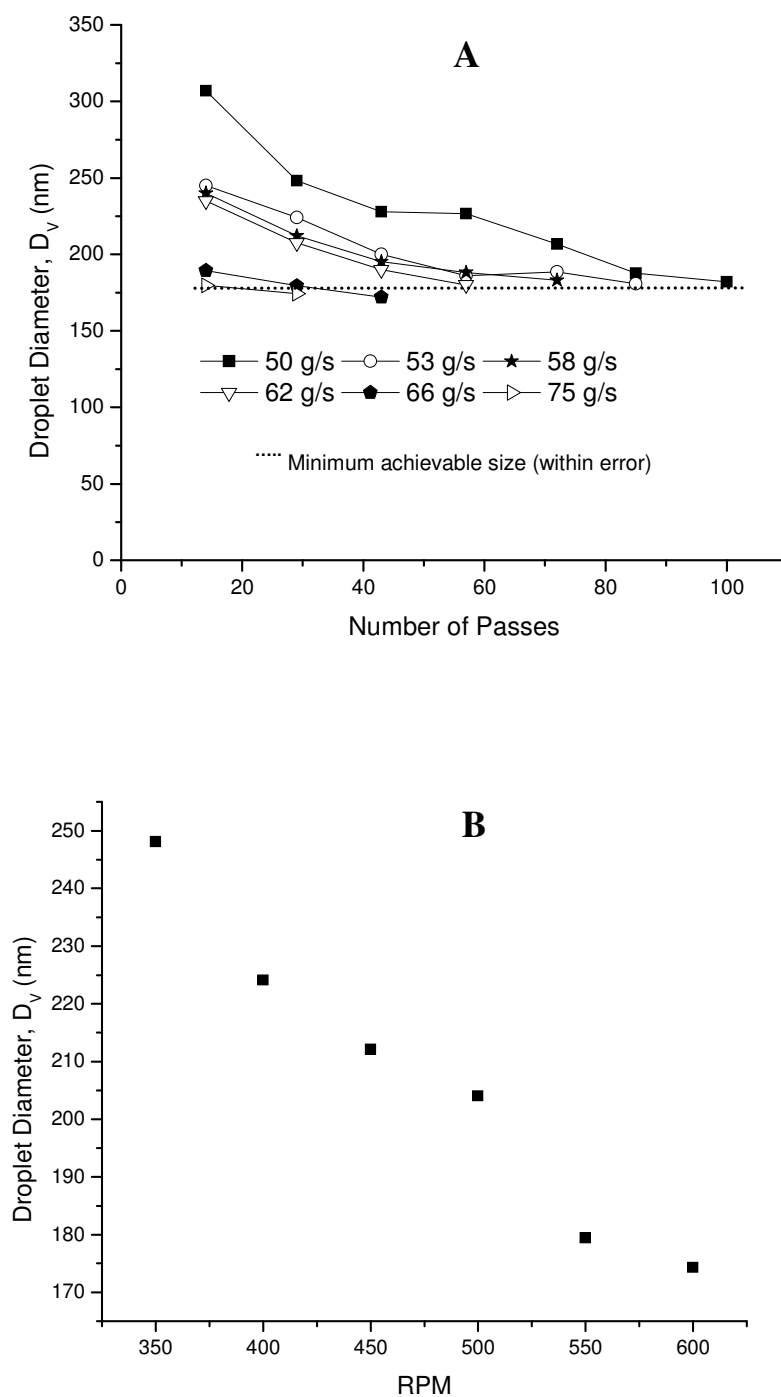
Droplet and particle size measurements were performed using a Malvern Nanosizer ZS. Samples were diluted with surfactant solution in concentrations above the CMC for droplet stability. For all runs, conversion was determined gravimetrically (See Appendix A1).

### 7.2 RESULTS AND DISCUSSION

#### 7.2.1 EFFECT OF VARYING FLOW RATE

In the initial phase of the investigation, we ran a series of emulsifications using a single bank of SMX elements (7 mixers) and formulation FM 1. The first parameter investigated was flow rate, which was varied by altering the pump speed from 350 to 600 RPM (50 to 75 g/s). We recorded the number of passes required to reach the minimum equilibrium stable droplet size (Figure 7.3) when operating in the laminar to transitional regime ( $Re \sim 10^3$  for an open pipe).





**Figure 7.3** A - Mean droplet size evolution for miniemulsions emulsified using 1 bank of SMX elements (7 mixers) and pumped through at flow rates ranging from 50 to 75 g/s (350 to 600 RPM). B - Mean droplet size evolution for miniemulsions prepared with increasing RPM and ~ 30 passes through 1 bank of SMX mixing elements.

Droplets prepared with formulation FM 1 gradually decreased in size as the number of passes through the elements increased. This is a general trend that is observed irrespective of the flow rate. Droplet size decreases after each successive pass through the elements until the asymptotic limit is reached, as indicated by the dashed line in Figure 7.3A.

We believe droplet breakage within mixing elements in a turbulent regime is a hybrid of two mechanisms. Initially, multiphase streams are split into striations that get reoriented, redistributed, recombined and then are subjected to further separation. As the number of striations increases, the thickness of each striation decreases until separation becomes impossible to visually detect. As the flow rate increases and enters the transitional flow regime, it is assumed that mixing on the macroscopic scale would take place on very short time scales and it would be almost undetectable upon exiting the mixing elements. It is assumed that at the microscopic scale, the droplet breakage process proceeds with turbulent eddies breaking droplets that are larger than eddy size, until they reach the Kolmogorov length scale (the smallest eddy size).<sup>[2]</sup> This is a chaotic environment due to dramatic pressure fluctuations varying considerably from one point to the next within the elements, ultimately affecting local velocity gradients. Increasing turbulence by increasing the flow rate ( $W_{\text{Breakage}}$ ) induces more droplet breakage for a given period of time and specified formulation ( $\gamma$ ), creating smaller droplets ( $\Delta A$ ) as shown by Equation 2:

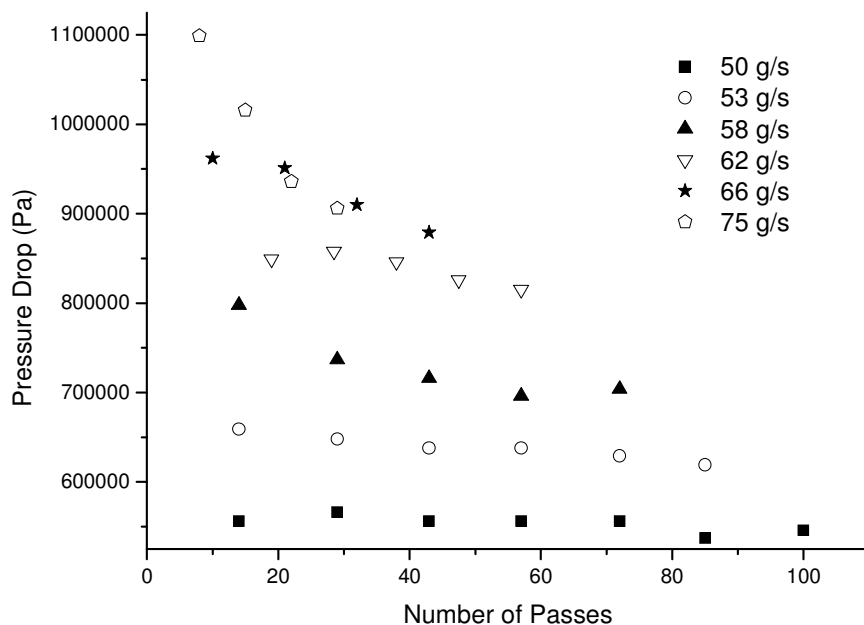
$$W_{\text{Breakage}} = \gamma \times \Delta A \quad (2)$$

Emulsifying formulation FM 1 at increasing RPM for the same number of passes (~30) results in decrease in the droplet size (Figure 7.3B). Increasing the amount of work done on a miniemulsion results in progressively larger surface areas and hence smaller

droplets. However, Figure 7.3A shows that the final stable droplet diameter ranges between 170 to 180 nm in size for any RPM; the only difference is the number of passes and time required to reach the equilibrium droplet diameter, which is dependent on the flow rate. The results strongly suggest that process parameters such as flow rate and formulation play a certain role in determining final droplet sizes.

For droplets ranging from microns to millimeters in diameter it has been computationally predicted and experimentally observed that droplets break along crossbars and cross points (intersection of crossbars) and that adjusting the number of elements along the axis and in parallel will ultimately affect the transverse flow profile of the multiphase streams. Additionally, varying the number of breaking point locations and the gaps within the crossbars will play a role in determining the droplet size evolutions. This is a reasonable explanation when dealing with “large” droplets, but one would expect that nano-sized droplets are more likely to flow around the crossbars and cross points and thus spend more time undergoing breakage due to eddies. In theory, if SMX elements are to resemble packed bed reactors, the pores constructed from the cross bars are the main channel for flow of miniemulsions and the size of the pores could determine the upper and lower limits of eddy sizes which are said to cause droplet breakage, in addition to any potential breakage along the crossbars and cross points. As shown in Figure 7.3A, irrespective of the flow rates, ~ 170 nm appears to be the lower limit of droplet size. Relating this value to the Kolmogorov length scale would require measurements of local velocity gradients along and within the perimeter of the pores, a process that is intrusive and requires specialised equipment and/or computational modeling.

It was observed that as the rotation rate of the pump head increased by 50 RPM, the number of passes required to obtain the minimum droplet size was reduced by approximately 14 passes through the mixing elements. However, increasing the flow rate came at a cost of higher pressure drop across the bank of elements (Figure 7.4).

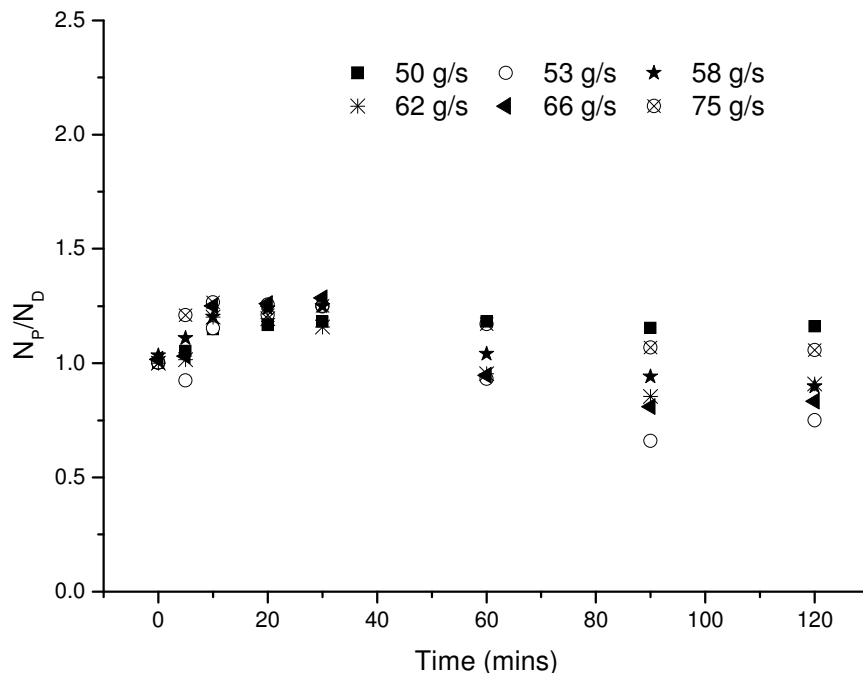


**Figure 7.4** Pressure drop evolution for miniemulsion formulation FM 1 emulsified at varying RPM.

Delivering fluid at a faster flow rate, and hence higher Reynolds number, to elements of the same size will cause a buildup of pressure at the entrance of elements (more so than at the exit which is essentially open to the atmosphere in our set up) (Figure 7.1). The higher the Reynolds number and hence the pressure drop, the more turbulent the environment and the more chaotic the droplet breakage process is expected to be, resulting in what appears to be more efficient droplet breakage, requiring fewer passages and subsequently less time. At lower flow rates (50 – 53 g/s), the pressure drop is relatively constant as the number of passes increases. As the flow rate increases (> 53

g/s), the absolute pressures across the bed increases, but decreases over a very short time span (~ minutes) as the resistance to droplet breakage decreases (i.e. as the droplets become smaller and stabilise). A similar investigation was performed using a set of 10 mm SMX static mixers however, the pressure drop along the length of the bed ranged from 0.5 to 2 bars depending on the flow rate (50 to 75 g/s) resulting in ill-defined and unstable droplets. Investigations into miniemulsification with 10 mm SMX mixers at higher flow rates (> 75 g/s) are scheduled for future study.

All final miniemulsion droplets prepared in this investigation were found to be stable (little variation in droplet size and distribution,  $\pm 5$ -10 nm) for a period of several hours and were subsequently polymerised in a batch process using water-soluble KPS as the initiator (Figure 7.5).

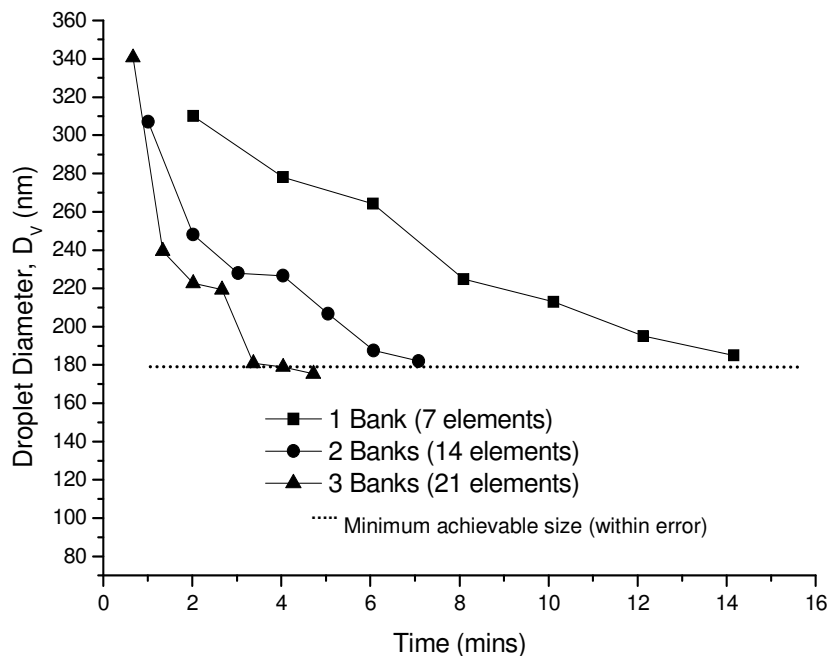


**Figure 7.5** The ratios of the number of particles to the number of droplets throughout the polymerisations for miniemulsions prepared with 2.0 wt% *in situ* KSA and homogenised at various flow rates ranging from 50 to 75 g/s.

In all cases, conversion reached 85 to 95% within two hours of polymerisation. Droplet diameters ( $D_v$ ) were measured and used to calculate the ratio of  $N_p/N_D$  (See Appendix A2 & A3). Miniemulsions polymerised with a nearly one to one mapping of droplets to particles ( $N_p/N_D = 1$  within  $\pm 5$ -25%). Overall, increasing the number of passes through the mixing elements generates droplets of smaller sizes. By increasing the flow rate through the mixing elements, the minimum droplet size can be attained in fewer passes but at a cost of higher pressure drop.

### 7.2.2 INCREASING THE NUMBER OF ELEMENTS IN SERIES

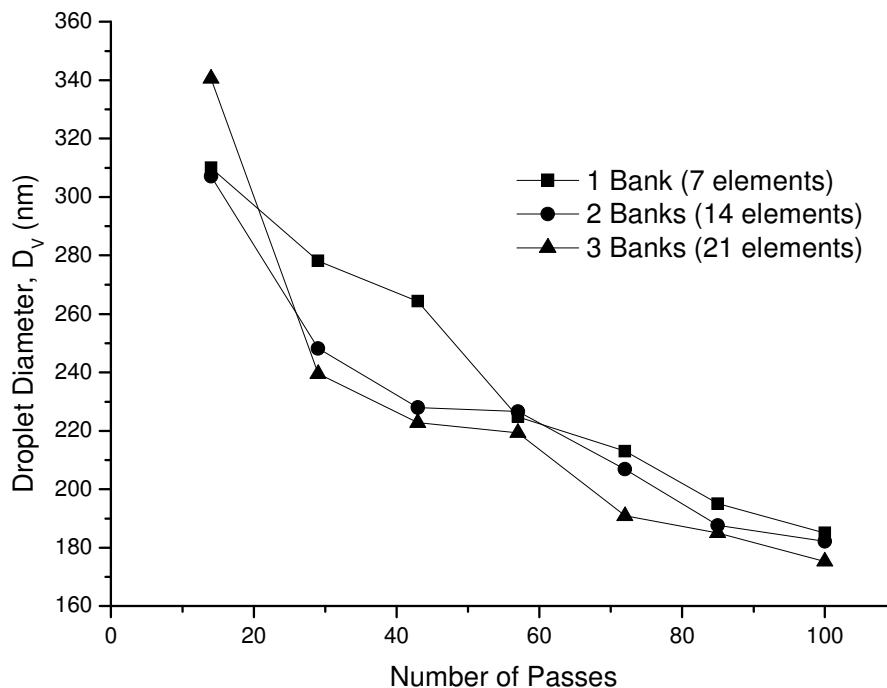
In the second phase of this investigation, we pose the question as to whether emulsification time can be reduced by increasing the number of elements in series, thereby reducing the amount of passes required per bank of elements. From Figure 7.3A, we found that when operating at 50 g/s, reaching the equilibrium droplet diameter required 100 passes through the mixing elements. Therefore, in addition to the pre-existing single bank that was used in previous emulsifications, a second and third bank were added in series to bring the total of SMX mixing elements to 14 and 21, respectively. Using formulation FM 1, we ran two emulsifications at 50 g/s using 2 and 3 banks separately and recorded the time required to reach minimum equilibrium droplet size (Figure 7.6).



**Figure 7.6** Mean droplet size evolution for droplets emulsified at 50 g/s using 1, 2 and 3 banks of mixers.

By increasing the number of elements in series, we were able to reach the minimum droplet equilibrium point significantly faster than when working with just 1 bank of elements. When emulsifying with 1 bank of elements (7 mixers), the homogenisation process required a total of ~ 14 minutes to reach ~ 180 nm sized droplets. By adding an additional bank, we were able to reduce the process down to half the time (7.5 minutes). With a third bank of elements, ~ 180 nm droplets were produced in less than 5 minutes. The reason for the significant decrease in time is that when 2 banks are in series a total of 100 passes is achieved for 1 complete circulation through the 2 banks (50 passes through each bank). Similarly, when 3 banks of elements are in series a total of ~ 33 passes through each bank is required to arrive at a total of 100 passes overall. Therefore increasing the number of elements in series reduces emulsification time, so

long as the number of passes required to achieve minimal droplet size is preserved (Figure 7.7).



**Figure 7.7** Mean droplet size evolution as a function of the number of passes for droplets emulsified at 350 RPM using 1, 2 and 3 banks of mixers.

As long as the total number of passes remains the same irrespective of the number of elements in series, a similar final droplet size will be attained. This trend has been reproduced at the other flow rates used in this work. As the results are very similar, they are not shown here for the sake of brevity. All final miniemulsions prepared in Figure 7.6 using formulation FM 1 were found to be relatively stable (little variation in droplet size and distribution) for a period of several hours and were subsequently polymerised in a batch process using water-soluble KPS as the initiator. In all cases, conversion reached 85 to 95% within two hours of polymerisation. Droplet diameters ( $D_v$ ) were measured and used to calculate the ratio of  $N_p/N_D$ . The miniemulsions polymerised with a nearly one to



one mapping of droplets to particles ( $N_P/N_D = 1$  within  $\pm 5$ -20%).

### 7.2.3 VARYING BOTH FLOW RATE AND THE NUMBER OF ELEMENTS IN SERIES

In the previous two sections we have shown that increasing the flow rate through 1 bank of elements or the number of elements in series (to a maximum of 3 banks) can significantly reduce the emulsification time and generate droplets similar in size. The objective of this section is to investigate the combined influences of varying the flow rates through the elements and the number of elements in series.

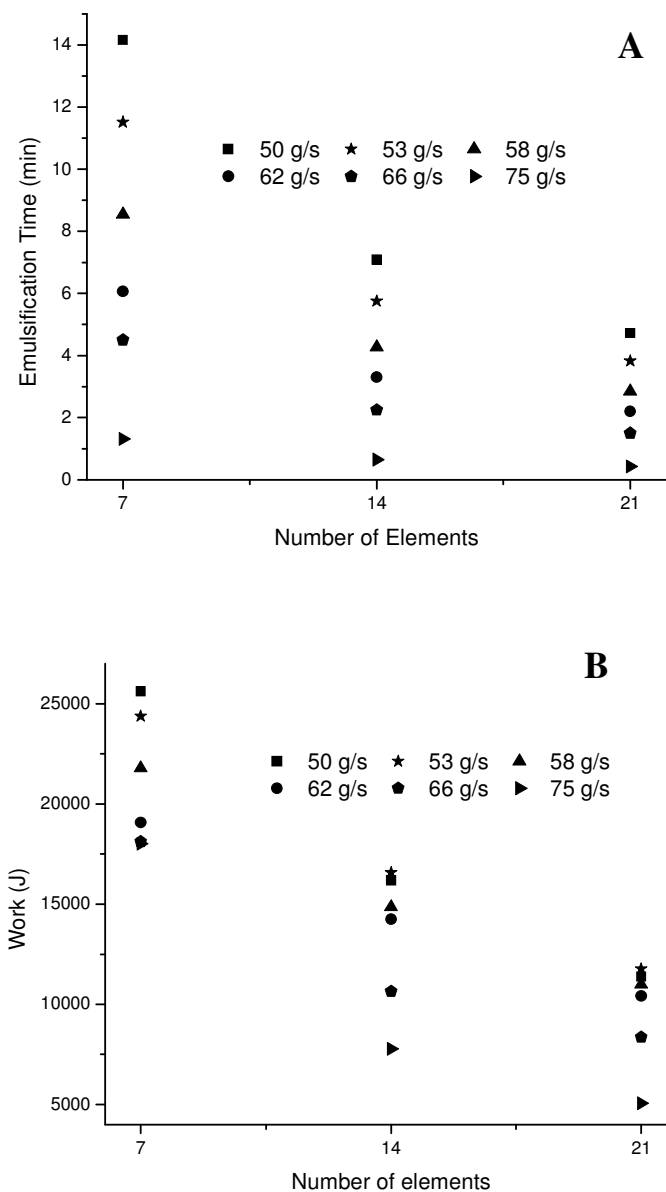
The overall objective is to develop a process that is time, cost and most importantly energy efficient. If a process requires excessive amounts of energy, independent of its effectiveness as a homogenisation device, it will not be amenable to scale up. Ideally, any device that is developed for commercial use should be scalable, reproducible and most importantly economically and energy efficient. The preceding observations have shown that in line SMX elements are scalable in series (at least to the extent studied in this work) and generate reproducible results, irrespective of the flow rate, so long as the number of passes required to emulsify the material is maintained. The question now lies as to whether or not their energy consumption is comparable to less than more traditional devices such as rotor-stators.

The amount of power ( $P_w$ ) (and hence energy) required to operate the static mixers (Figure 7.8), is based on the flow rate ( $Q$ ) and pressure drop ( $\Delta P$ ) along the length of the elements (Equation 8).

$$P_w = \Delta P \times Q \quad (9)$$

In this study, the total work required is defined as the product of the power input and the

emulsification time needed to generate droplets ranging between 170 to 180 nm. The work requirement was calculated at flow rates ranging from 50 to 75 g/s.



**Figure 7.8 Time (A) and energy (B) evolution for 170 to 180 nm droplets generated at various flow rates (50 to 75 g/s) with varying number of elements in series.**

From Figure 7.8A, it is observed that as the flow rate increases, the emulsification time required to generate 170 to 180 nm diameter droplets drops significantly as the

number of elements in series increases. Operating at 50 g/s with only 1 bank of elements (7 mixers) requires an emulsification time of ~ 14 minutes. This can be compared to operating at 75 g/s and 3 banks (21 elements), which requires approximately ~ 30 seconds to reach a similar droplet size. When we increase both the flow rate and the number of elements in series, there is a significant reduction in emulsification time required to reach similar droplet sizes. Such a reduction could not be achieved by varying one parameter alone with the current set up. However, varying the two operating parameters simultaneously facilitates the emulsification process.

Similarly, as the volumetric flow rate and the number of elements in series are increased, the amount of work required to generate droplets of comparable sizes decreases by a factor of 5. It was found that ~25 000 J of work was required to generate ~170 nm droplets when operating at 50 g/s with 1 bank of mixers (7 elements), over a total emulsification time of ~14 minutes. By comparison ~5 times less work (~5 000 J) was required when operating at 75 g/s with 3 banks in series (21 elements) to generate droplets comparable in size. More importantly, only 30 seconds were required representing an almost 30 fold reduction in emulsification time. This demonstrates that while operating at higher flow rates creates larger pressure drops across the banks of mixers the additional cost associated with this is more than compensated for by a very large reduction in emulsification times.

In comparison to other devices (Table 7.3) such as rotor-stators, it has previously been shown that emulsifying formulation FM 1 required ~ 20 minutes to generate ~ 170 nm sized droplets (Run #5) (Chapter 6) The emulsification process consumes a total of ~ 197 KJ/KG of work which utilises ~ 16 times more energy in comparison to working at

the upper limit of our SM process of 75 G/S with 3 banks in series (Run #8) or ~ 3 times more at the lower limit (Run #7). Additionally, when preparing miniemulsions using static mixers and *in situ* KSA at the lower limit of our SM set up (Run #7) we are consuming ~ 2 to 3 times less energy than when using SDBS under similar SM conditions and nearly 7 to 10 times less compared to systems prepared with the rotor-stator (depending on rotor-stator head size). Overall, the SMX elements are more energy efficient. They are more effective at breaking down larger droplets due the even spread and breakage of the flow stream across the width of the elements, thereby generating narrower distributions, in a reasonable amount of time.

**Table 7.3** Estimation of the energy consumption required by ultrasonication, the rotor-stator and static mixers in the preparation of miniemulsion systems. 2 wt% surfactant was used throughout all emulsifications.

Run #	Emulsification Device	Operating Conditions	Surfactant (2 wt %)	Droplet Diameter (nm)	Time (min)	Energy Consumption (KJ/KG)	Reference
1	Ultrasonication	80 % amp.	SDBS	156	1	87	Chapter 5
2	Rotor-Stator (7.5 cm head size)	3000 RPM	SDBS	185	60	433	Chapter 5
3	Rotor-Stator (5.5 cm head size)	3000 RPM	SDBS	192	60	577	Chapter 5
4	Rotor-Stator (5.5 cm head size)	3000 RPM	<i>p</i> KSA	176	40	385	Chapter 6
5	Rotor-Stator (5.5 cm head size)	3000 RPM	<i>In situ</i> KSA	174	20	197	Chapter 6
6	Static Mixers (7 x 6 mm SMX)	~ 50 g/s	SDBS	170	30	161	Chapter 5
7	Static Mixers (7 x 6 mm SMX)	~ 50 g/s	<i>In situ</i> KSA	176	14	60	Lower Limit
8	Static Mixers (21 x 6 mm SMX)	~ 75 g/s	<i>In situ</i> KSA	172	0.5	12	Upper Limit

#### 7.2.4 CONTINUOUS EMULSIFICATION/POLYMERISATION OF MINIEMULSIONS

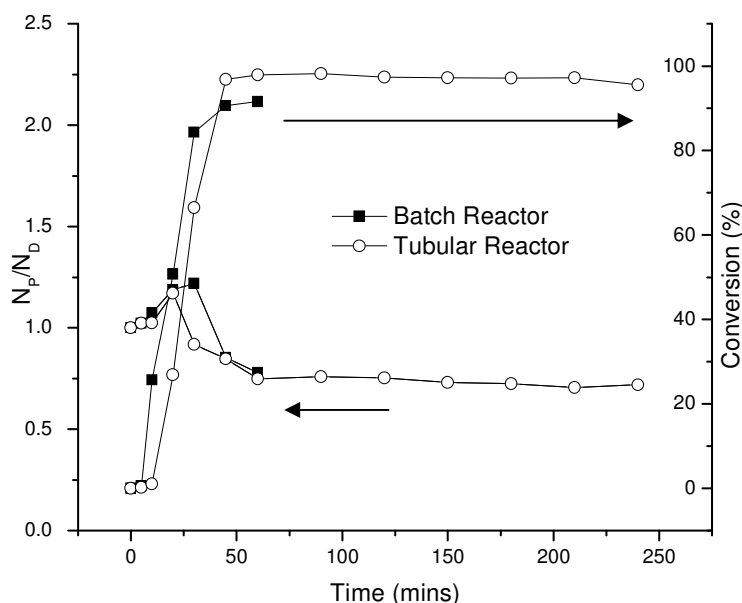
The ability to continuously generate miniemulsions that could be immediately polymerised would have a number of advantages, including eliminating the need to store and transport intermediate emulsions, and to exploit the numerous advantages inherent in a continuous process.<sup>[3,4]</sup>

The choice of reactor is important in this context, and while many options are open, the use of continuous stirred tank reactors (CSTR) is not recommended because the wide residence time distribution would lead to the inclusion of un-polymerised droplets in the exit stream. For this reason, either (semi-)batch reactors or continuous tubular reactors seem to be better choices since all of the particles in the reactor will have the same residence time. In order to exploit the advantages of a continuous system, we will focus on the use of a linear flow tubular reactor.

Linear tubular reactors are simple to design and construct, can operate for an extended period of time with very little maintenance, and have large surface area to volume ratio which allows for efficient heat removal. Previous studies have demonstrated successful polymerisation of miniemulsions using tubular reactors on a laboratory scale.<sup>[5, 6]</sup>

The goal of the final step of our investigation is to develop a process whereby miniemulsions are continuously produced and polymerised on a laboratory scale. A schematic illustration of the set up is shown in Figure 3. The organic and aqueous phases are introduced into the emulsification vessel and emulsified for the appropriate number of passes (depending on flow rate). Working at 75 g/s and 3 banks of elements in series requires ~ 30 passes to emulsify ~0.4 litres of a mixture of water and monomer (FM1). As described above, an initial emulsification step is used to fill up a holding tank situated

between the emulsification loop and the reactor, and to fill the reactor itself. Once both the reactor and the holding tank are full, a second gear pump is used to pump the stable miniemulsion from the holding tank through the tubular reactor at a flow rate of  $\sim 12$  g/min (this corresponds to a residence time of 1 hour in the tube). Given the difference between the residence time of the reactor and the time required to generate the emulsion, it is rather straightforward to occasionally open the T-valve between the emulsification loop and the holding tank to ensure that the latter always contains enough emulsion to keep the tubular reactor full. Due to the nature of the set up, purging with nitrogen proved difficult and so an excess amount (0.2 wt % with respect to monomer mass) of initiator was used at a slightly elevated temperature compared to our previous polymerisation experiments (80 vs. 70 °C). The tubular reactor process was compared to a batch polymerisation also operated with excess initiator and at 80 °C (Figure 7.9).



**Figure 7.9** Conversion and  $N_p/N_d$  profiles for miniemulsions emulsified in the static mixers at 600 RPM with 3 banks of elements in series and polymerised in a batch (■) or one step emulsification/polymerisation process with a tubular reactor (○).

Both the continuous and the batch processes were initiated using water-soluble KPS. In both cases, conversion reached between 90 to 97% within one hour of polymerisation. Droplet diameters ( $D_V$ ) were measured and used to calculate the ratio of  $N_P/N_D$ , which is approximately 0.8 for both the batch and continuous reactors. The batch process was stopped after 1 hour while that of the one step continuous emulsification/polymerisation process was left to run for 4 hours (4 residence times.) It can clearly be seen here that the continuous process is stable.

Comparing the novel continuous approach we developed with a conventional batch approach we observe similar reaction profiles both in terms of conversion and droplet/particle nucleation. This has a wide range of implications, both in terms of the ability to control product quality as well as the efficiency of production and control of the reaction kinetics and conversion. In previous works from our group, it has been demonstrated that changing the surfactant concentration allows one to change the particle diameters rather easily. In addition, this set-up allows one to work at different solid contents or formulations without needing to shut down the reactor.

### 7.3 CONCLUSIONS

The work presented here demonstrates that SMX static mixer elements can be used to effectively and efficiently create polymerisable miniemulsions. The rapid stabilisation of the droplets generated in this manner due to the acid/base neutralisation reaction that forms the surfactants at the surface of the particle means that this emulsification can be done more rapidly with the *in situ* surfactant than with preformed surfactant that must diffuse to, then absorb on the droplets.



Furthermore it was shown that the reduction in the time required to produce a stable emulsion for high flow rates and an increased number of mixing elements more than compensated for the higher pressure in the emulsification loop. In other words, although the instantaneous energy requirements were greater at 75 g/s with 21 mixing elements than they were at 50 g/s and 7 elements, the time required to create the emulsion was 15 times shorter for the former configuration.

Subsequently, a continuous process for polymerisation of miniemulsions was studied at the laboratory scale using *in situ* surfactants with 3 banks of SMX mixer elements (21 total elements). Comparing this process with a batch process, similar results for the  $N_P/N_D$  ratio and conversion were obtained, but the continuous process was accomplished in a single step. This novel approach offers important opportunities for improved efficiency when studying processes at the laboratory scale and may be a feasible approach for industrial polymerisation processes.

## 7.4 LITERATURE CITED

1. El-Jaby U, Cunningham MF, McKenna TFL. The Advantages of *in situ* Surfactant Generation for Miniemulsions. *Macromol. Rapid Commun.* – In press (MACP.200900698)
2. Walstra, P. Turbulence Depression by Polymers and its Effect on Disruption of Emulsion Droplets. *Chem. Eng. Sci.* **1974**; 29, 882-885.
3. González, I.; Paulis, M.; de la Cal, J.C.; Asua, J.M. (Mini)emulsion Polymerisation: Effect of the Segregation Degree on Polymer Architecture. *Macromol. React. Eng.* **2007**; 1, 635-642.
4. Asua, J.M. Introduction to Polymerisation Processes. In *Polymer Reaction Engineering*. Ed: Asua, J.M. **2009**, Wiley-Blackwell Publishing Ltd: Oxford. pg: 1-28.
5. Schork, F.J.; Guo, J. Continuous Miniemulsion Polymerisation. *Macromol. React. Eng.* **2008**; 2, 287-303.
6. Ouzineb, K.; Graillat, C.; McKenna, T. F. Continuous Tubular Reactor as a Seed Reactor in Miniemulsion Polymerisation. *DECHEMA Monographien.* **2001**, 137, 293-301.

# 8

## ***SIGNIFICANT CONTRIBUTIONS***

---

The objective of the thesis was to investigate a number of different emulsification devices for the preparation of miniemulsions and to develop the first lab scale, single step emulsification/polymerisation process for the continuous production of miniemulsions. Currently, there is a considerable amount of industrial effort is being invested in an attempt to scale up miniemulsion technology from the lab to production scale. However, the lack of a commercially viable, energy efficient emulsification device is impeding the transition from laboratory to marketplace.

From the experimental results of this work the following significant findings were made:

- Preliminary investigations using the rotor-stator demonstrated that we are able to generate stable polymerisable miniemulsion droplets.
- Static mixer requires the least amount of energy to operate and impose the least amount of shear generating a narrower droplet distribution in a reasonable amount of time compared to miniemulsion droplets prepared with the ultrasonicator or the rotor-stator.
- *In situ* generated surfactant allows us to stabilise newly generated surfaces more rapidly resulting in a more efficient and reproducible homogenisation/polymerisation process, whereby secondary nucleation is avoided due to the hydrophobic nature of the surfactant.
- Combining the mixing efficiency of the static mixers with the inherent advantages of using *in situ* generated surfactants we were able to develop the first lab scale single step emulsification/polymerisation process for the continuous production of miniemulsions.

The first emulsification device we investigated was the rotor-stator. We found that we are able prepare stable miniemulsions at industrially pertinent solids content (47-55%) ranging from 2  $\mu\text{m}$  to 300 nm in size, by increasing the surfactant concentration and the

rotational speed. The advantages to using the rotor-stator is that it can handle large volumes and it is a device which has already been scaled to industrial production levels. To assess whether the rotor-stator met the objectives set out at the beginning of the thesis (an energy efficient, continuous emulsification process), we compared the efficiency of the rotor-stator in terms of power imparted to the fluid, imposed nominal shear and energy consumption to the static mixers, with ultrasonication as a reference. From the results it was found that the static mixers consumed the least amount of energy, imposed the least amount of shear and generated narrower droplet size distributions within a reasonable amount of time compared to droplets prepared with the rotor-stator and sonicator, making them the optimal choice for the preparation of miniemulsions.

We then began to investigate ways to improve the emulsification process by reducing the amount of coalescence during the droplet breakage/formation cycles, with the intention to increase energy savings. We implemented a long established technique whereby we neutralised a long chain carboxylic acid with a water-soluble base at the oil water interface, creating a surfactant and almost instantaneously generating micron size droplets. We found that the characteristic time to stabilise newly-formed droplet surfaces using *in situ* generated surfactants is approximately 50% faster than the characteristic stabilisation time for preformed conventional surfactants to diffuse, collide and adsorb onto the surfaces. This approach allows us to stabilise newly exposed surfaces more rapidly and therefore makes the emulsification process more efficient, reducing the emulsification time scale and increasing energy savings compared to when using commercially known preformed surfactants. Additionally, any concern with respect to secondary nucleation in the water phase due to the presence of surfactants (free or in

micelles) when using preformed surfactants is alleviated as the *in situ* generated surfactants reside in the organic phase.

Combining the inherent advantages of *in situ* generated surfactants with the efficiency of the static mixers, we were able to generate polymerisable miniemulsions in under 14 minutes, compared to 30 minutes when using SDBS, at the same operating conditions using our original experimental set up. We continued to reduce process time from 14 minutes to 0.5 minutes by simultaneously increasing the number of elements in series and the flow rate through the pump. Although, this came at a cost of higher pressure drop in the emulsification loop, resulting in larger instantaneous energy consumption, the total process energy requirement in terms of energy per kilo of latex produced was ultimately lower due to significantly shorter processing time.

Subsequently, we investigated the feasibility of integrating a continuous tubular reactor in line with the emulsification loop in order to develop the first fully-integrated continuous emulsification/polymerisation process for the preparation of miniemulsions using *in situ* generated surfactants. The reaction profiles and final product characteristics were nearly identical to those obtained during batch operation, demonstrating that the miniemulsion processes described herein can be successfully adapted to continuous operation, thus realizing additional savings in process time and energy consumption.

# 9

## ***FUTURE WORK***

---

The work completed thus far has left a solid ground work for establishing further experiments via experimental investigation or computational modeling that can help explore and expose the fundamentals of our working systems. The following projects are recommended for further examination:

1. Fundamental study of nano-sized droplet formation.

Such a project will involve experimental investigations and CFD modeling of droplet breakage of colloidally stabilised nanometer sized droplets in different types of devices with a focus on the rotor-stators and static mixers. The results should be compared to fluid flow dynamics within each respective device.

Thus far, we have shown that a fundamental understanding of the stabilisation system led to major improvements and a novel emulsification process. However, if we are to scale such novel processes, a more in-depth understanding of what forces control breakage of colloidally stabilised nanometer size droplets and where the breakage is most likely to occur.

The majority of the droplet breakage models developed account for large unstabilised droplets; thus these models fail to account for the constant change in interfacial tension due to dynamic surfactant adsorption and for the osmotic pressure contribution instated by the presence of a costabiliser. These factors should be taken into consideration when performing a numerical simulation of stabilised droplets flowing through different emulsification devices in a flow regime comparable to what is expected in the emulsification device. These numerical results should be paralleled with experimental runs measuring conductivity, turbidity, viscosity and in-line light scattering.



2. Experimental studies should be performed relying on basic engineering knowledge in an attempt to isolate which hydrodynamic and geometrical parameters control the final droplet size when emulsifying with SMX static mixers. The results and methodology could then be used when developing scale up criteria for SMX mixers.

This study should be carefully performed whereby a single geometrical or process parameter would be varied at a time. A number of experiments are proposed that may help to deduce the determining factor controlling the droplet size:

- Perform repeated emulsifications at a constant flow rate using a series of SMX mixers of different diameters (i.e. changing mixer pore size) but with similar number of cross bars along the axis and in parallel (i.e. the pore size should grow proportionally with the diameter of the mixing element).
- Similarly, the emulsifications should be repeated whereby a constant pressure drop is maintained across the length of the mixing elements. In order to perform these emulsifications for larger SMX mixers, flow rates must be increased in order to accommodate the increase mixer diameter. The difficulty in performing such experiment at increasing Reynolds numbers is the corresponding increase in inertial forces, making it more difficult to determine whether droplet breakage is caused by an increased chaotic environment and turbulent eddies or by laminar shear forces.
- Working at same pore sizes irrespective of the SMX mixer size, while maintaining the flow rate or the pressure drop constant, separately.

Trends for the number of passes, emulsification time and energy consumption required to reach minimum droplet size should be recorded and compared. The significant

contribution drawn from these results is determining whether similar trends can be extracted from all sets of mixers and whether there is a global trend that can be followed when selecting SMX mixers for emulsification purposes. Ultimately, isolating the determining factor controlling droplet sizes facilitates the scale up process of the static mixers; i.e. keeping a constant pore size, flow rate or pressure drop across the elements, etc.

3. A deeper understanding of the physico-chemical aspect of *in situ* generated surfactants and their integration into the polymer backbone is required.

Saturated long chain carboxylic acids are considered semi-volatile organic compounds. Switching to unsaturated counterparts, one could attempt to integrate the surfactant into the polymer backbone by reacting the double bonds; resulting in a 'greener' process.

Additionally, to date, interfacial tension measurements performed with *in situ* generated surfactants have not been reported with absolute confidence. Understanding and modeling the dynamics of the various acid complexes and their contributions to the interface is essential, especially when trying to understand the mechanisms of droplet breakage and stabilisation (point 1 & 2).

It is acknowledged that interfacial measurements of *in situ* generated surfactants have proven to be extremely complicated and unreliable, however attempts should be made to understand the interfacial activity of the preformed counterparts as it was shown in Chapter 6 that equal amounts of *in situ* or preformed surfactants generate droplets of comparable size. Such measurements require elaborate measurement techniques and

devices as mentioned in Chapter 6. Additionally, understanding the dynamics of stabilisation between the two forms of surfactants can highlight some knowledge on the characteristic time of stabilisation using *in situ* generated surfactants compared to the time for diffusion, collision and adsorption for the preformed counterparts.

A

## *Appendix*

---

### A.1 Calculating Conversion

In all polymerisation presented, monomer conversion was determined gravimetrically. Samples which were withdrawn from the reactor were left to cool down to room temperature. The samples were then transferred into an aluminum tray and moved to an oven set between 85 to 100 °C in order to evaporate any residual monomer and water.

The following is a sample calculation used to determine the amount of monomer conversion throughout the polymerisation.

- Determine initial mass of aluminum tray:  $M_{tray}$
- Transfer sample into tray and measure mass of “wet tray”:  $M_{wet}$
- Move tray to oven until sample is dry
- Measure mass of “dry tray”:  $M_{dry}$

Based on these small calculations, the mass of the “wet” sample and “dry” sample can be determined:

Mass of wet sample ( $M_{ws}$ ) :  $M_{wet} - M_{tray}$

Mass of dry sample ( $M_{ds}$ ) :  $M_{dry} - M_{tray}$

Calculate mass fraction of each chemical component used:

Monomer: 
$$F_{mon} = \frac{m_{mon}}{m_{tot}}$$

Costabiliser: 
$$F_{cos} = \frac{m_{cos}}{m_{tot}}$$

Surfactant: 
$$F_{sur} = \frac{m_{sur}}{m_{tot}}$$

Initiator:

$$F_{ini} = m_{ini} / m_{tot}$$

Water:

$$F_{wat} = m_{wat} / m_{tot}$$

Using mass fractions, determine the mass of each component in each “wet sample”:

$$\text{Mass of monomer in wet sample: } M_{mon} = M_{ws} * F_{mon}$$

$$\text{Mass of costabiliser in wet sample: } M_{cos} = M_{ws} * F_{cos}$$

$$\text{Mass of surfactant in wet sample: } M_{sur} = M_{ws} * F_{sur}$$

$$\text{Mass of initiator in wet sample: } M_{ini} = M_{ws} * F_{ini}$$

$$\text{Mass of water in wet sample: } M_{wat} = M_{ws} * F_{wat}$$

Using the above amounts, and assuming that all the water has evaporated once the sample is considered “dry”, the total mass of polymer ( $M_{pol}$ ) is:

$$M_{pol} = M_{cos} - M_{sur} - M_{ini}$$

Conversion is then:

$$\% (X) = \left( \frac{M_{pol}}{M_{mon}} \right) \times 100$$

### A.2 Calculating the number of droplets ( $N_D$ ):

$$N_D = \frac{M_{pol} \times 6}{d_{mon} \times D_d^3 \times \pi}$$

Where,  $M_{pol}$  is the mass of polymer (see Appendix A1),  $d_{mon}$  is the density of the monomer and  $D_d$  is the average diameter of the droplet.

### A.3 Calculating the number of particles ( $N_P$ )

$$N_P = \frac{M_{TOT} \times 6}{D_d^3 \times \pi} \times \left( \frac{X}{d_{pol}} + \frac{1-X}{d_{mon}} \right)$$

where,  $M_{TOT}$  is the total mass of monomer,  $D_d$  is the average diameter of the droplet,  $X$  is the conversion (see Appendix A.2),  $d_{pol}$  and  $d_{mon}$  is the density of polymer and monomer respectively.

Therefore, the ratio of the number of particles to the number of droplets:

$$N_P / N_D$$